Virtual Source Method: Imaging Steeply Dipping Structures In a Heterogeneous Medium using a Walk-Away VSP Survey

Submitted by: Kyle Foley

A thesis submitted to the Department of Earth Sciences
Memorial University
St. John's, NL, Canada
in partial fulfillment of the degree of
Masters of Science

Date of Completion: May 2017

Abstract

The virtual source technique is a relative new seismic imaging method with the ability to create virtual sources at the location of receivers. This technique has a broad range of applications, which could be attractive to the petroleum and mineral exploration industry. However, much of the research has been completed imaging a target in a homogenous background. To make the virtual source method more applicable this research focused on more geologically realistic models by changing the homogeneous background to a heterogeneous background (ex sedimentary layering or gneissic foliations). The ultimate goal of this thesis was to test whether seismic scattering, caused by heterogeneities, could enhance the imaging capabilities of the virtual source technique on a complex target. Understanding how different heterogeneous fields affect scattered wavefields and then applying this knowledge to the processing sequence of the virtual source method, was the approach taken for this research to appropriately study the results.

Acknowledgments

I would like to thank my supervisor **Dr. Charles Hurich** for spending countless hours helping me with all aspects of this project. The guidance Dr. Hurich gave me during this project will help me succeed in my future endeavors.

I would like to thank my second reader **Dr. Colin Farquharson** for the guidance during my graduate courses and answering any questions I had.

Thank you to **Sharron Deemer** for her help and technical guidance throughout this project.

Also thanks to **Peter Bruce** for spending time to help me with any linux or software issues.

I would also like to thank Landmark© Software, for supplying me with the processing program ProMAX© which was used to process the seismic modeling of this project.

Table of Contents

List of Tables

List of Figures

Chapter 1 Introduction

Surface seismic surveys have limited effectiveness when imaging steeply dipping geological features, which are common in hard rock geology and salt dominated environments. These surveys are biased towards imaging shallow dipping reflectors due to the geometric relationship between the reflectors, sources and receivers. The problem with recording reflections from sub-vertical targets is that there will be no reflections emanating off the sub vertical reflector back to the surface, as illustrated in figure 1.1A. In order to provide a recording geometry appropriate for these steeply dipping features, a survey known as a Vertical Seismic Profile (VSP) can be utilized. A VSP survey

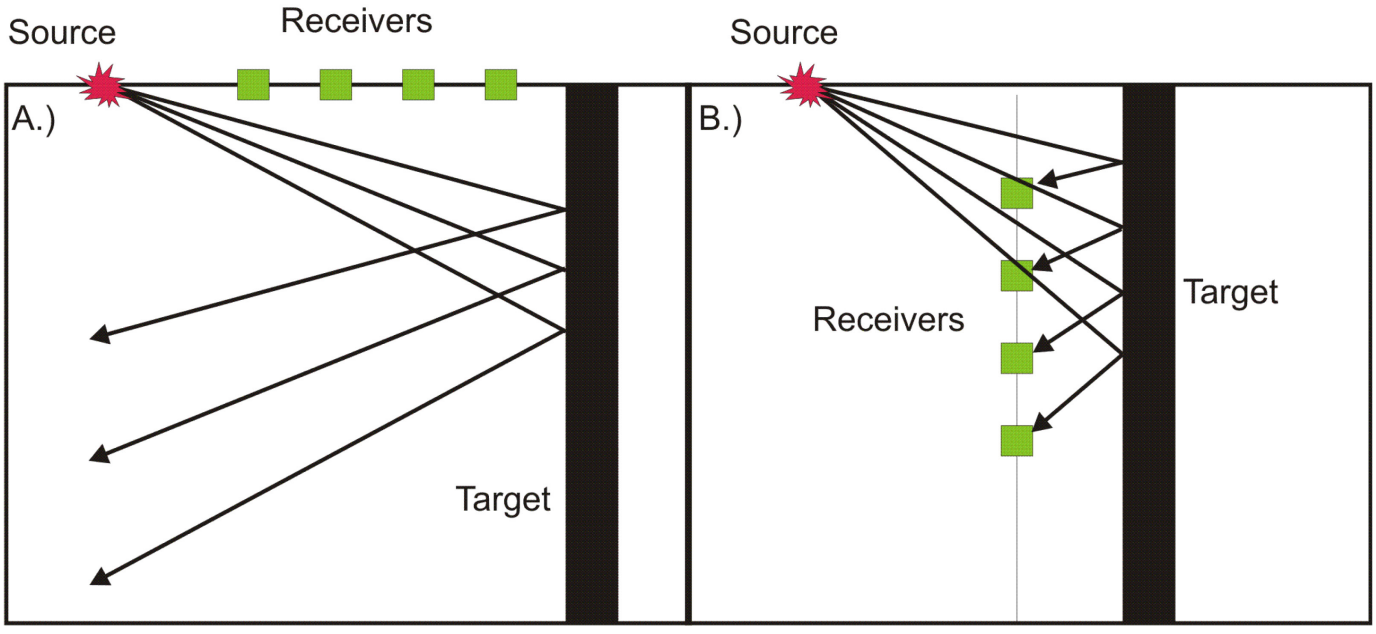

Figure 1.1 Tradition vs VSP Seismic Survey
A.) Surface Seismic Survey. Geometry cannot properly image the steeply dipping target.
B.) VSP Survey. Since the receivers are located in the borehole the targets reflected waves are recorded.

geometry differs from a surface survey because the receivers are located in the borehole and sources are on the surface (figure 1.1B), creating a favorable geometry for imaging steeply dipping targets. Unfortunately, the data cannot be processed with all the CMP noise cancelling capabilities of a surface seismic survey, since the sources are not in the same plane as the receivers. Within the past two decades a relatively new technique that processes VSP data with all the noise cancelling capabilities of a surface survey has been developed, known as the virtual source method, which solves the issue of imaging steeply dipping structures.

The virtual source method uses seismic interferometry to re-datum sources from the surface to the borehole at receiver locations, allowing the virtual sources and receivers to be located in the same plane (figure 1.2 A). In order to re-datum surface sources to the receiver's kinematically correct location a specific geometry must be achieved (travel path D1 to R1 to R2). Producing enough virtual sources at receiver locations to properly image a steeply dipping reflector requires a wide distribution the surface sources. Due to cost of shooting a sufficient distribution of surface sources, as well as environmental limitations the amount of angle ranges produced from surface sources will be limited. The limited source aperture will limit the image quality produced by the virtual source method, and potentially causes the introduction of artifacts.

In the petroleum and mineral exploration industry increasing the seismic resolution on targets that have steeply dipping features is important, due to the economic

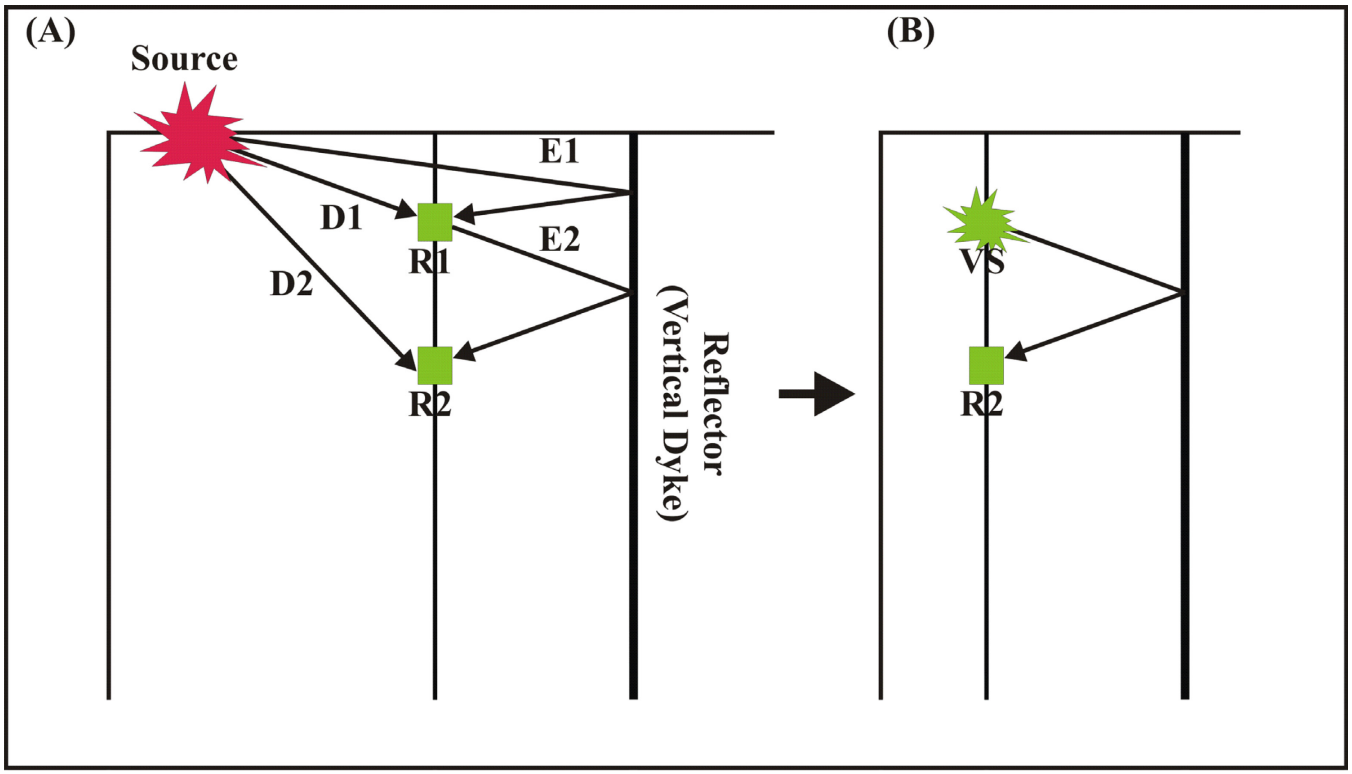

Figure 1.2. Kinematically Correct Event Location for the Virtual Source Method. (A) Simplistic geometry of a VSP survey with the sources located at the surface and receivers in the borehole. (B) R1 is transformed into a virtual source. D1=direct arrival recorded at R1, D2=direct arrival recorded at R2, E1=specular refection recorded at R1, E2=specular reflection recorded at R2, VS=virtual source.

possibilities that these areas contain. For the petroleum industry there are significant amounts of hydrocarbons trapped in overturned, and steep edges of many salt structures. The mining industry also has valuable materials in steeply dipping, and complicated mineralized dykes. The use of a surface seismic survey poses a problem to the exploration industries that are attempting to properly image the steeply dipping, and irregular shapes produced by salt domes and mineralized dykes. Using the virtual source method with a VSP walk away survey is a more attractive imaging technique for this geometric arrangement. However, the potential limitations placed on the surface source

aperture do not allow the survey to produce a large range of angles, required to image these complicated structures. In a number of research papers it has been pointed out that seismic scattering in response to geologic heterogeneity may help to mitigate the problem, by utilizing the increased range of propagation angles produced by scattering. This project will be testing to see if a heterogeneous medium can increase the range of illumination angles that can be captured on the already proven virtual source method. If successful then this imaging technique will be able to produce higher resolution images of these complex geological features, thus increasing the amount of industry interest in the virtual source method.

Bakulin and Calvert (2006) discussed the possibility of a scattered wavefield having the potential to increase the reflection angles that are properly recorded by a seismic survey (figure 1.3). To this date limited practical research has been completed on the subject. To examine the effectiveness of increasing reflection angles a single point scatter is introduced into a homogeneous medium (figure 1.3). Using a zero offset VSP survey, with receivers located in a vertical borehole it is possible to image the ray paths emanating from the point scatter (figure 1.3). The zero offset VSP survey recorded both upgoing and downgoing waves, demonstrating that the point scatter increased the amount of illumination angles in the subsurface. The VSP survey could take advantage of the heterogeneities because this medium will create countless scatterers, causing the seismic ray paths to scatter in all directions. The increased illumination angles from the scattered wave field could have significant effects on the image quality of the target: (i) by increasing the amount of kinematically correct information in the virtual sources, and

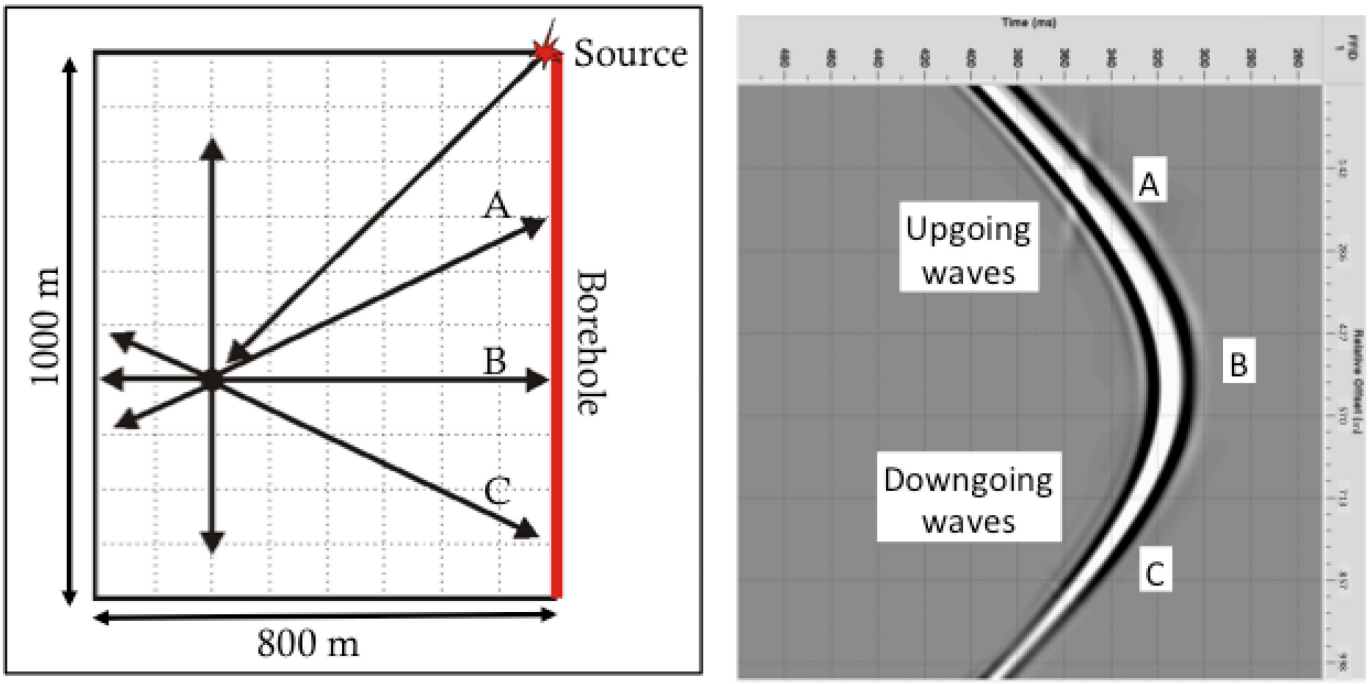

Figure 1.3 Point Scatter
A zero offset VSP shot gather shows that a point scatter causes the seismic wavefield to scatter in all directions, creating both upgoing and downgoing wavefields which can impinge on a receiver.

(ii) reducing the amount of artifacts created during the interferometry process through cancellation of kinematically incorrect information.

To study the affects of geologic heterogeneity on the virtual source technique this research will be using a suite of computationally generated (synthetic) VSP surveys. The imaging study is preceded by an analysis of the forward scattered wave field in a variety of scattering media with different properties, by studying the FK spectra. The FK analysis examines the direct wave and the cone of energy created by each scattered wavefield, to demonstrate the strength and nature of each scattered wavefield. This work, develops an understanding of how to best utilize the scattered wavefield while using

geologically realistic scattering parameters. The next critical element of the experiment is to develop a reference model that consists of geometries appropriate for assessing the affects of heterogeneity. Once the reference model has been defined, systematic inclusion of heterogeneity is used to determine if and under what conditions heterogeneity may contribute to increasing the amount of kinematically correct virtual sources. This requires examination of the nature of geological heterogeneity, which includes an investigation into amount of coda that is appropriate to cross correlate during the virtual source method. During this portion of the project a CMP processing flow properly images these steeply dipping structures. Using all of information from the models, this research will extend upon the current literature by demonstrating the affects a heterogeneous medium has on the virtual source method.

Chapter 2 Literature Review

2.1 Introduction

"Seismic Interferometry of any data only requires two steps: The two recorded signals from each source are cross-correlated and the resulting cross-correlograms are summed" (Curtis, 2006). Many researchers are utilizing seismic interferometry at this time and some examples of research being done in this field include day-light acoustic imaging, time-reversal acoustics and the virtual source method. The theory for the cross-correlation and summation to create virtual sources in the earth is of particular interest for this master's thesis. Over the past 15 years this method has been developed and has been proven to work in both theory and real world practice (Schuster, 2001; Bakulin and Calvert, 2006; Hornby and Yu, 2007; Mehta and Snieder, 2008; Schuster, 2009; Brand and Hurich, 2012; Hurich and Deemer, 2013). Even though there have been leaps forward in the virtual source method, limited research has been completed on the effects of using the virtual source technique in a heterogeneous medium.

2.2 Virtual Source Method

Gerald Schuster (2001) proved it was possible to partially satisfy the requirements for seismic interferometry with active seismic acquisition parameters. Active seismic data uses man made sources and receivers and via cross correlation and summation

virtual sources are created at receiver locations. The research performed for this master's thesis will also use active seismic acquisition parameters during the virtual source method.

Research has been advanced implementing the virtual source method in the past two decades using several types of seismic surveys. With these different seismic geometries the virtual source technique has been used for the suppression of surface waves (Vasconcelos et al, 2008; Xue et al, 2009), time lapse imaging (Hornby and Yu, 2004), imaging the edges of salt domes (Hornby and Yu, 2006) and imaging steeply dipping dykes with complex geometries in a hard rock environment (Brand and Hurich, 2012; Hurich and Deemer, 2013). The research for this masters thesis uses a VSP walk away survey to image steeply dipping and complex mineral bearing dykes, which is similar to how the virtual source technique was utilized by Yu and Hornby (2006), Schuster (2009), Brand and Hurich (2012) and Hurich and Deemer (2013). They proved by redatuming surface sources to receivers in the subsurface reflectors are not only imaged but can improve the resolution of the reflector. In 2012 Brand and Hurich used synthetic models with rock properties resembling a hard rock environment to further advance the work completed by Yu and Hornby. By closely examining the source aperture and source density they were able to determine under what survey conditions this method is optimal in a homogeneous environment. The work completed on this master's thesis will closely resemble and expand on the work completed by Brand and Hurich in 2012.

Brand and Hurich primarily worked on synthetic models with a homogeneous country rock surrounding a steeply dipping reflector. In reality geology will have heterogeneities that will cause the seismic wavefield to scatter. Limited research has been completed in this field but Baulkin and Calvert (2006) concluded that scattering the seismic wavefield could extend the virtual source aperture by introducing heterogeneities to near surface conditions. Bal and Ryzhik (2005) showed that time reversal acoustics was improved in a heterogeneous medium due to the increase in angles at which the wavefields are travelling with. Brocea (2006) used seismic interferometry to increase the imaging capabilities of a seismic Kirchhoff migration in a cluttered medium. The importance of this new work lays the potential of using the scattered wave field to increase the range of illumination angles and mitigate artifacts introduced by the limited number of surface sources.

Chapter 3 The Virtual Source Method

3.1 Introduction to the Virtual Source Method

The virtual source method is a form of seismic interferometry that can be used to re-datum surface sources into a borehole to produce virtual sources at the location of borehole receivers. In order to properly implement the virtual source technique and all its benefits, the surface sources must be re-datumed to the correct spatial receiver location in the borehole. Brand and Hurich (2012), as well as Hurich and Deemer (2013) used ray tracing as an intuitive method to explain how surface sources are re-datumed to proper receiver locations. Ray tracing is also used in this thesis to explain the virtual source method. Figure 3.1 depicts a simplistic model that helps to explain the virtual source technique using a surface source, two receivers in a vertical borehole and an adjacent reflector oriented parallel to the borehole. The survey is setup in such a way that the difference in travel time between the direct arrival emanating from a surface source recorded at R1 and the travel time of the reflection recorded at R2 is equal to the reflection produced by a virtual source at R1 and being recorded at R2 (figure 3.1 A) (Mehta, 2008). This geometry allows the cross-correlation between the direct wave recorded at R1, and the reflection recorded at R2 to produce a reflection between R1 and R2. The cross-correlation re-datum's the surface source to be a virtual source that is located at R1 (figure 3.1 B). When this cross-correlation creates a virtual source at a receiver and this virtual source is recorded at another receiver, a kinematically correct event has been produced. It is required to produce numerous kinematically correct virtual

source and receiver pairs during a VSP walk away survey in order for the virtual source method to properly work and successfully image the target.

When completing a VSP survey not every cross-correlation between two receivers results in kinematically correct virtual source locations (figure 3.2). In this case the cross-correlation will still represent the travel time difference between the direct arrival at R1 and the reflection at R2, but it will not equal the travel time of a reflected event emanating from R1 and being recorded at R2 (figure 3.2). In the field there is no way of knowing if the survey has produced a kinematically correct virtual source and this poses a problem for our experiment. Fortunately if careful consideration is taken when designing the acquisition parameters this problem can be overcome.

3.2 Practical Applications of the Virtual Source Technique

Many geological environments contain targets with complex geometries and steep dips that are not readily imaged with surface seismic surveys. Commonly, these targets would include mineral bearing dykes, steep edges of salt domes and the reflections off steeply dipping fault zones. In the mining industry electromagnetics, gravity and magnetics are the common geophysical surveys that are used, because these surveys can image anomalies produced by mineral bearing structures. These surveys do not provide the high-resolution capabilities that a seismic survey does; therefore it is difficult

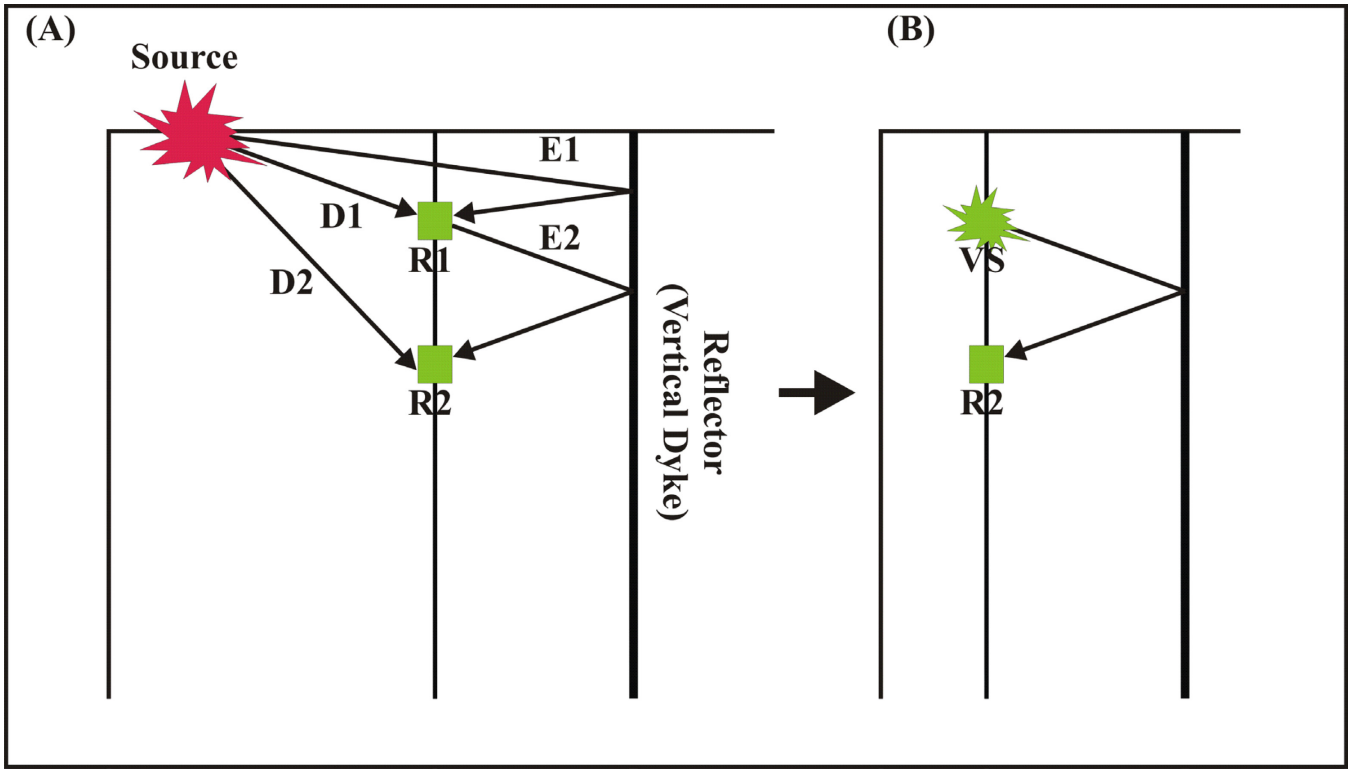

Figure 3.1. Simple Geometry for Virtual Source Method (Duplicate of Figure 1.2)
(A) Simplistic geometry of a VSP survey with the sources located at the surface and receivers in the borehole. (B) R1 is transformed into a virtual source. D1= direct arrival recorded at R1, D2= direct arrival recorded at R2, E1= specular refection recorded at R1, E2= specular reflection recorded at R2, VS=virtual source

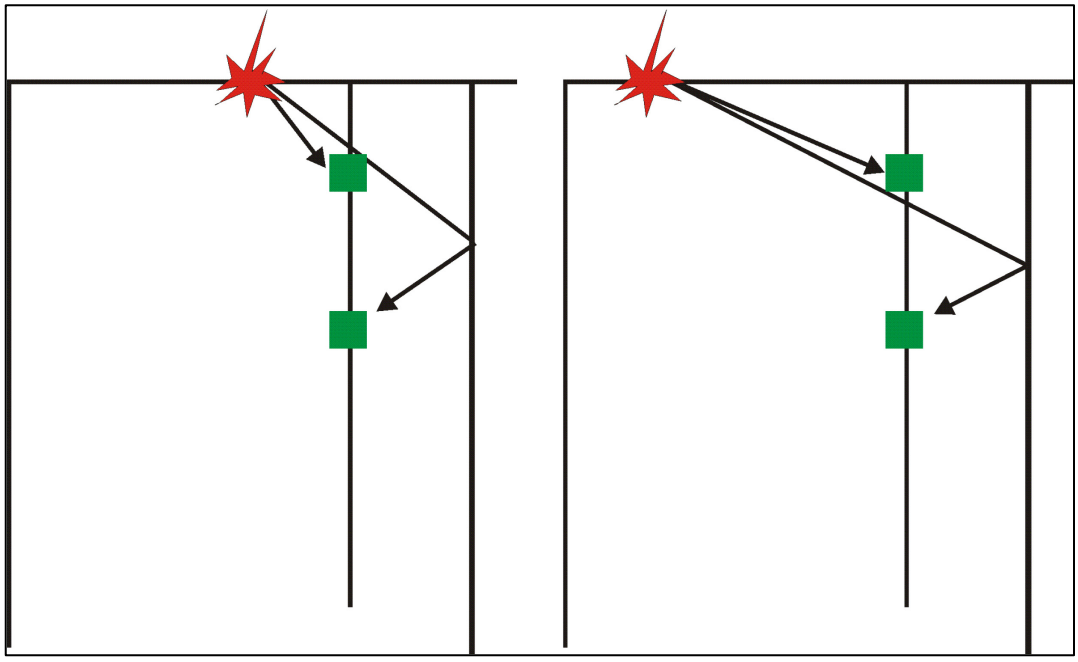

Figure 3.2. Geometry for Kinematically Incorrect Event Creation
A simplistic model representing travel paths that will not produce a kinematically correct virtual source.

to make a detailed prediction of the complex nature of the geology. In the petroleum industry surface seismic surveys are commonly used because most beds containing oil and/or natural gas are sub-parallel to the surface, which acts as the datum for seismic acquisition. In some sedimentary environments there are steeply dipping salt structures that have hydrocarbons trapped on the edges. Unfortunately, a land or marine seismic survey won't be able to properly image these steeply dipping targets due to the geometric set up of the survey. To properly image these features, this master's thesis will implement a synthetic model of a VSP walk away survey that will process the data using the virtual source technique to increase the angles of illumination on the steeply dipping target.

The virtual source method has been tested in geological scenarios such as a sedimentary salt dome (Hornby and Yu, 2007) and a hard rock environment (Hurich and Deemer, 2013) with encouraging results coming from both research papers. In both instances it was demonstrated that by re-datuming the surface sources into the borehole there are a number of benefits that improve the final result of this specially designed VSP survey, which can be identified as: (i) Relocating the surface sources to lie in the borehole allows sources and receivers to be in the same sub-vertical plane. Since receivers and sources are in the plane sub-parallel to the target the imaging bias can be mitigated (Hurich and Deemer, 2013). (ii) When the virtual sources are re-datumed to the borehole the data can be processed like a surface seismic survey via the CMP method with all its noise attenuation capabilities (Brand and Hurich, 2012). (iii) By relocating surface sources to receiver locations in the borehole it is only necessary to create a

velocity model that represents the geology between the borehole and the target of interest (salt dome or mineralized dyke) (Bakulin and Calvert, 2004; Hornby and Yu, 2007). This is helpful, as I don't have the information to create a velocity model of the near surface. (iv) The re-datumed sources can be processed with pre-stack migration techniques, which are becoming more popular for imagining complex geometries (Hornby and Yu, 2007). The noted points provide our specially designed VSP survey with better means to properly image steeply dipping features.

3.3 Effect of Source Spacing and the Stationary Phase Requirement

As mentioned previously, there is no way of knowing which surface source – receiver pairs produce kinematically correct virtual sources, but fortunately mathematics can be used to understand how to isolate the correct ray paths. Schuster (2001), showed that the integral equations defining the virtual source method must have two receivers completely surrounded by a continuous distribution of sources to create a kinematically correct virtual source – receiver pair. Cross-correlating the response recorded by the two receivers with each surrounding source is completed to create a correlation gather (figure 3.3). The summation of the correlation gather into one single virtual source trace allows for the destructive interference of all incorrectly placed events and constructive interference of all the correctly placed events. When a virtual source is placed kinematically correct after summation it is defined as a stationary phase point (Brand and Hurich, 2012). Surrounding the two receivers with sources will ensure that the virtual

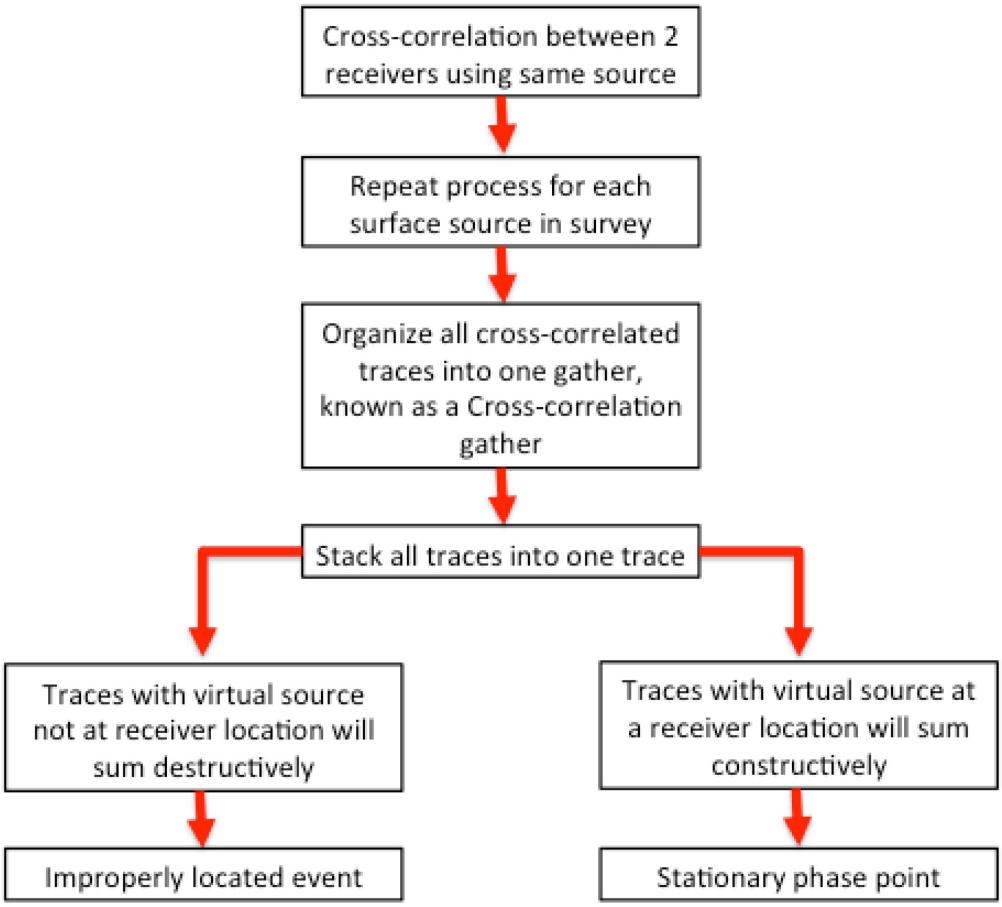

Figure 3.3 Stationary Phase Points
Flow chart explaining the processing technique of the virtual source method.

source is kinematically correct (figure 3.3) during integration of the correlation traces. Proving that without knowing the geometry or information regarding the velocity of the subsurface a virtual source can be properly located at a receiver in the subsurface (Schuster, 2001).

However, it is unrealistic to completely surround a buried receiver with buried sources. Mehta and Snieder (2008) demonstrated that only a narrow range of angles between the virtual source and the receiver actually contributes to stationary phase, demonstrating that it is possible to design a realistic VSP walk away survey that partially

satisfies the requirements of the virtual source technique. The geometry of the seismic sources must be carefully considered to achieve stationary phase of the virtual sources when the receivers are not completely surrounded by sources. Source aperture (i) and source density (ii) (Brand and Hurich, 2012) are two parameters, which must be taken into consideration when designing a VSP walk away survey to guarantee the target is imaged when processing with the virtual source technique.

Brand and Hurich (2012) explain the importance of having an adequate source aperture when processing with the virtual source method, by designing an experiment that looks at the effects of increasing the surface source aperture. Their research explained that by increasing the source aperture the input model would produce a higher quality image. This is expected because if you increase the number of sources the number of correlation traces will increase in the correlation gathers. The more correlation traces you sum in the integration process does not necessarily mean more stationary phase but rather provides more destructive interference that removes artifacts (figure 3.4). Another portion of the acquisition to consider is source density. If the source spacing is not dense enough the model could be susceptible to poor destructive interference causing improperly placed events during the summation process and spatial aliasing (Mehta, 2008). Mehta proves that by decreasing the density of the surface sources the travel time between traces will increase, causing the correlation gathers to be more vulnerable to poor cancellation of improperly located events (figure 3.4).

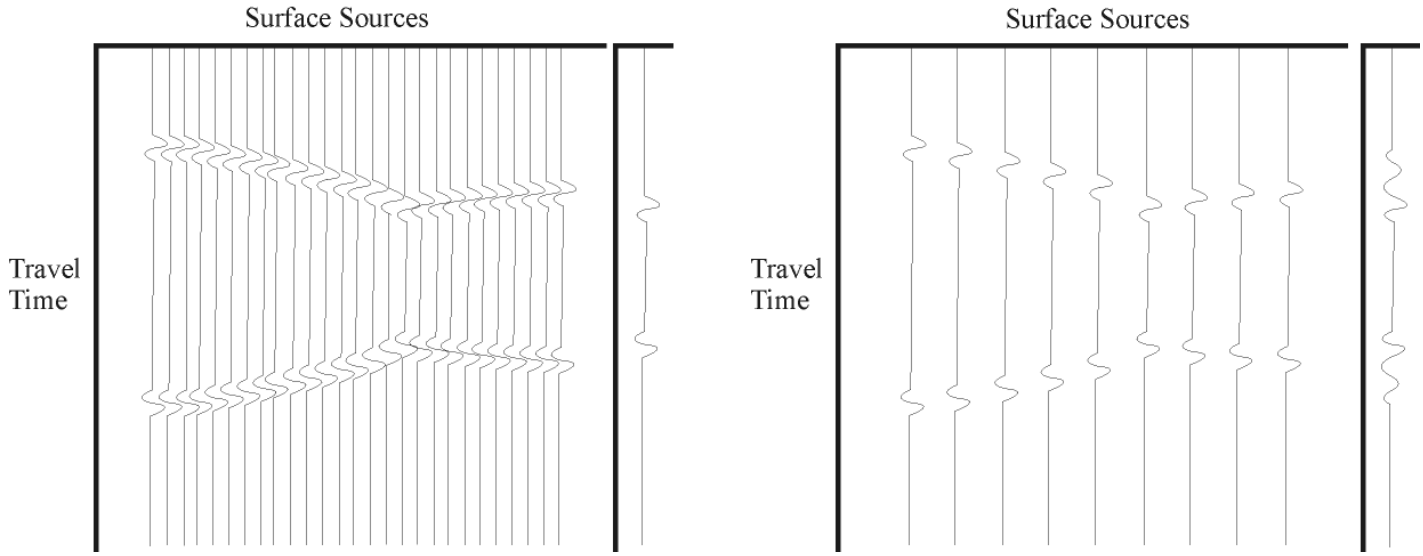

Figure 3.4 Effect of source density during summation
When the density of the surface sources is reduced by a third the slope of the correlation gather increases causing poor cancelation of non-stationary phase events. Modified image from Mehta (2008)

3.4 Ray Tracing Analysis

If the cross-correlation process is unable to achieve constructive interference of kinematically correct events when summing the correlation gathers the target of interest will be poorly imaged. This means that stationary phase (figure 3.2) was not achieved, and the summation of the correlation gathers produced incorrectly located events in the virtual source data. To ensure this does not occur, special consideration must be taken when designing the ideal source spacing and source aperture for the VSP walk away survey. A ray tracing analysis, experimenting with different geological and acquisition scenarios is utilized to determine their effects on the overall quality of the virtual source method. Producing these models will help to develop an understanding of how to properly maximize stationary phase for different geological scenarios.

3.4.1 Reflector Orientation

Mineralized dykes, and salt structures are very complex and can have a wide range of dip angles associated with them, which will effect how well VSP walk away survey's can image the target of interest. Conducting a straight ray theory analysis on three different target angles, with a vertical borehole adjacent to the target (figure 3.5), demonstrates the effects dip angles have on the required surface sources needed to produce stationary phase of the same virtual source – receiver pairs. The reflector of interest has a different dip angle in each of the three scenarios, and is surrounded by a homogeneous country rock (figure 3.5), for simplicity of the straight ray analysis. Figure 3.5 (C) displays the most favorable set up for producing stationary phase for two reasons: (i) the reflector dips towards the borehole allowing for the same stationary phase points to be created with a smaller surface source aperture than if the reflector was oriented vertically (figure 3.5 A) or dipping away from the borehole (figure 3.5 B). (ii) Correct stationary phase can also be produced from upcoming waves, which increases the fold of the data. Figure 3.5 (B) has the least desirable scenario because the reflector is dipping away from borehole making it difficult to obtain enough stationary phase points with a realistic source aperture. In order to produce the same stationary phase points as seen in figure 3.5 (A) and (C), an unrealistic real world source aperture would have to be employed in scenario (B).

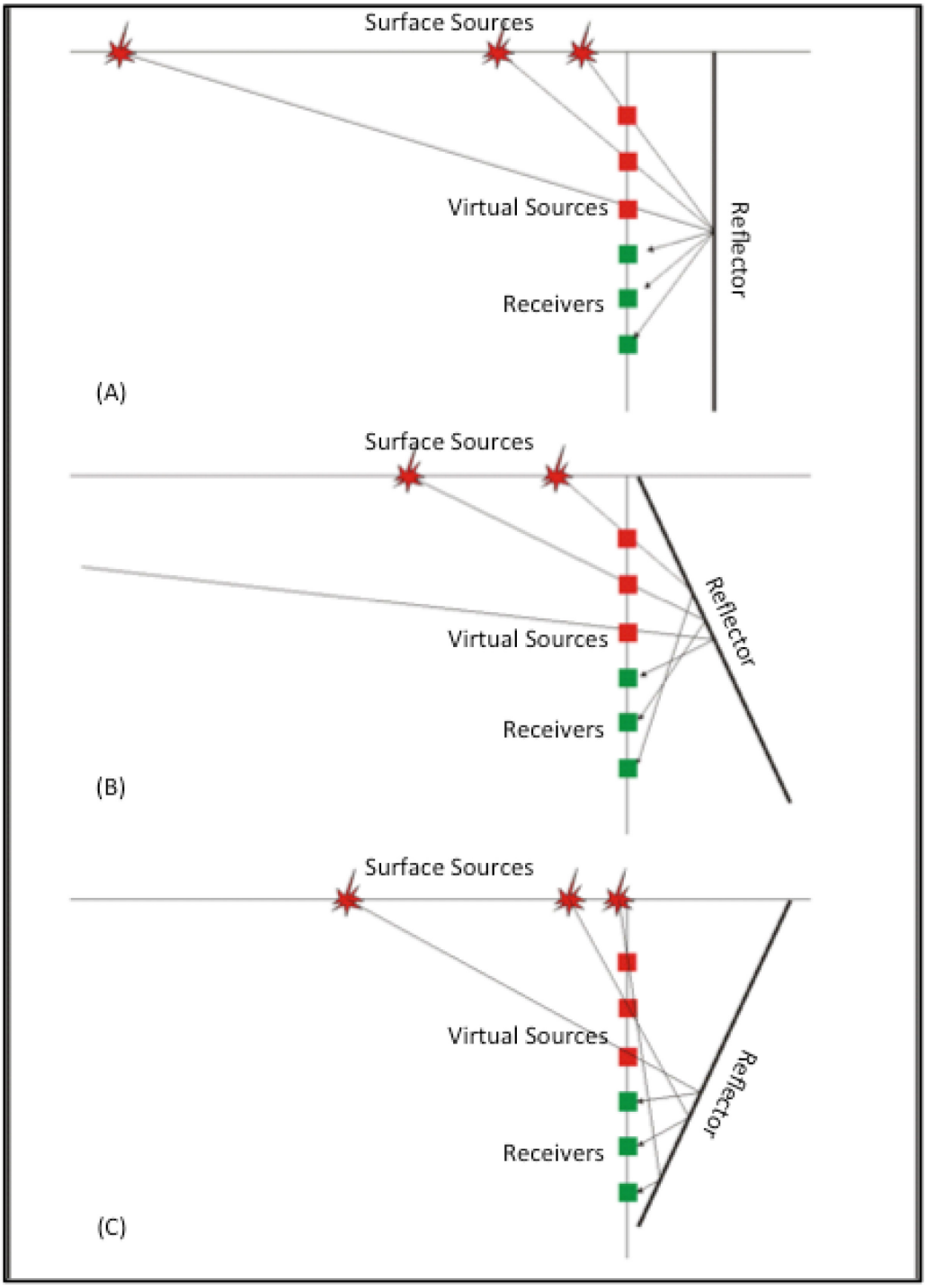

Figure 3.5 Dip orientation affecting VSP Geometry
(A) A vertically dipping reflector. (B) Reflector dipping away from borehole. (C) Reflector dipping towards borehole.

3.4.2 Source Aperture

An onshore seismic survey has many obstacles (e.g. forest, roads, ect), which limits the extent of the source aperture that an offshore survey does not have to be concerned with. To test the outcome that different source apertures has on the virtual source method, an experiment was conducted using two different surface source apertures while leaving the rest of the survey parameters consistent. A vertically dipping reflector, surrounded by a homogeneous country rock will be the synthetic model so that a straight ray analysis can be completed on each survey design. The research used a MATLAB code to perform the ray tracing analysis.

The reference survey for this experiment is model 1, and the geometry can be seen in table 3.1. This seismic survey is designed to demonstrate a VSP walk away seismic survey with a 1500 m surface source aperture. The ray tracing analysis demonstrates that stationary phase is produced only for virtual sources occurring down to a depth of approximately 1200 m (figure 3.6), leaving the bottom third of the borehole without the ability to produce kinematically correct virtual sources. The limited depth of stationary phase points only allows for a maximum CMP depth of 1500 m (figure 3.7). Both of those observations indicate that the deeper portion of the reflector is poorly imaged, and will be located in the wrong position kinematically. Another important observation is that there are a large number of stationary phase rays created by surface sources less than 500 m away from the borehole (figure 3.6). Most of these stationary

Model Number	Receiver Spacing (m)	Number of Receivers	Borehole Depth (m)	Distance to Reflector (m)	Source Aperture (km)
1	18	100	1800	300	1.5
2	18	100	1800	300	10
3	18	100	1800	600	1.5

Table 3.1 Geometric set up of models for Straight Ray Tracing analysis

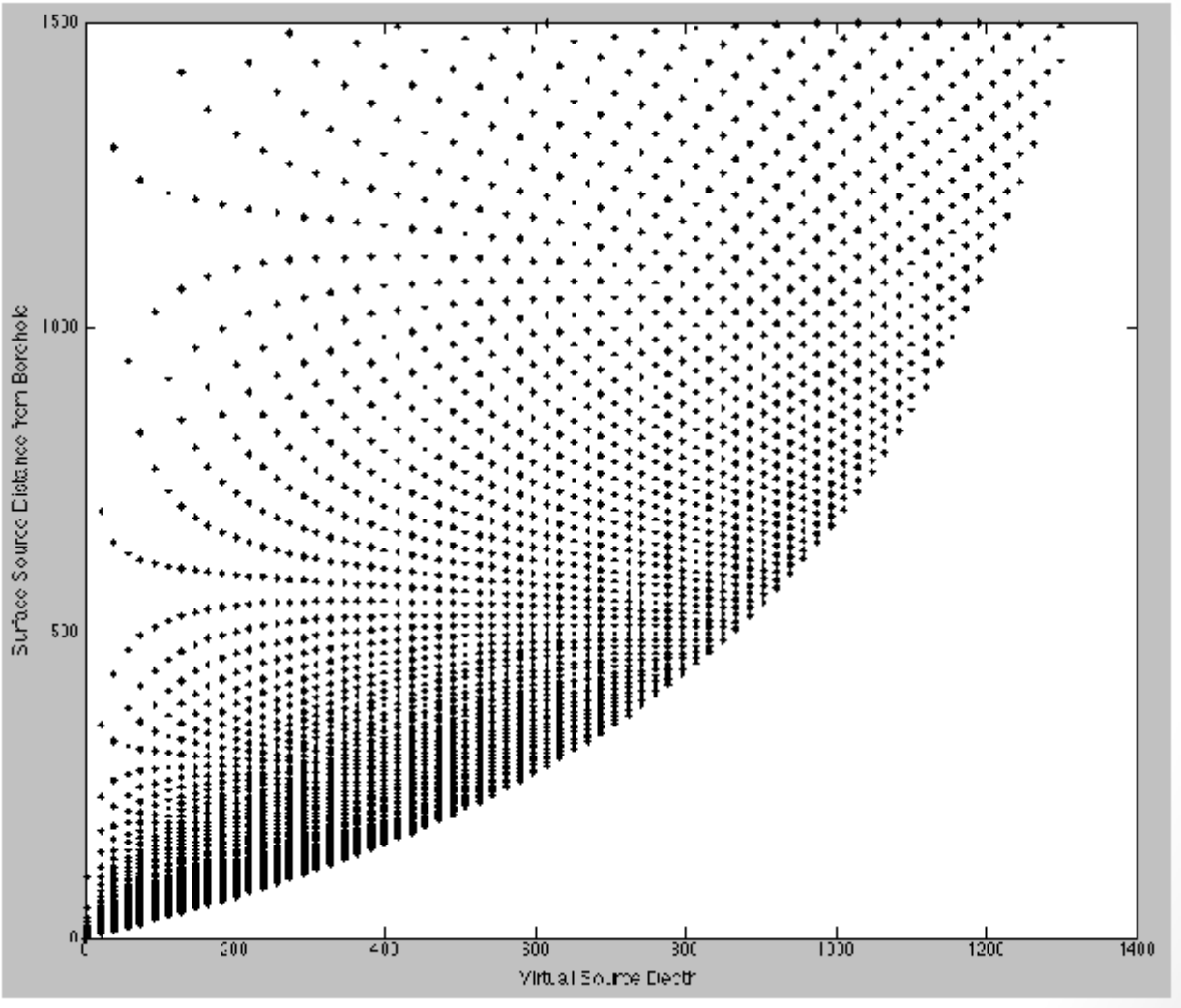

Figure 3.6 Surface Source Distance from Borehole vs. Virtual Source Depth for Model 1 Each point on this graph represents a stationary phase virtual source. The x-axis denotes the depth of each virtual source in the borehole and the y-axis denotes the surface source distance from the borehole. This figure demonstrates how the surface source distance from borehole affects the virtual source depth in the borehole. An important observation, at larger surface source offsets the spacing between stationary phase points becomes larger indicating most of the benefits from imaging a shallow target come from near offset surface sources.

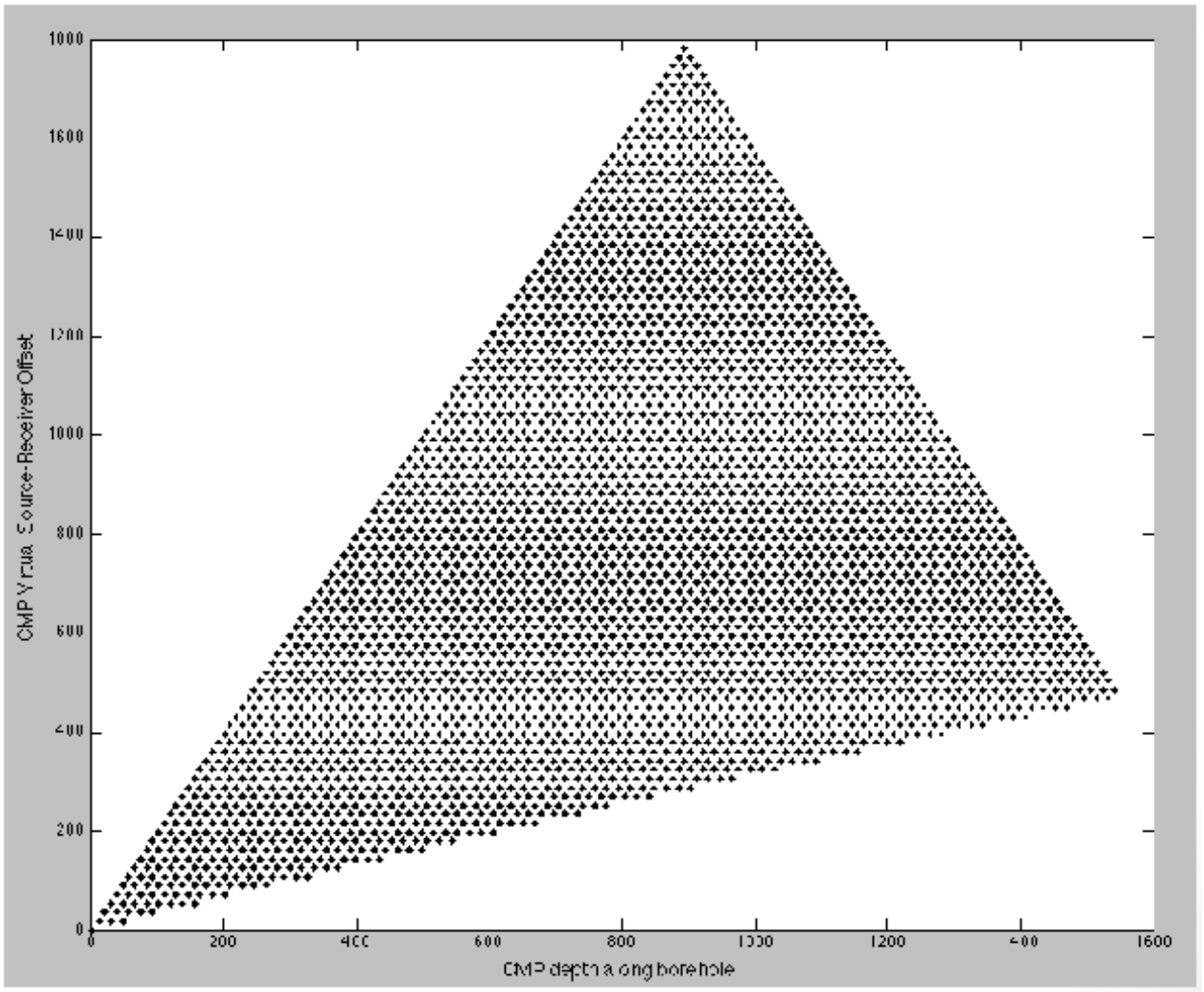

Figure 3.7 CMP depth along borehole vs. CMP virtual source-receiver offset for Model 1 Each point represents a stationary phase virtual source, the x-axis is the depth of the midpoint of each source - receiver pair, and y-axis is the offset of each source – receiver pair. This figure shows which CMP offsets are contributing to the fold of the data.

phase rays are redundant, because they are within the same Fresnel zone with respect to the adjacent surface locations. So, multiple surface source locations within 500 m of the borehole satisfy proper stationary phase geometry for the same virtual source receiver pair. One final point to note is from figure 3.8, which demonstrates that no receivers shallower than any virtual sources produce stationary phase points. Due to this geometry, any traces from a receiver shallower than a virtual source can be removed during processing.

Model 2 in table 3.1 depicts a VSP walk away survey design with a source aperture of 10 km. In this survey design the extended surface source aperture produces stationary phase down to 1600 m into the borehole (figure 3.9), which is 300 m deeper than originally observed in model 1. The depth of the borehole is likely the limiting factor for not creating stationary phase rays deeper than 1600 m because there are fewer receivers deep in the borehole. Since there is an increase in the depth and amount of virtual sources created, the fold in the CMP gathers increases (figure 3.10), causing a narrower spatial filter when stacking the data that is biased towards imaging waves traveling orthogonal to the receiver array toward the middle of the borehole. The increased fold in CMP gathers causes more of the artifacts created during cross-correlation to be stacked out, as they will be travelling at angles not orthogonal to the receiver array. The change in CMP gathers between the source aperture of 1.5 km (figure 3.7) and 10 km (figure 3.10) is most noticeable in the near virtual source – receiver

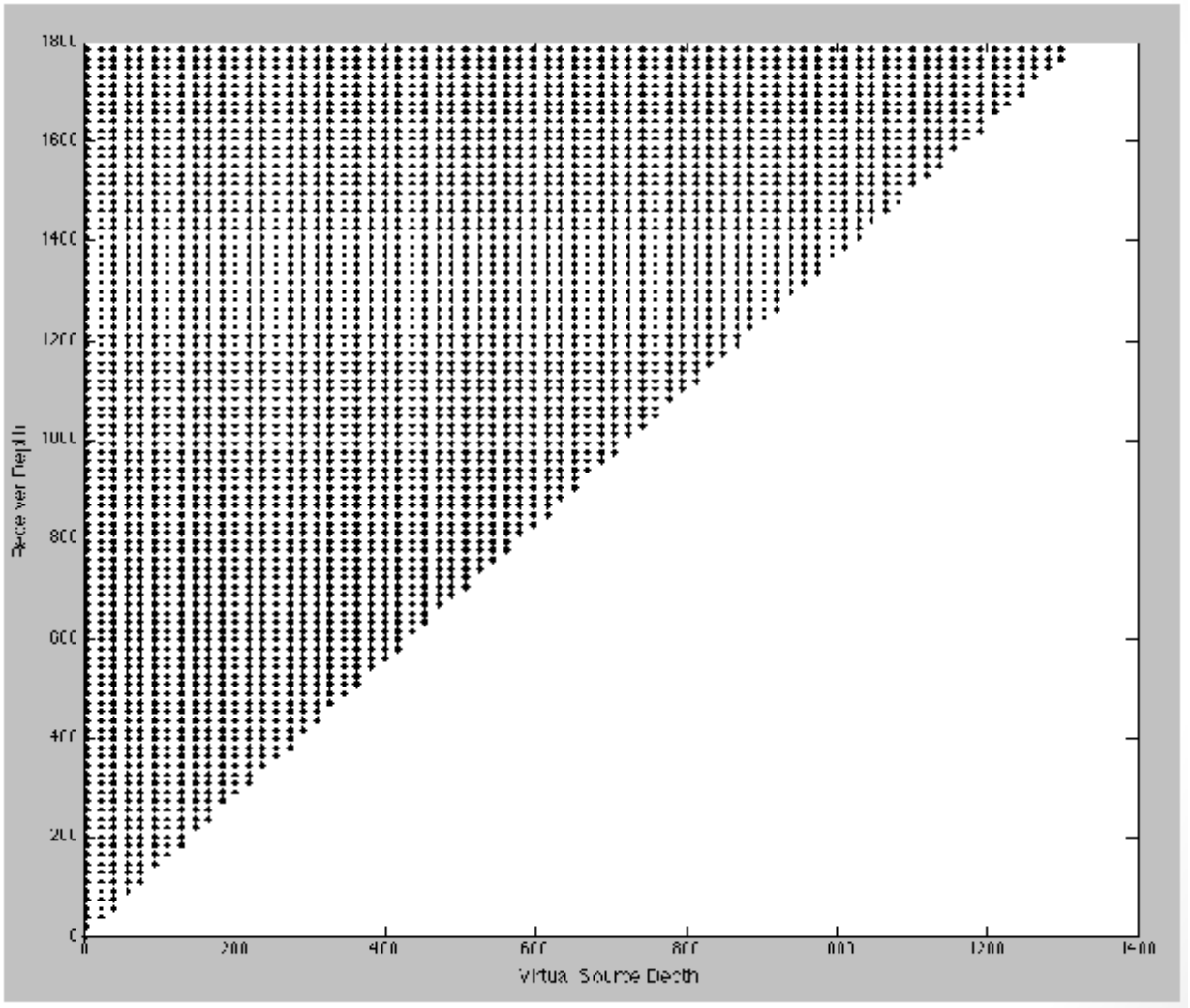

Figure 3.8 Receiver Depth vs. Virtual Source Depth for Model 1
The graph demonstrates, with this geometric set up no upgoing rays will produce stationary phase points and thus should be removed during processing.

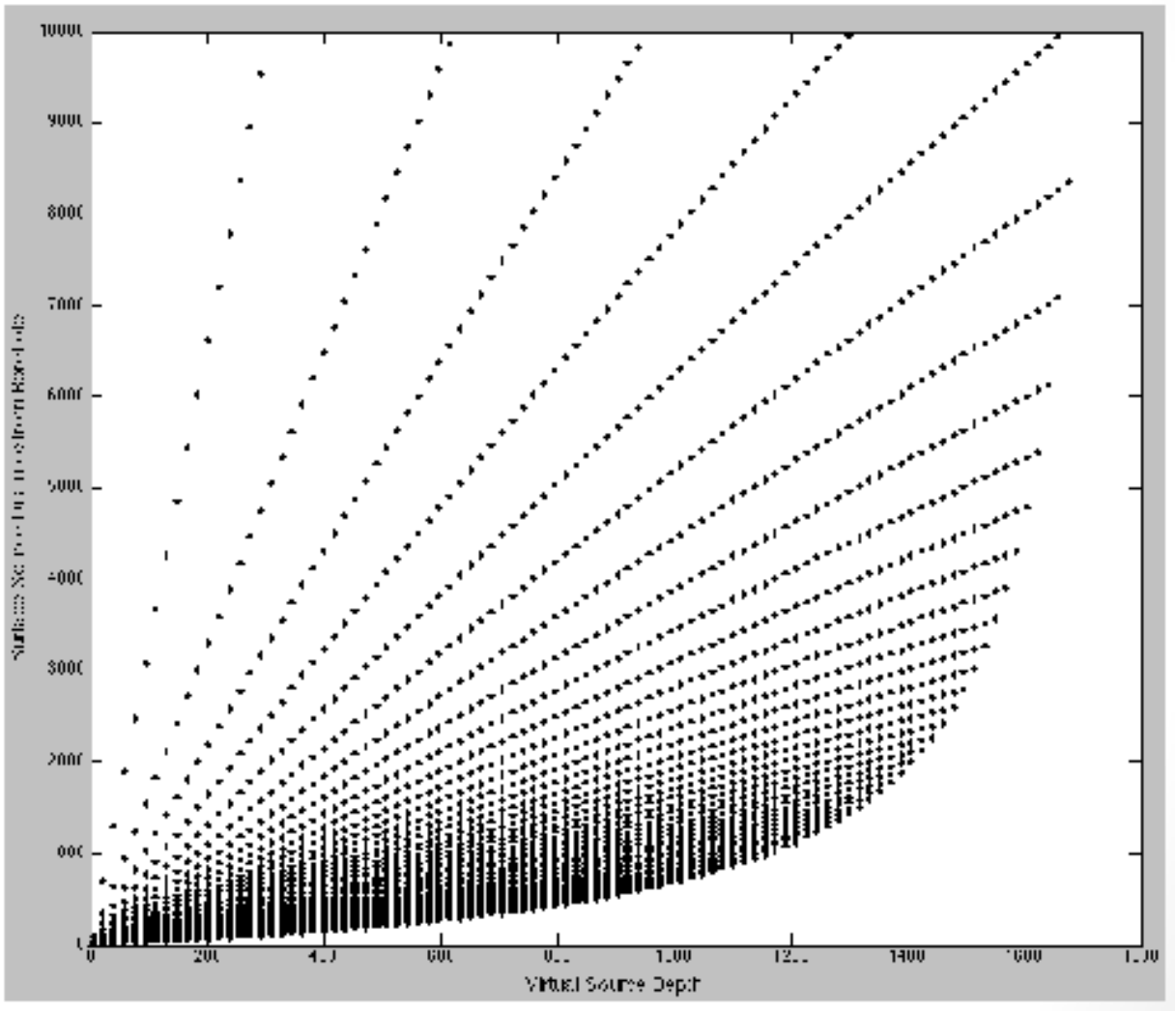

Figure 3.9 Virtual source depth vs. Surface source distance from borehole for Model 2. The source aperture of 10 km is able to produce kinematically correct stationary phase to a depth of 1600 m in the borehole. Similar to figure 3.6 a significant portion of the stationary phase points are created by the near offset surface sources.

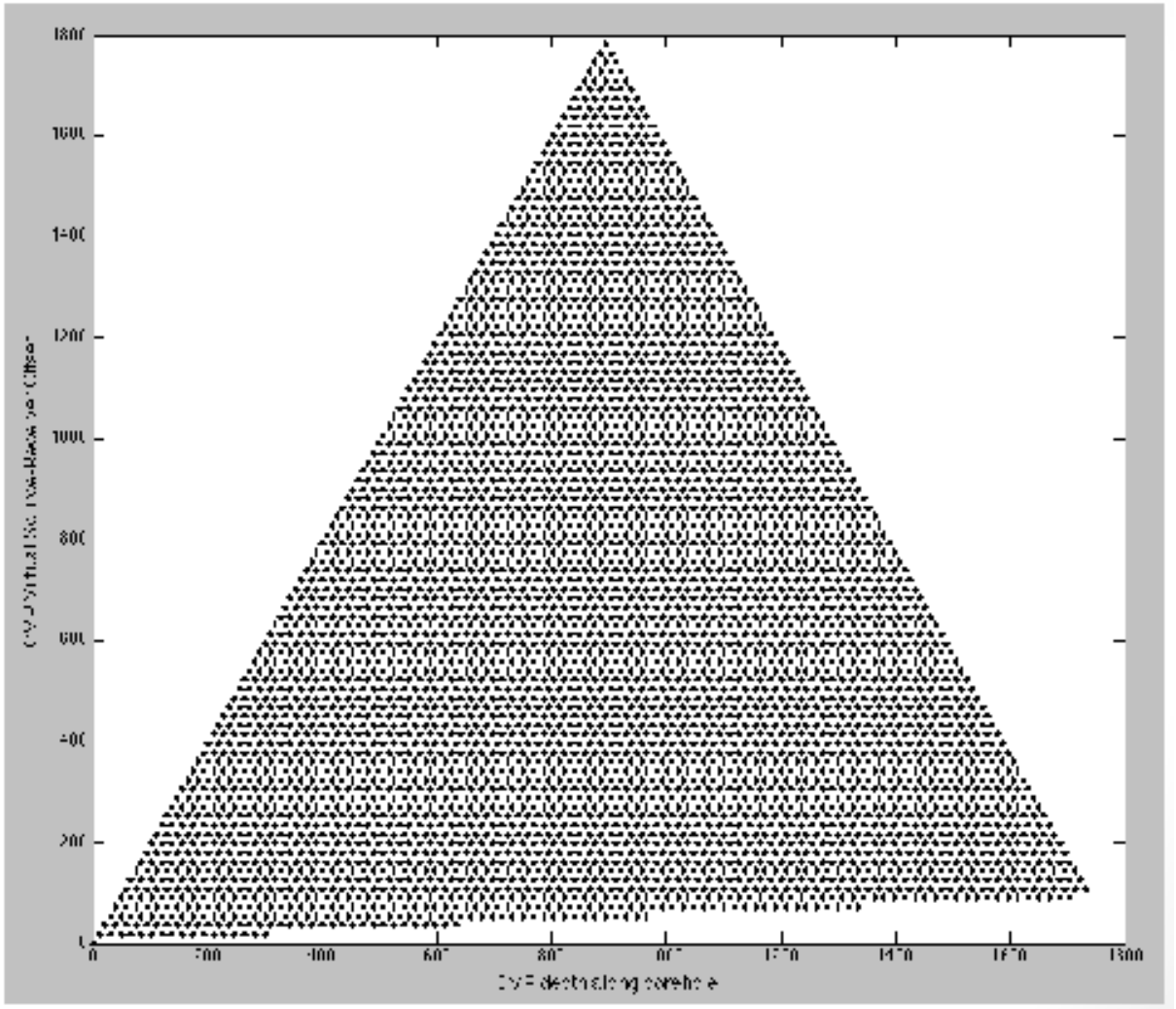

Figure 3.10 CMP depth along borehole vs. CMP virtual source-receiver offset for Model 2

The difference between this graph and figure 3.7 is the increase of kinematically correct near offset virtual source – receiver pairs.

offsets. This is critical to the experiment, as I hope to fill the gaps in the near offset virtual source – receiver pairs of a limited source aperture by simulating a larger source aperture with the use of the increased ray paths caused by a scattered wavefield. One final point to note is that, although model 2 images deeper into the subsurface a lot of the surface sources will be redundant when creating stationary phase rays and the financial implications of performing a source aperture of 10 km would be much greater than if the source aperture was 1500 m. A source aperture of 10 km would be better suited for a survey that was trying to image a reflector located deeper in the subsurface.

3.4.3 Reflector Distance from Borehole

This section develops an understanding of the implications of increasing the distance between the borehole and the vertically dipping reflector, by creating a third model. The third model uses the same survey parameters from model 1, but doubles the spacing between the borehole and reflector (table 3.1). A ray tracing analysis was conducted on model 3, so it can be compared to the results of model 1 (figure 3.11 and figure 3.12). The ray tracing results from model 3 illustrates that: (i) most of the virtual source – receiver pairs have decreased near CMP offsets and (ii) CMP's are not imaged as deep in the borehole (figure 3.11). The result demonstrates that as the borehole distance is increased the amount of proper stationary phase decreases. Although this is an important observation, seismic surveys will also suffer from near surface imaging problems if the target of interest is too close to the borehole. Another important observation to make, is that by increasing the spacing between the reflector and borehole

the source aperture would also need to be increased to produce a similar virtual source geometry.

3.5 Concluding Remarks

Shuster (2001) showed that in theory the receivers must be completely surrounded by sources to produce stationary phase. However, in this chapter practical work by Brand and Hurich, and a ray tracing analysis have been discussed, proving that if special consideration is taken during the design of the VSP survey the need for surrounding the receiver's completely by sources can be overcome. The source aperture must be broad enough to create a sufficient amount of virtual sources with proper stationary phase, and the source density is such that the incorrectly located events are summed destructively.

Chapter 3 has demonstrated that the surface source aperture and the distance between borehole and reflector can have significant impacts on the quality of the final image. These effects can be generally seen in the CMP fold, the offset of the virtual source – receiver pairs and the depth at which virtual sources can produce stationary phase. The reflector orientation will also have a significant impact on the amount of stationary phase points that will be recorded. Only receivers located below the virtual source will be able to produce stationary phase unless the reflector is dipping toward the borehole. So, great care must be taken when designing a realistic VSP walk away survey to ensure enough stationary phase points without oversampling are captured in order to image the target of interest.

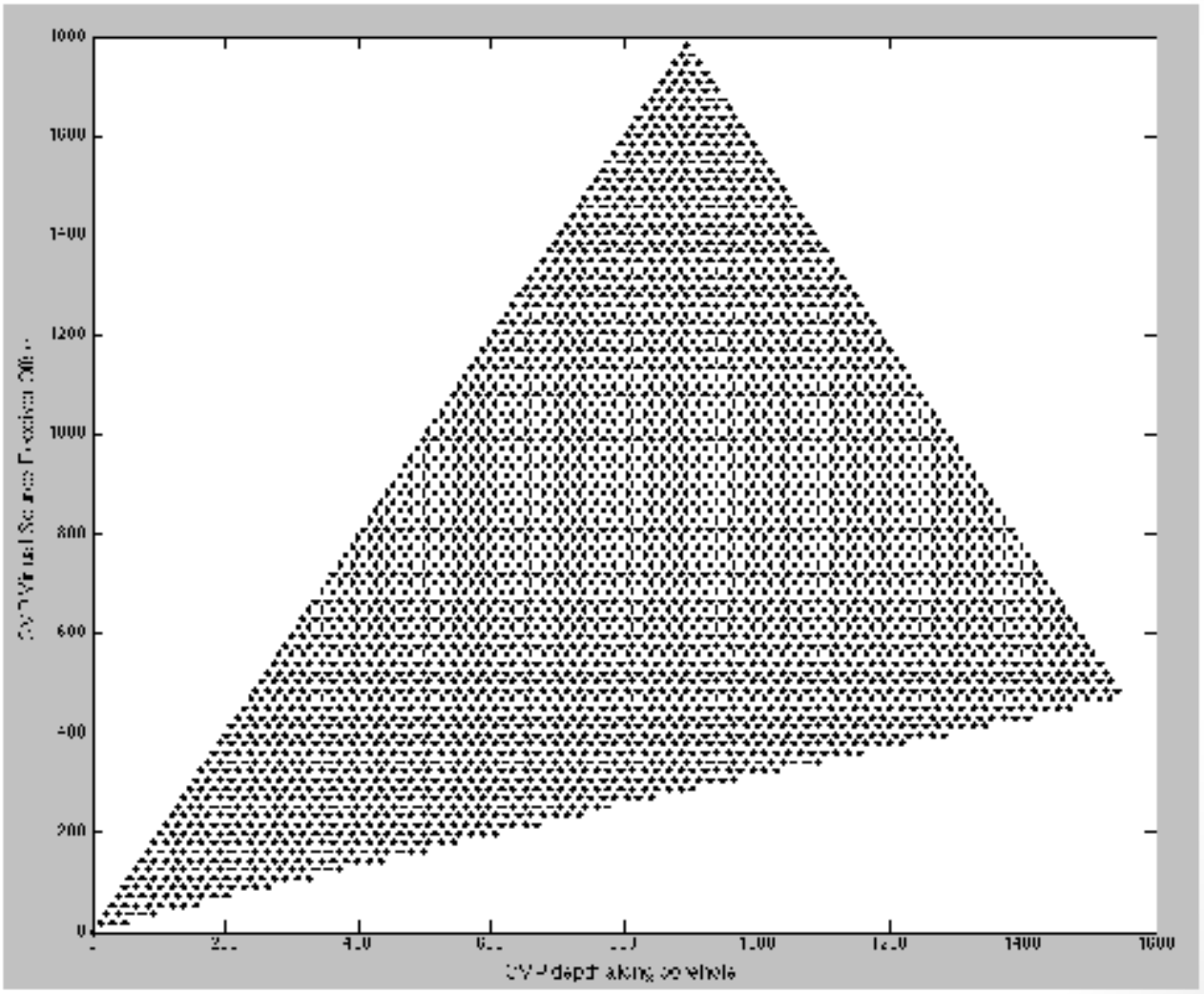

Figure 3.11 CMP depth along borehole vs. CMP virtual source-receiver offset for Model 1.

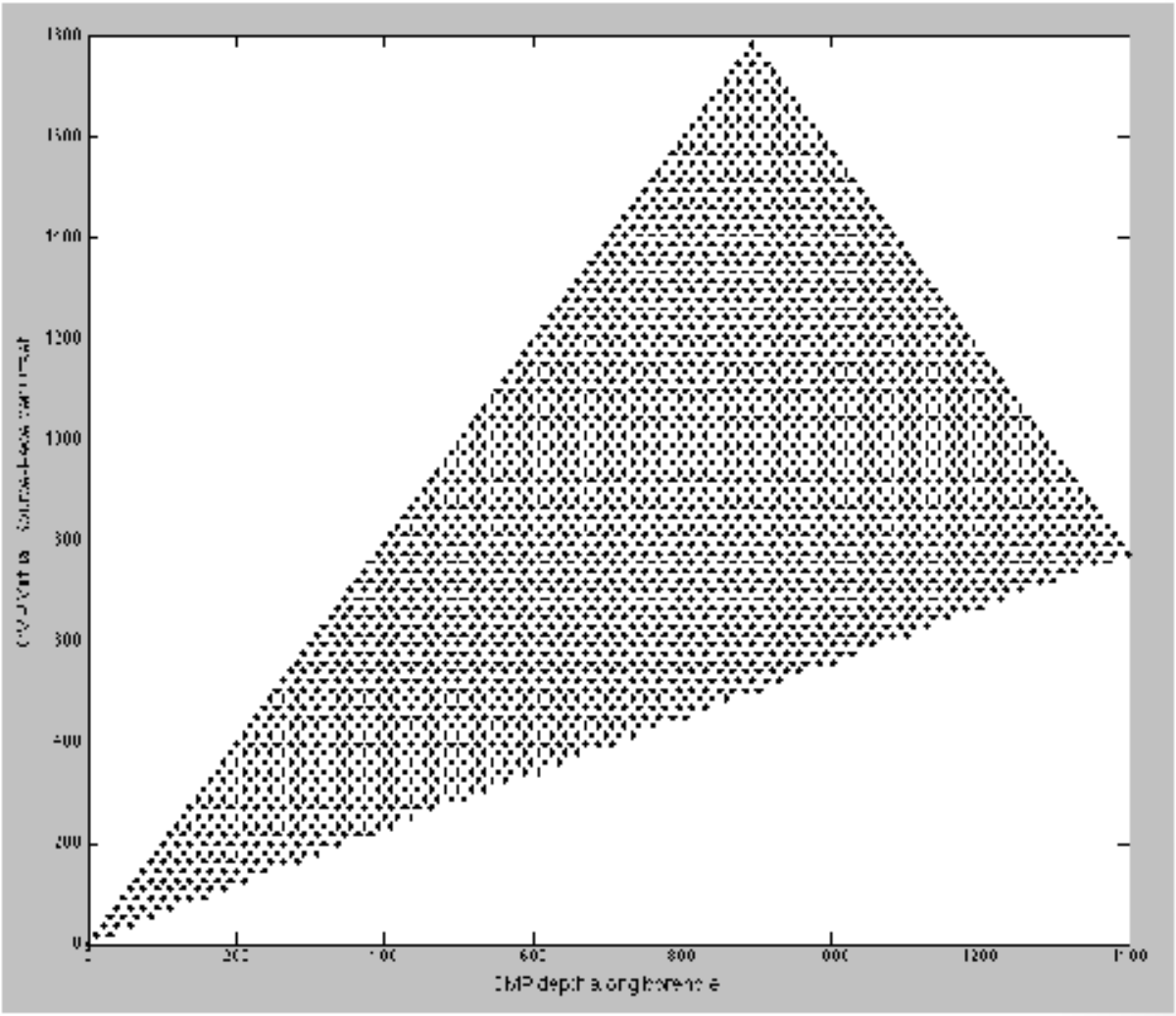

Figure 3.12 CMP depth along borehole vs. CMP virtual source-receiver offset for Model 3

Increasing the distance between the target and the borehole causes a dramatic decrease in the kinematically correct near offset virtual source – receiver pairs.

Chapter 4: Understanding the Capabilities of the Virtual Source Method

4.1 Introduction

Chapter 3 discussed the requirement for stationary phase events with sufficient coverage too properly image the subsurface in its kinematically correct location. In Chapter 3, and most of the research completed on the virtual source method has been carried out assuming a homogeneous environment (Brand and Hurich, 2012; Bakulin and Calvert, 2006). Since it is rare for real geology to be homogeneous, this chapter discusses the affects geologic heterogeneity has on imaging a target using the virtual source method. A number of heterogeneous models are studied to investigate the affects of scattering, and clarify how scattering may help or hinder the virtual source technique.

The first portion of the experiment uses 2D synthetic models to examine the results different heterogeneous parameters will have on a seismic wavefield. The heterogeneous models are created with realistic geological parameters by varying the velocity distributions and correlation lengths (L'Hereaux, 2005; and Holliger, 1996). A zero and 1000 m offset VSP survey are completed on each heterogeneous model, to study how differing forms of heterogeneity affect the nature of the scattered wavefield. The virtual source method is then applied on a reference model containing a vertically dipping target and a homogeneous country rock. The final portion of the experiment applies our previously gained knowledge of scattering fields and replaces the homogenous country

rock in the reference model with heterogeneous mediums. An analysis of all models using the virtual source gathers, pre-stack CMP virtual source gathers and the final stacked virtual source image is used to determine how heterogeneities change the imaging capabilities of the virtual source method.

4.2 Generating 2D Synthetic Data and Preprocessing

In order to create a seismic response for the synthetic models in Chapter 4, an already developed program that approximates the wave equation is used. The synthetic seismic data is calculated using a finite difference, acoustic solution of the wave equation, which is sufdmod2 in Seismic Unix terms (Brand and Hurich, 2012). The program uses a 2^{nd} order accurate acoustic finite difference algorithm to construct a numerical approximation of a wavefield. In addition, the finite difference algorithm accurately represents a VSP walk away survey with sources located on the surface and receivers in a vertically oriented borehole, in order to preform the virtual source method.

The 2^{nd} order finite difference algorithm creates low frequency numerical noise in each VSP shot gather (figure 4.1), which creates a problem during the cross-correlation stage of the virtual source method. A butterworth bandpass filter was applied to the data in order to remove the low frequency noise. A zero offset VSP survey with 300 receivers in the borehole was designed to determine the bandpass filter that best preserves the phase of the modeled wavelet for this synthetic modeling. A zero phase (figure 4.2) and minimum phase (figure 4.3) filter, with parameters of 10-20-100-160 were first applied to the data. Both filters removed the low frequency noise, but added reverberations to the

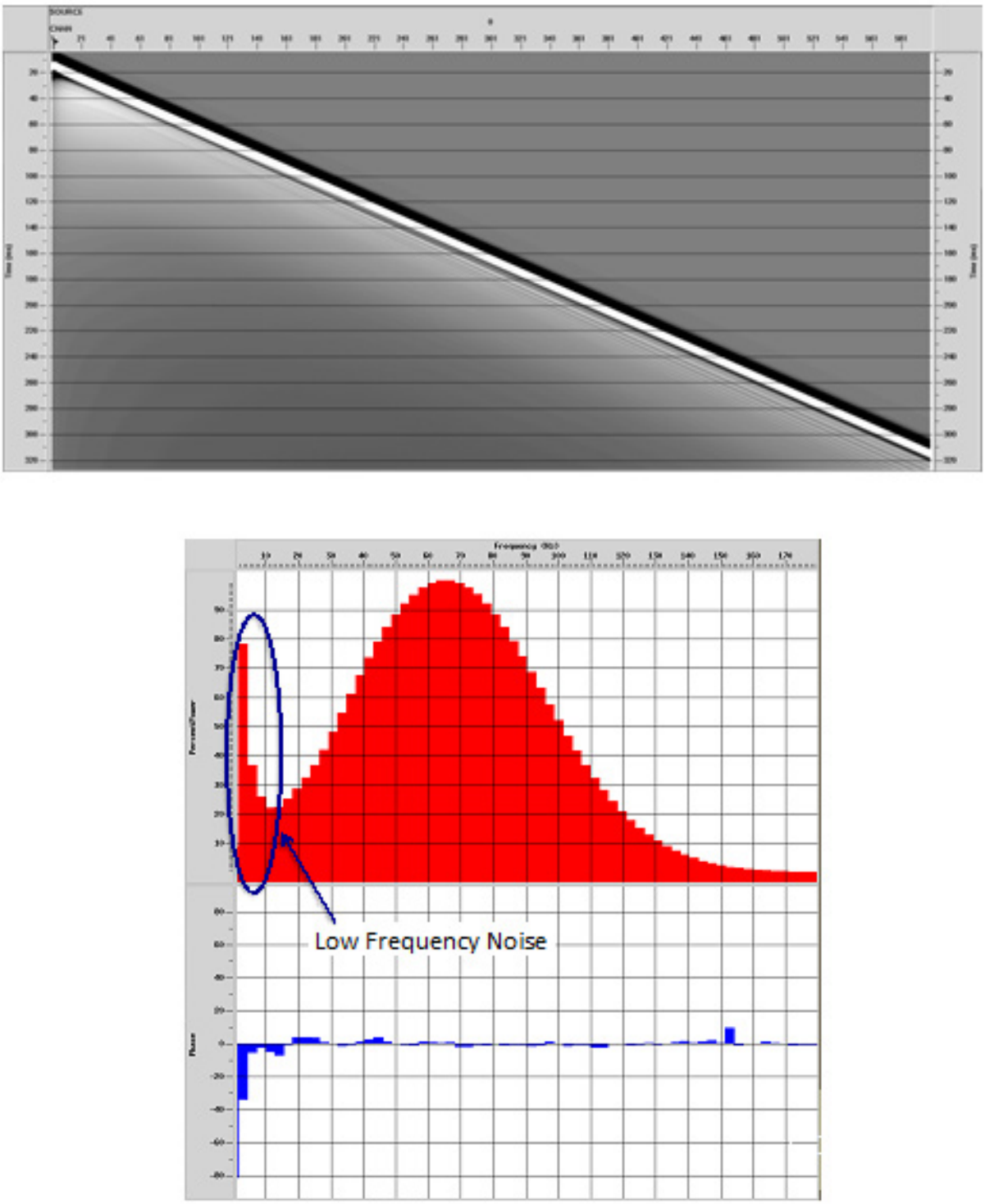

Figure 4.1 Spectral Analysis on the direct wave of a Zero Offset VSP survey

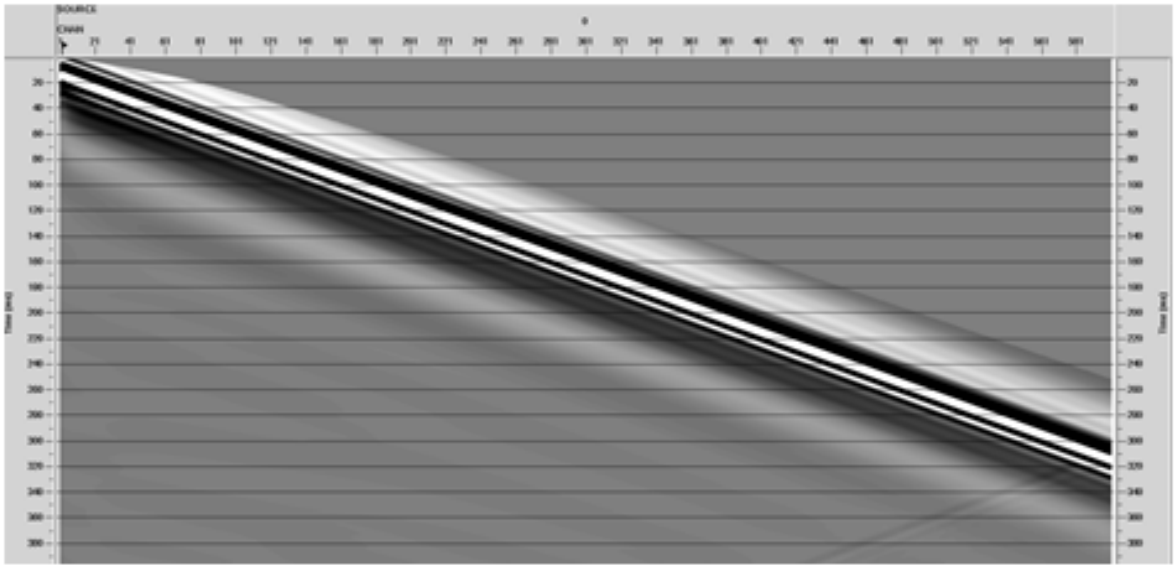

Figure 4.2 Zero Phase Bandpass Filter
A Zero Offset VSP shot gather with a zero phase bandpass filter applied. The bandpass filter has cut offs of 10-20-100-160 Hz.

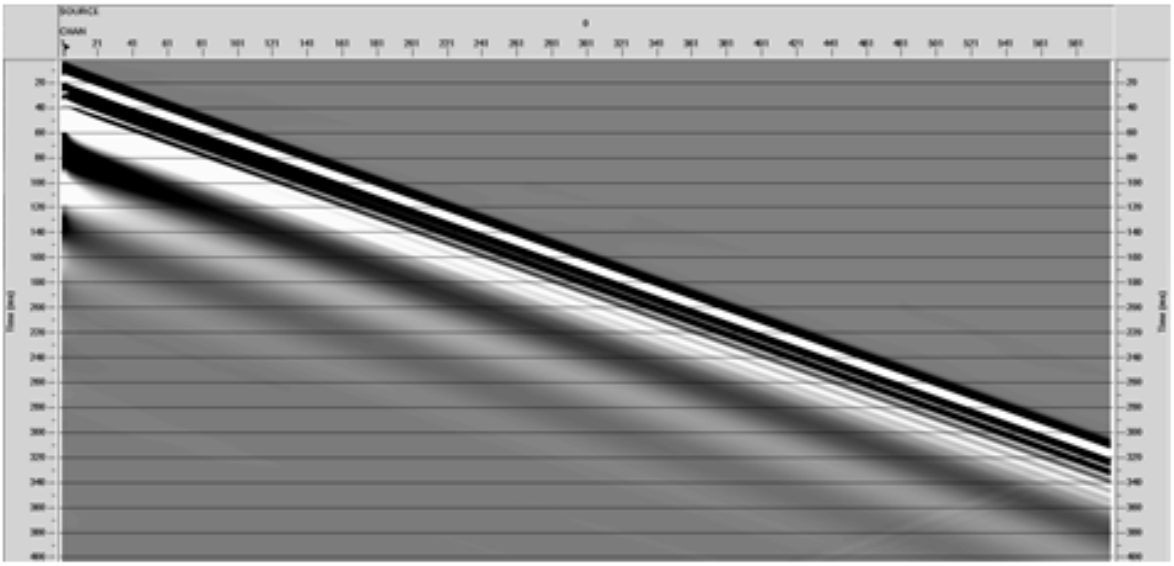

Figure 4.3 Minimum Phase Bandpass Filter
A Zero Offset VSP shot gather with a minimum phase bandpass filter applied. The bandpass filter has cut offs of 10-20-100-160 Hz.

data. However, the minimum phase filter only created reverberations after the first arrival of the direct wave (figure 4.3), which can be reduced by determining the proper cut-offs. An analysis of the amplitude spectrum from figure 4.1 concluded that the most appropriate filter cut-offs for the minimum phase butterworth bandpass filter were 5-20-100-200 (figure 4.4). These cut-offs allow for two full octaves on the low cut off and a full octave on the high cut off minimizing artifacts created when applying the bandpass filter.

Once a bandpass filter has been applied to the data it is necessary to demonstrate that the phase of the seismic wavelet is stable within the space of the synthetic models. To test the stability of the wavelet a spectral analysis was completed on the direct wave. Figure 4.5 displays the spectral analysis of a number of channels throughout the shot gather to see if the direct wave is stable. In the first five channels (figure 4.5 A) the amplitude of the direct wave decreases and the phase of the wavelet is fairly mixed, but in the further offset channels the amplitude of the direct wave is constant and phase of the wavelet is close to minimum phase (figure 4.5 B, C, D). So, after the first 5 to 10 channels the phase and amplitude spectrum is stable for the domain of the synthetic models created for this masters thesis.

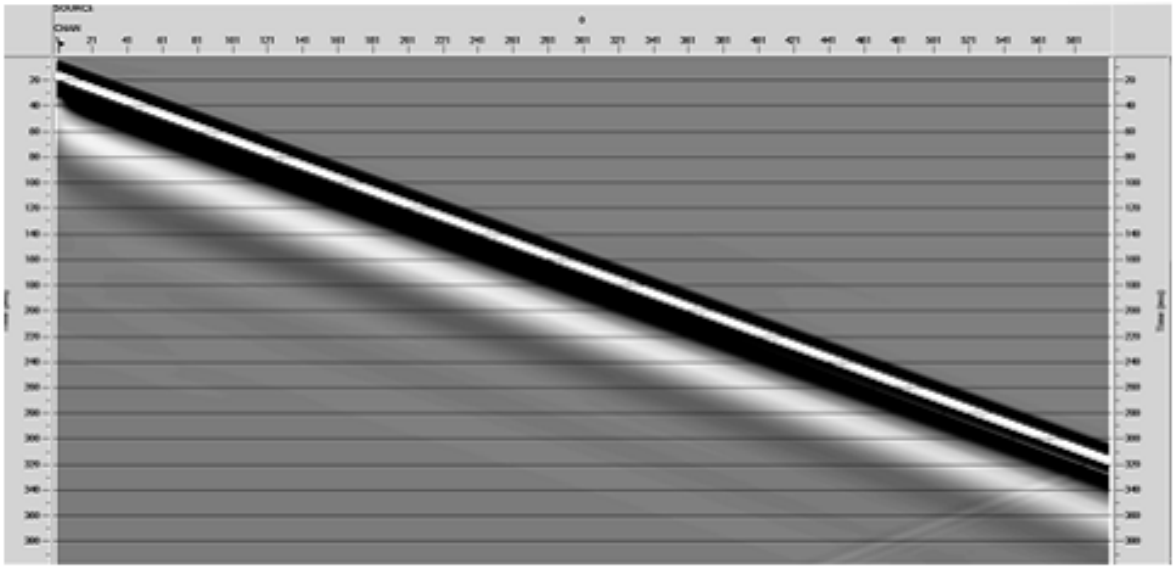

Figure 4.4 Optimized Bandpass Filter
Zero Offset VSP shot gather with a minimum phase bandpass filter applied. The bandpass filter has cut offs of 5-20-100-200 Hz.

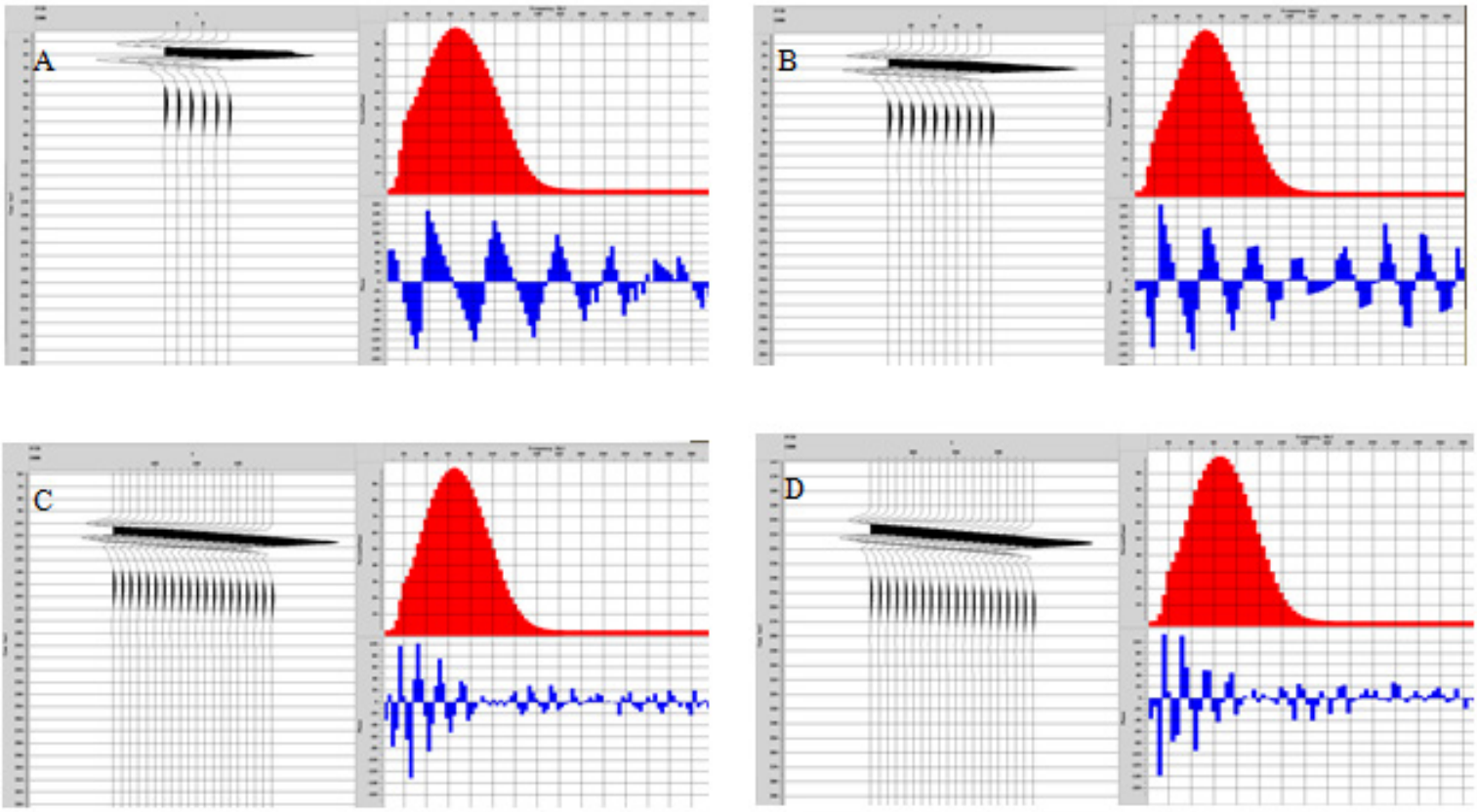

Figure 4.5 Testing Phase Stability
Spectral Analysis completed on the direct wave of a Zero Offset VSP with a minimum phase bandpass filter of 5-20-100-200 applied. (A) Spectral Analysis of Channels 0-5, (B) Spectral Analysis of Channels 20-30, (C) Spectral Analysis of Channels 180-200, (D) Spectral Analysis of Channels 380-400.

4.3 Analyzing Heterogeneous Fields

Geological heterogeneity is a term used to describe the variability of rocks in the subsurface. In seismic terms this relates to variations in velocity and density, as well as the spatial distribution between adjacent rocks. These values vary in different geological environments causing the scale of the heterogeneities in the subsurface to change significantly. To examine how the scale of heterogeneity will affect the scattered wavefields a series of randomly distributed fields, known as stochastic fields are generated. Each stochastic field has same starting point (seed) in the random numerical generator, in order to keep each experiment consistent. The rest of the heterogeneous field is populated from the same starting point by the random numerical generator within the constraints of the correlation coefficient and variability of velocities that are input into the program. A limitation of these stochastic fields is that they are in 2-D, but heterogeneity associated with scattering occurs in 3-D in the real world.

L'Hereaux (2005, 2006) and Holliger (1996) completed a statistical analysis on a number of hard rock environments around the world using sonic logs. They determined spatial distributions in the subsurface by calculating the correlation coefficient, while the variability of the velocities in adjacent rocks was calculated from the standard deviation of the sonic logs. An additional sonic log data was acquired from the Voisey's Bay mine in Labrador (table 4.1). The correlation length and standard deviations calculated from the sonic logs for each geological location, except for Voisey's bay where only the standard deviation was given (L'Hereaux, 2005, 2006; Holliger, 1996), gives an

indication of the values appropriate for simulating real geological conditions (table 4.1). Based on the data taken from L' Hereaux (2005, 2006) and Holliger (1996) (table 4.1), a zero and 1000 m offset VSP survey were created to evaluate different heterogeneous mediums. One important point to note, is that the sonic logs only give information about the heterogeneity in the direction of the borehole trajectory. Therefore, an assumption has been made in our experiments that the heterogeneity is the same in all directions. Commonly the heterogeneity varies in all directions, but due to lack of information this is another limiting factor in our experiment.

Location	Correlation Length (m)	Standard Deviation (m/s)
Leuggern	60	317
Bottstein	80	370
KTB	150	358
Stenburg	160	300
Sudbury	47	500
Abitibi	60	241
Cajon Pass	140	400
Voisey's Bay		1100

Table 4.1 A summary of the correlation length and standard deviation calculations conducted by L' Hereaux (2005, 2006) and Holliger (1996).

4.3.1 Continuous vs. Bimodal Velocity Distributions

Two end-member heterogeneous models are created to test the affect variations in the heterogeneity of the geology has on the seismic wavefield. The two heterogeneous models used in this research are a continuous velocity distribution and a bimodal velocity distribution. Both of these heterogeneous distributions are randomly generated in the synthetic model, with the addition of two components: (i) a fractal (power law) spatial distribution of velocity and density values that are superimposed onto (ii) Gaussian and bimodal distribution of velocity (Frankle and Clayton, 1986). The spatial distribution of the continuous and bimodal models are generated using a von Karman autocorrelation function, which creates a smoothly varying, fractal pattern of velocity values. The continuous distribution represents a smoothly varying geological environment and the bimodal distribution represents a geological environment with abrupt changes. The continuous distribution in our model uses a Gaussian velocity distribution with a range of approximately 5250-6750 m/s (figure 4.6) and a standard deviation of 200 m/s. These values were determined based on the velocity ranges seen in table 4.1. The bimodal distribution requires a two-end member velocity distribution (figure 4.7), with a velocity range of 5600 m/s - 6400 m/s, creating a reflection coefficient of 0.067. The reflection coefficient is a measurement of the velocity fluctuation in all the heterogeneous fields, because our models are assuming that density is constant. Both velocity distributions center on a mean velocity of approximately 6000 m/s.

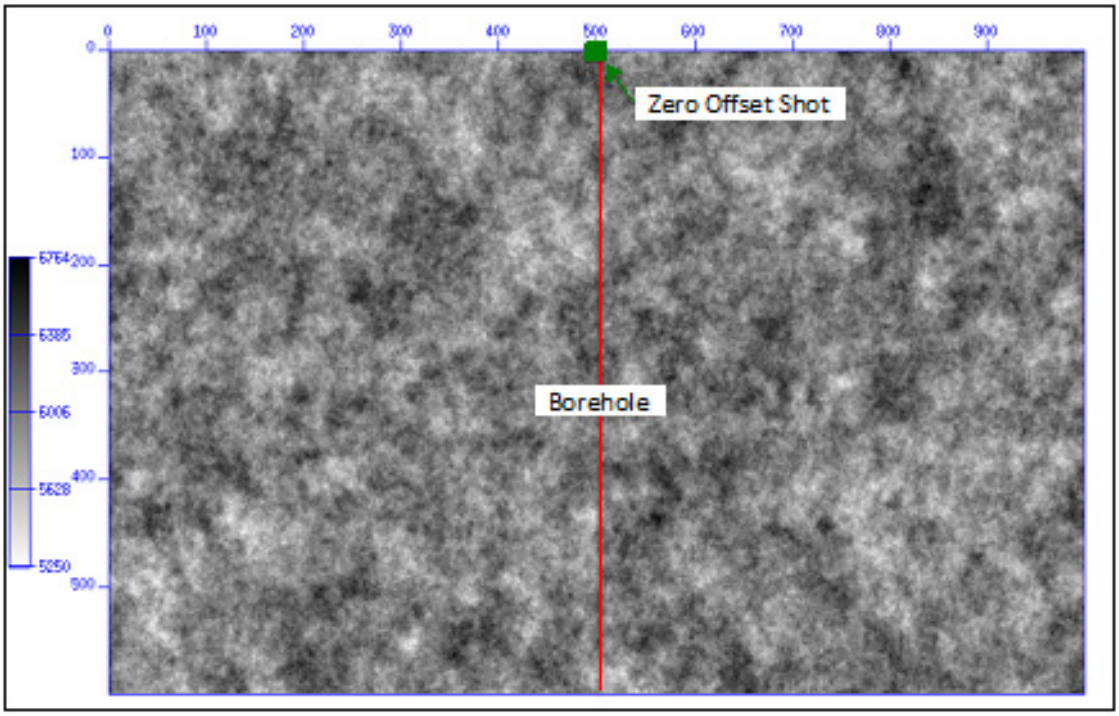

Figure 4.6 Continuous Velocity Distribution
A Continuous Velocity Distribution with a 60 m isotropic correlation length and a range of velocities between 5250-6750 m/s.

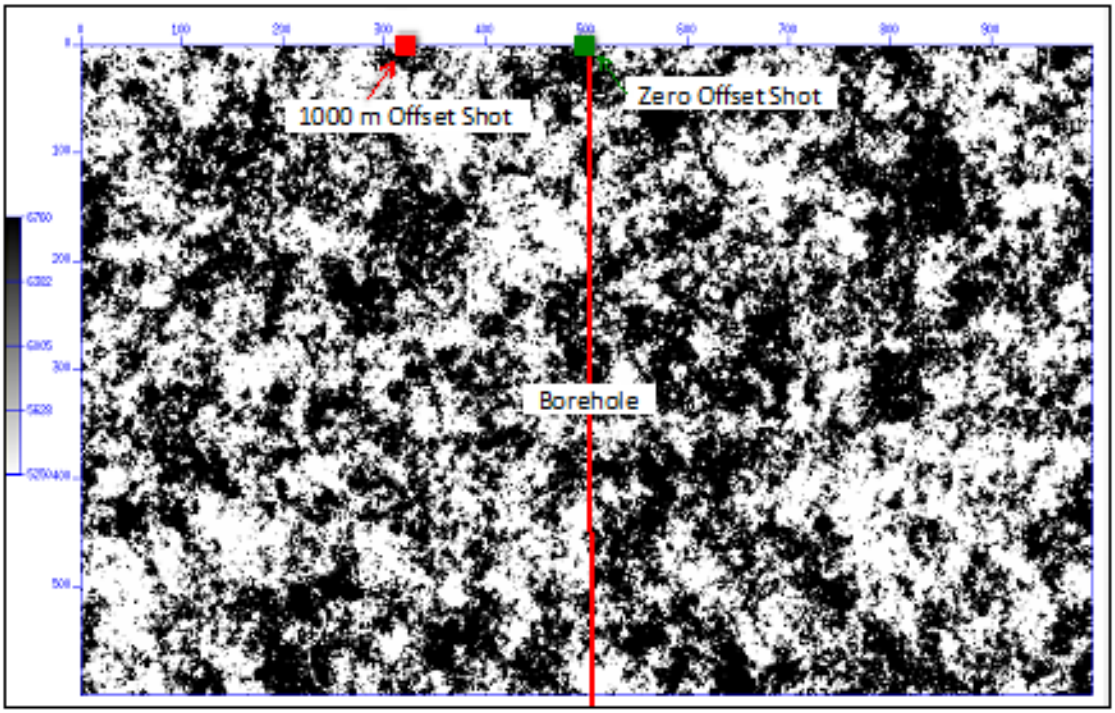

Figure 4.7 Bimodal Velocity Distribution
A Bimodal Velocity Distribution with a 60 m isotropic correlation length and two velocity end members (5600-6400 m/s) equally a reflection coefficient of 0.067.

To test the differences, continuous and bimodal distributions have on the scattered wavefield the correlation length is kept constant in the two models created for this section. Based on the sonic logs in the literature (L'Hereaux 2005, 2006; Holliger, 1996) and the frequency content of the synthetic model a correlation length of 60m would be a realistic and effective value for a heterogeneous environment. Due to lack of information the directionality of the correlation length is isotropic for both models.

The FK spectrum was used to examine how each heterogeneous field alters the seismic scattered wavefield. Analysis of this spectrum can be used to study the range of apparent velocities, and thus the angles of incidence recorded by the receiver array. The larger the spread of energy over the wavenumber domain gives a greater range of incidence angles. So, performing an FK analysis on a zero offset VSP survey helped to determine: i.) how much distortion occurs in the wave front and ii.) the angles of propagation of the direct wave plus trailing coda. The spectrum of energy in the frequency-wave number (FK) spectrum, seen in figure 4.8, 4.9 and 4.10, represents the range of apparent velocities associated with the scattered waves and the colour bar is an indication of the amplitude of the seismic waves. In the negative wavenumber domain the edge of the spectrum of energy is defined by the direct wave in the VSP survey as it represents the mean velocity of the medium (figure 4.11). In the FK and time-space (TX) domain it is clear that the scattered waves being produced by the bimodal distribution have stronger amplitudes than in the continuous distribution (figure 4.8 and 4.9). Another important point to note in the FK analysis is that the forward scattered waves (those in the negative K domain) are recorded at a number of different apparent velocities

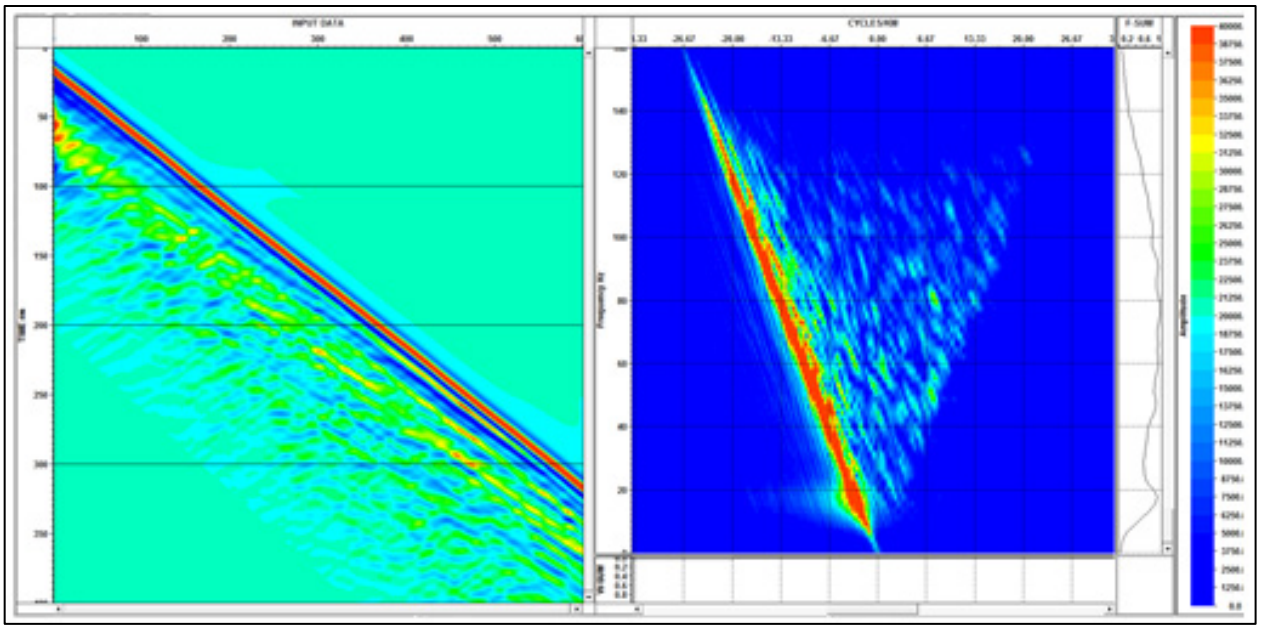

Figure 4.8 The FK spectrum of a Zero Offset VSP in an isotropic continuous heterogeneous velocity field with a correlation length of 60 m and a RMS of 3%
The cone of energy in the FK domain represents the apparent velocity range of the direct wave and trailing coda.

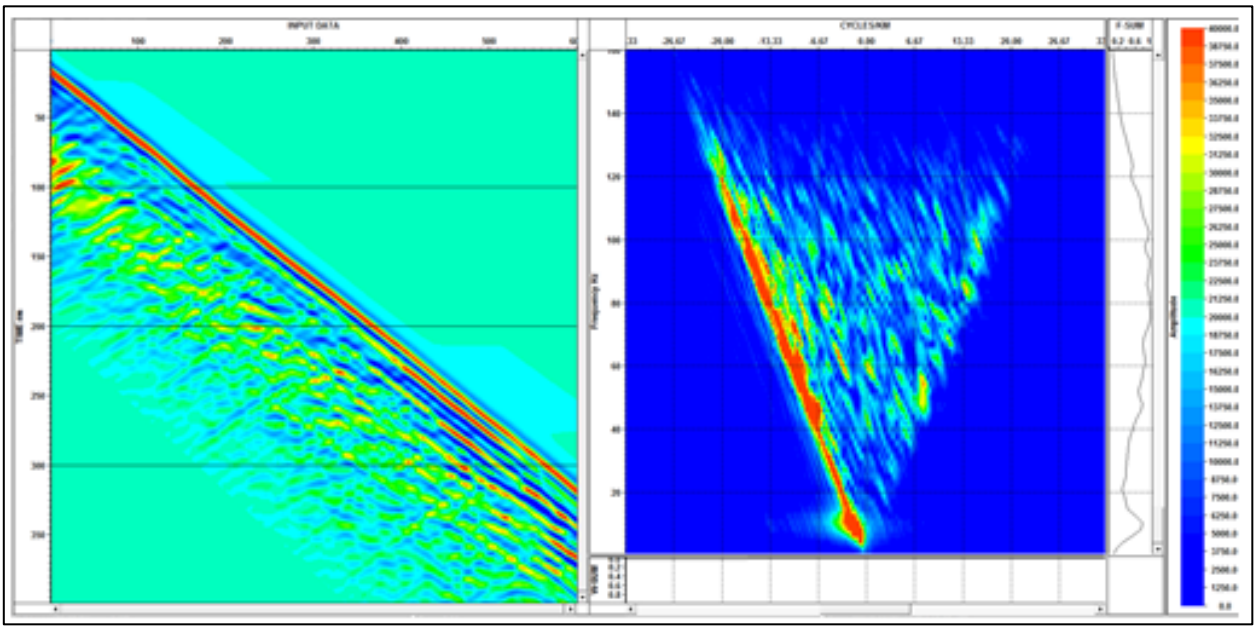

Figure 4.9 The FK spectrum of a Zero Offset VSP completed in a heterogeneous field with a correlation length of 60 m and a reflection coefficient of 0.067.

with strong amplitudes in the bimodal velocity distribution (figure 4.9). The range of apparent velocities in the FK spectrum is attributed to an increase in the travel angles of the scattered wavefield. Since more energy is partitioned from the direct wave to scattered waves, which travel with increased angles, the chance to produce stationary phase rays when applying the virtual source method will improve.

A 1000 m offset VSP survey was also examined on the bimodal heterogeneous model, to assess the affect the heterogeneous field has on the scattered wave at longer offsets. The scattered waves fronts in the Offset VSP (figure 4.10) are more distorted and have higher amplitudes than the zero offset VSP (figure 4.8). Since it is the same heterogeneous field (with no directional bias) and survey design, the amplitude increase of the coda can be attributed to the length the seismic waves have traveled through the heterogeneous medium. This is another important observation, because the further offset VSP shots have more energy distributed to the scattered wavefield, thus increasing the amount of illumination angles on a target.

4.3.2 Correlation Lengths

The data in table 4.1 (L'Hereaux 2005, 2006; Holliger, 1996) indicates that there is a wide range of correlation lengths for different geological environments. To evaluate the influence correlation lengths have on a scattered wavefield, three isotropic heterogeneous fields were created. The size of each correlation length was chosen based on the ranges of correlation lengths observed in the literature. The size of the correlation

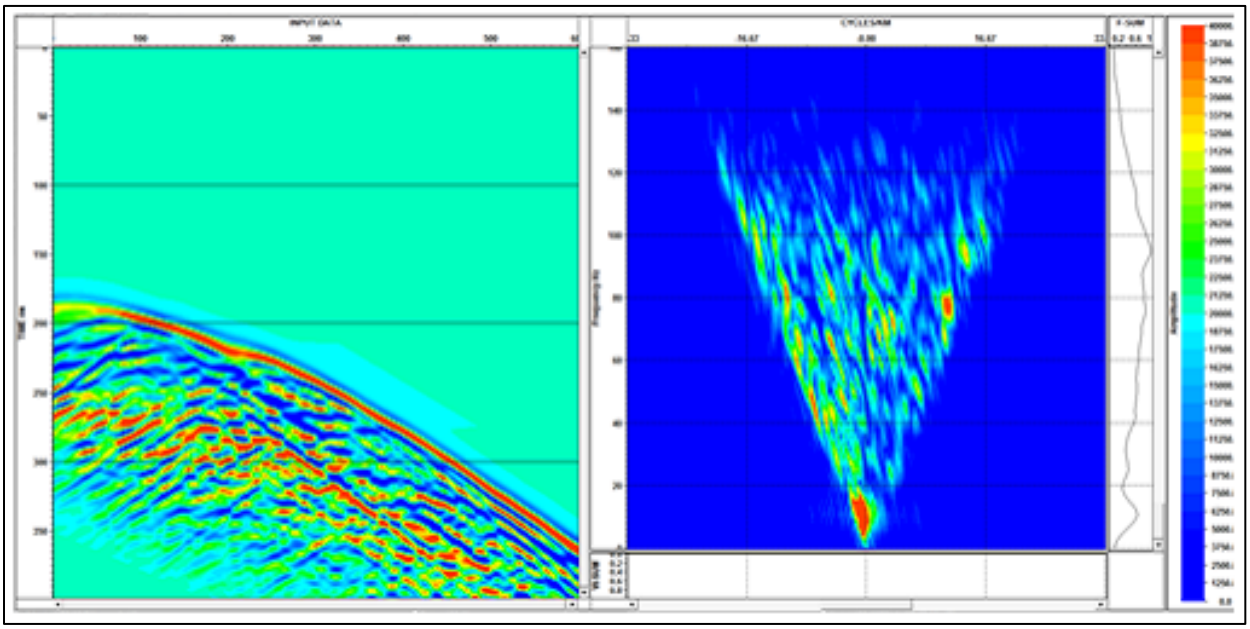

Figure 4.10 The FK spectrum of a 1000 m Offset VSP in a heterogeneous field with a correlation length of 60 m and a reflection coefficient of 0.067
Most of the energy from the direct wave is partitioned to the scattered wavefield.

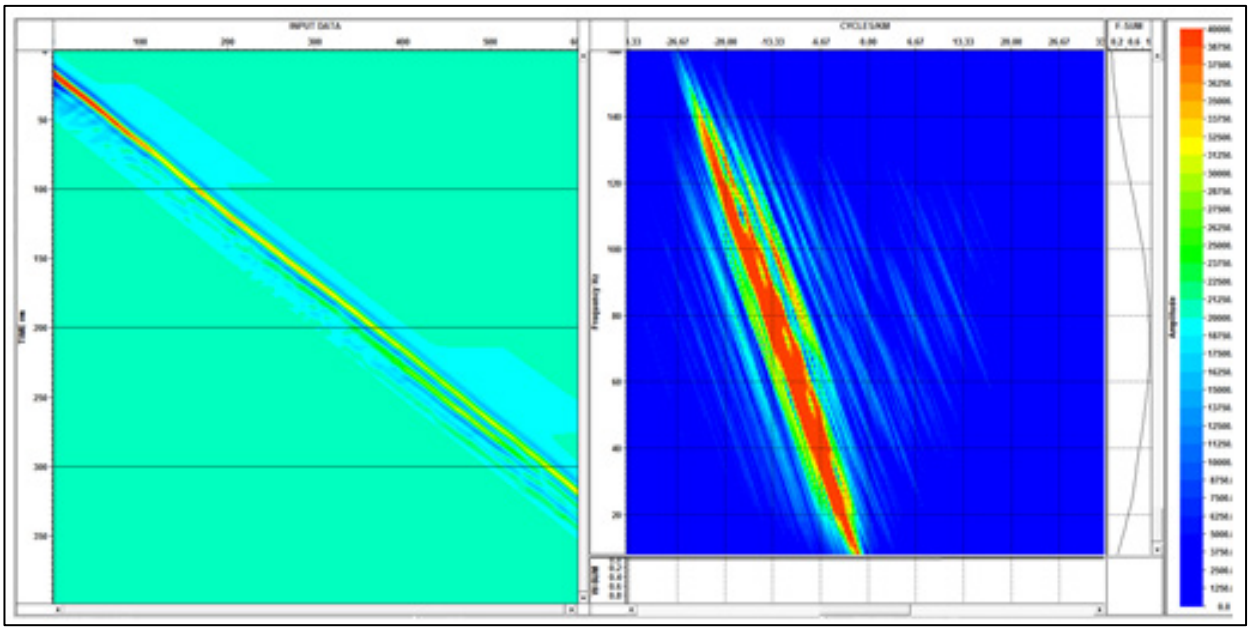

Figure 4.11 The FK spectrum of the direct wavefield.

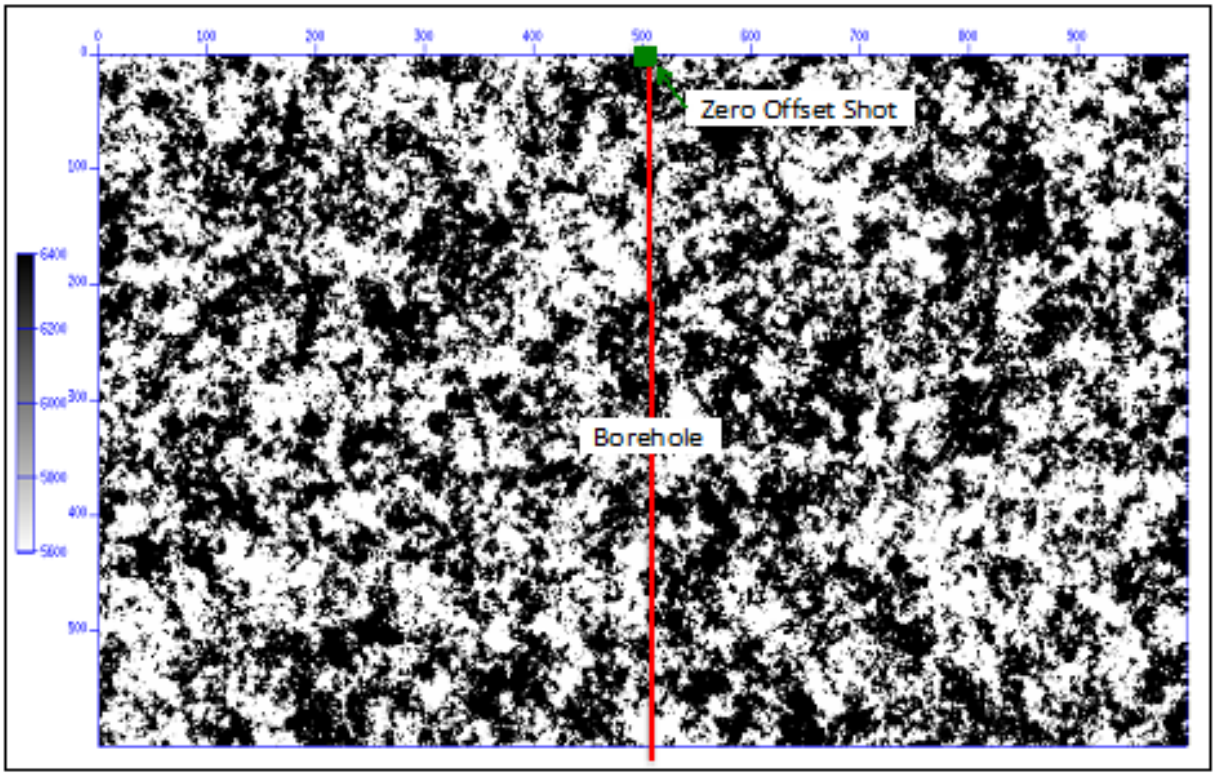

Figure 4.12 A Bimodal Velocity Distribution with an isotropic correlation length of 30 m and a reflection coefficient of 0.067.

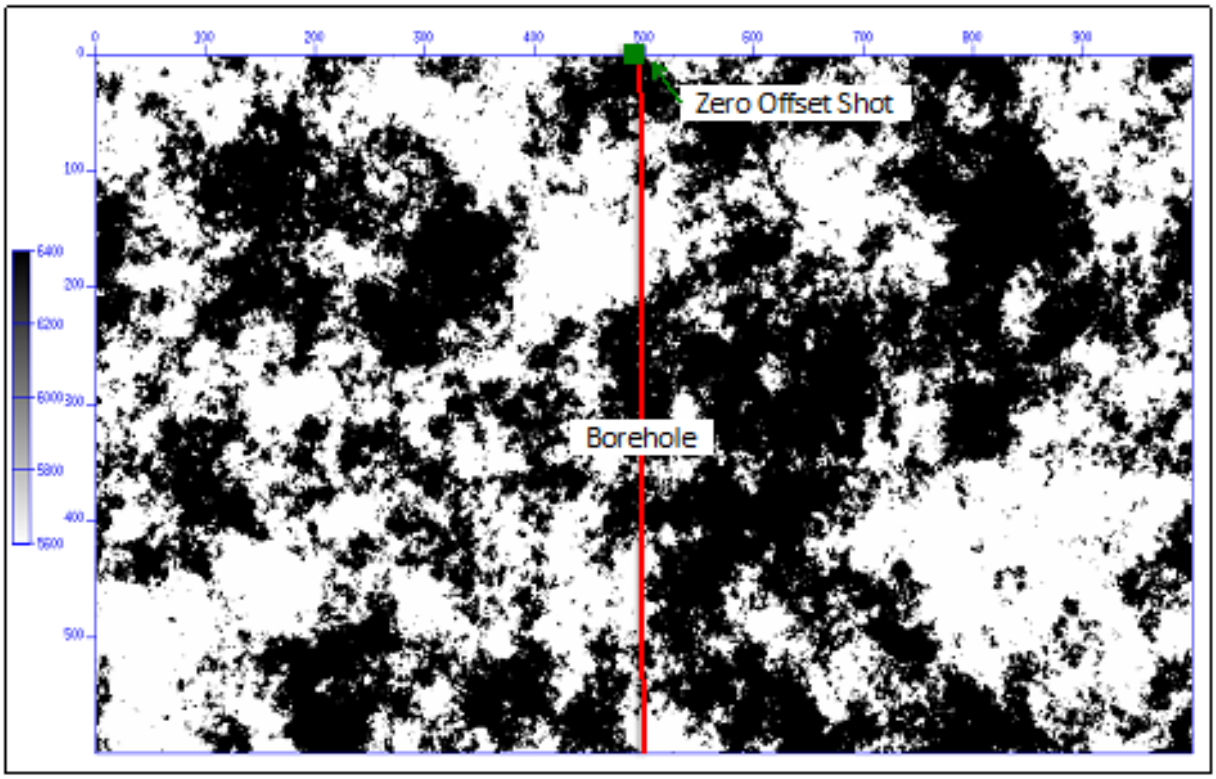

Figure 4.13 A Bimodal Velocity Distribution with an isotropic correlation length of 150 m and a reflection coefficient of 0.067.

length's were: 30 m (figure 4.12), 60 m (figure 4.7) and 150 m (figure 4.13). Each model has a mean velocity of 6000 m/s and a bimodal velocity fluctuation, which gives a reflection coefficient of 0.067 for each model.

The FK spectrum provides an estimate of the average amplitude of the scattered wavefields created by the three different heterogeneous velocity fields. The FK spectrum used the same parameters as the evaluation of the continuous versus bimodal velocity distribution to make these observations. Figure 4.14, 4.15, and 4.16 represent the FK spectrums with the correlation lengths of 30 m, 60 m and 150 m respectively. The strength of the codas amplitude is best exemplified in the TX domain, where overall the strongest amplitudes are seen when the correlation length is 60 m (figure 4.15). A correlation length of 60 m is well within the geological parameters seen in table 4.1 and is close to the dominant wavelength, which gives an end member (strongest scattering) result, thus creating the greatest chance of increasing the angles of illumination on the target.

4.3.3 Reflection Coefficients

Testing different reflection coefficients is the next step in optimizing the illumination angles created by the scattered wavefield. Bimodal velocity distributions with three different reflection coefficients were used in this section to understand the most fit for purpose distribution to increase illumination angles. Utilizing standard deviations from the sonic logs seen in table 4.1 (L' Hereaux, 2005, 2006; Holliger, 1996),

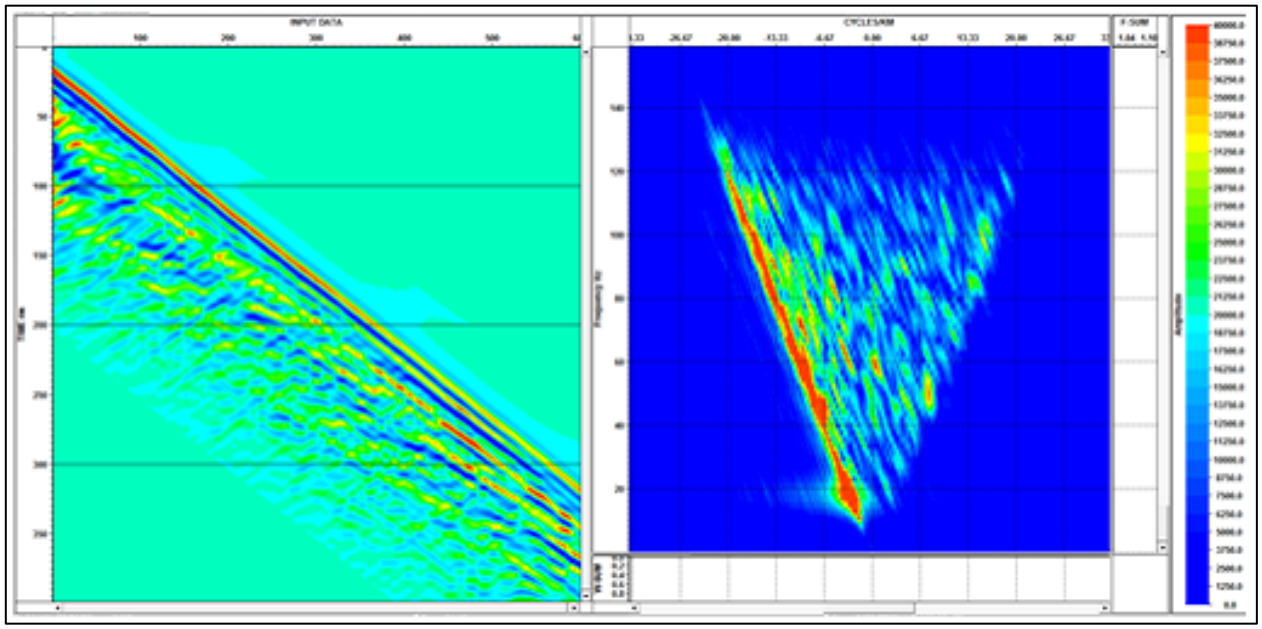

Figure 4.14 The FK Spectrum of a Zero Offset VSP in a heterogeneous field with a correlation length of 30 m and a reflection coefficient of 0.067.

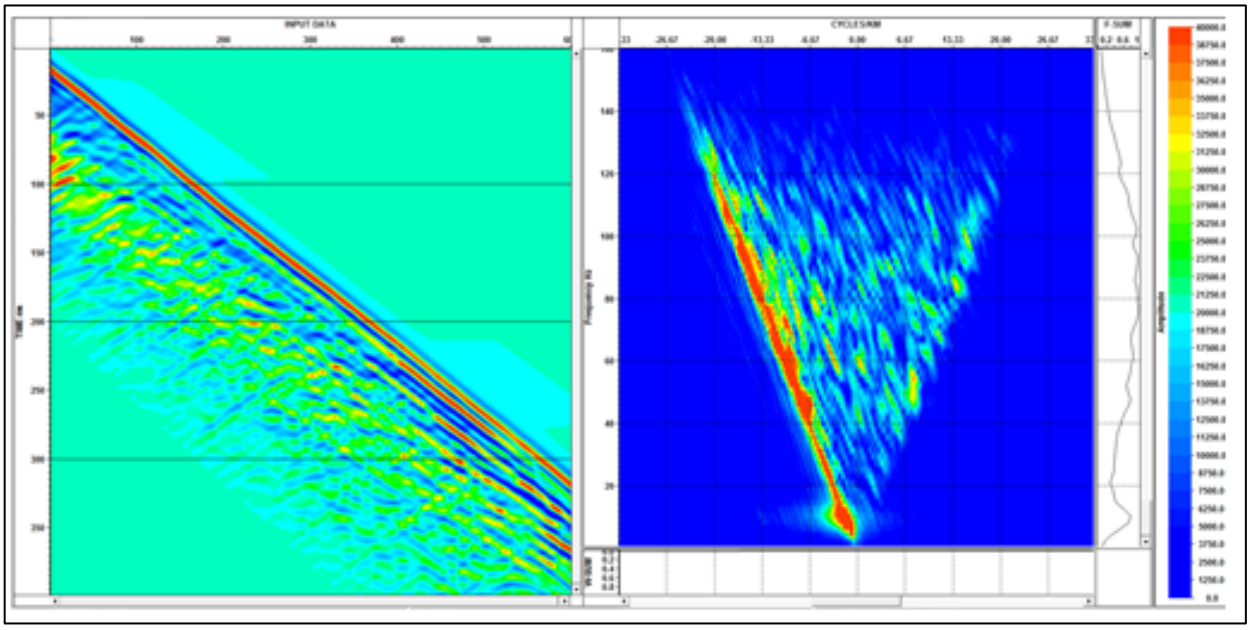

Figure 4.15 The FK spectrum of a Zero Offset VSP completed in a heterogeneous field with a correlation length of 60 m and a reflection coefficient of 0.067.

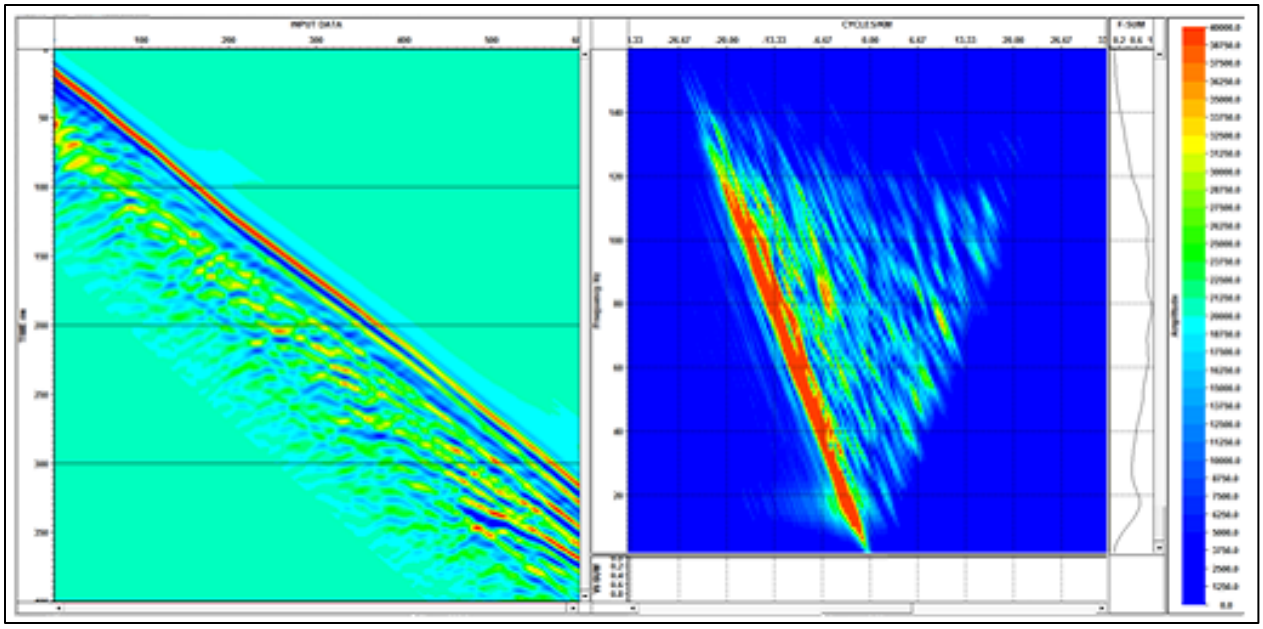

Figure 4.16 The FK spectrum of a Zero Offset VSP in a heterogeneous field with a correlation length of 150 m and a reflection coefficient of 0.067.

three reflection coefficients were calculated based on a mean velocity of 6000 m/s (0.1, 0.067 and 0.033). Using the results of the two previous sections all three models had a bimodal velocity distribution and an isotropic correlation length of 60 m.

A zero offset VSP survey is completed on each model so that an FK analysis will highlight the amplitudes of the apparent velocities (figure 4.17, 4.15, 4.18). It is clear that the range of apparent velocities in the forward propagating wave field has the largest amplitudes when the reflection coefficient is 0.1 (figure 4,17), and the model with a reflection coefficient of 0.033 (figure 4.18) has the weakest amplitudes. This result is expected, because as the reflection coefficient decreases so does the impedance contrast of the heterogeneous medium. It is noted that a reflection coefficient of 0.1 is on the outer limits of what is realistic for a geological environment. However, a reflection

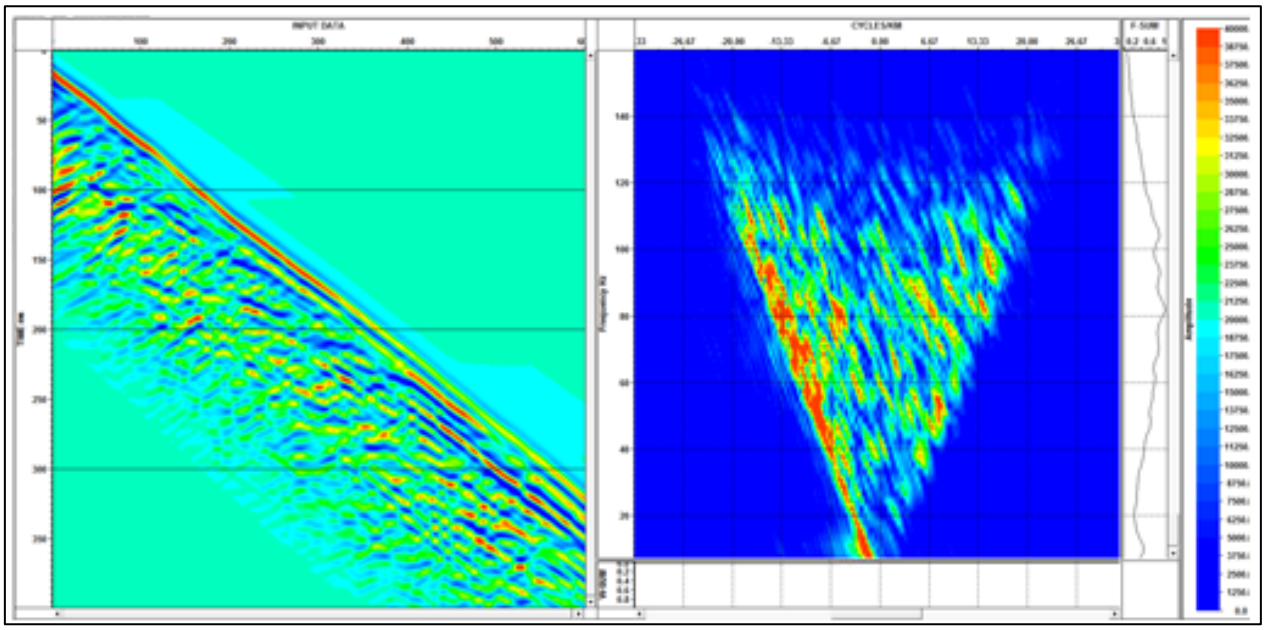

Figure 4.17 Zero Offset VSP in a heterogeneous field with a correlation length of 60 m and a reflection coefficient of 0.1.

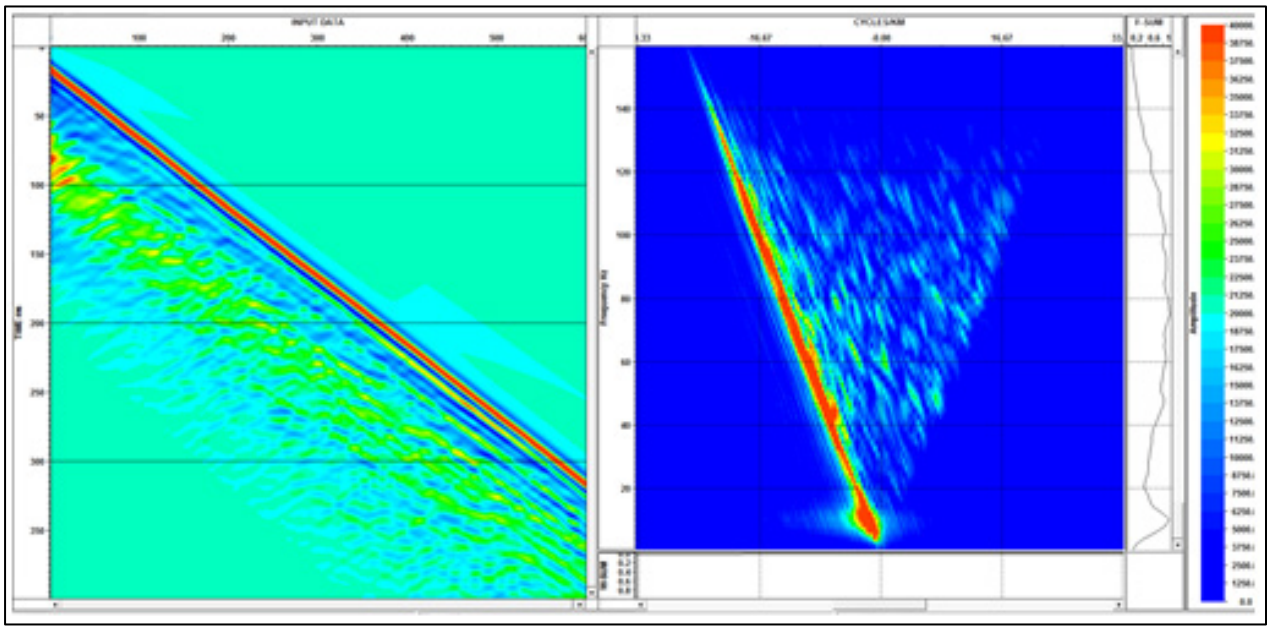

Figure 4.18 Zero Offset VSP in a heterogeneous field with a correlation length of 60 m and a reflection coefficient of 0.033.

coefficient of 0.067 is well within the range of a realistic velocity distribution (table 4.1), and produces significant scattering of the seismic waves (figure 4.15).

4.3.4 Anisotropic Scattering

Many geological environments have correlation lengths greater in one direction than the other. For example, siliciclastic sedimentary deposits often alternate between sandstone and mudstone beds, as well as mineral rich environments can differ between felsic and mafic rocks. Both of these geological environments have anisotropic correlation lengths with a longer correlation length in the plane of bedding/foliation. To simulate these geological scenarios two different end-member anisotropic models were created: one simulating horizontally oriented beds/foliations (figure 4.19) and the other representing vertically dipping beds (figure 4.20). To create an anisotropic model for the horizontal case a 300 m correlation length was used in the X direction and a 60 m correlation length was used in the Z direction. The two correlation lengths were reversed for the vertically dipping case. The two models used a bimodal velocity distribution with a reflection coefficient of 0.067, which is consistent with research noted in earlier sections of this master's thesis.

Similar to the previous sections a zero offset VSP survey was conducted on both models. An FK analysis was then performed on each survey to evaluate the power and nature of the scattered wave field. Although the amplitude of the scattered waves is similar between the vertically dipping and horizontally oriented case, the range of angles

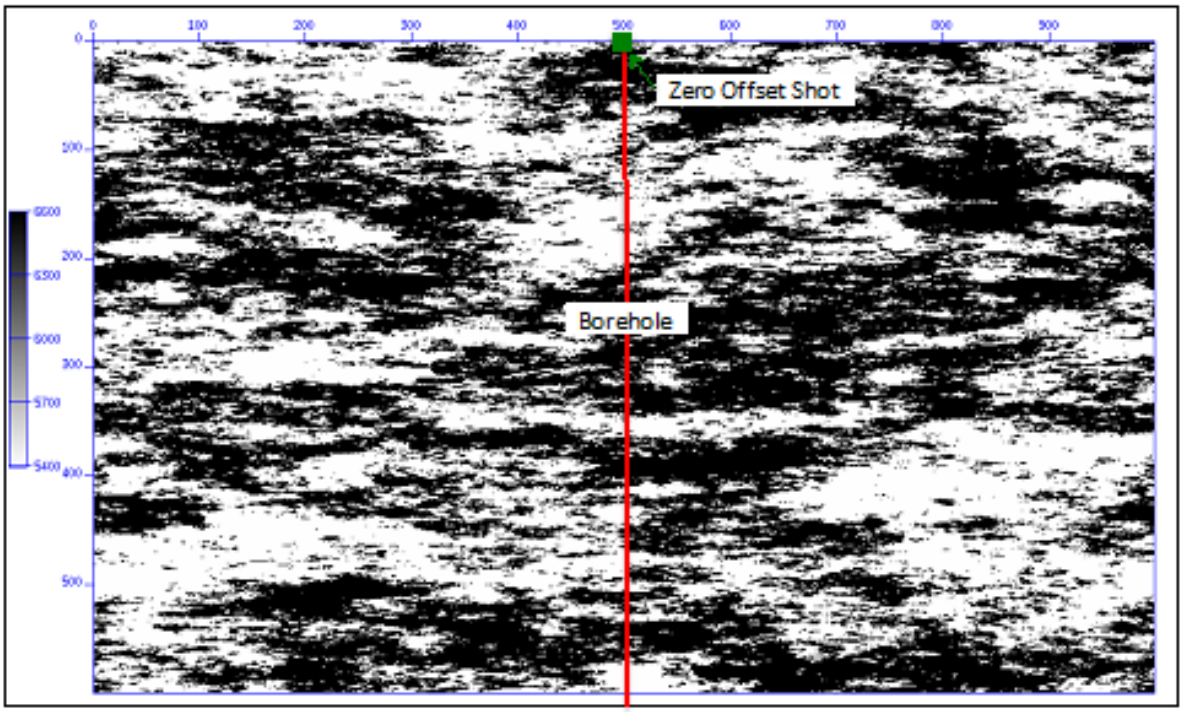

Figure 4.19 Horizontally Dipping Bimodal Velocity Model
300 m X correlation length, **60 m** Z correlation length and **0.067** reflection coefficient.

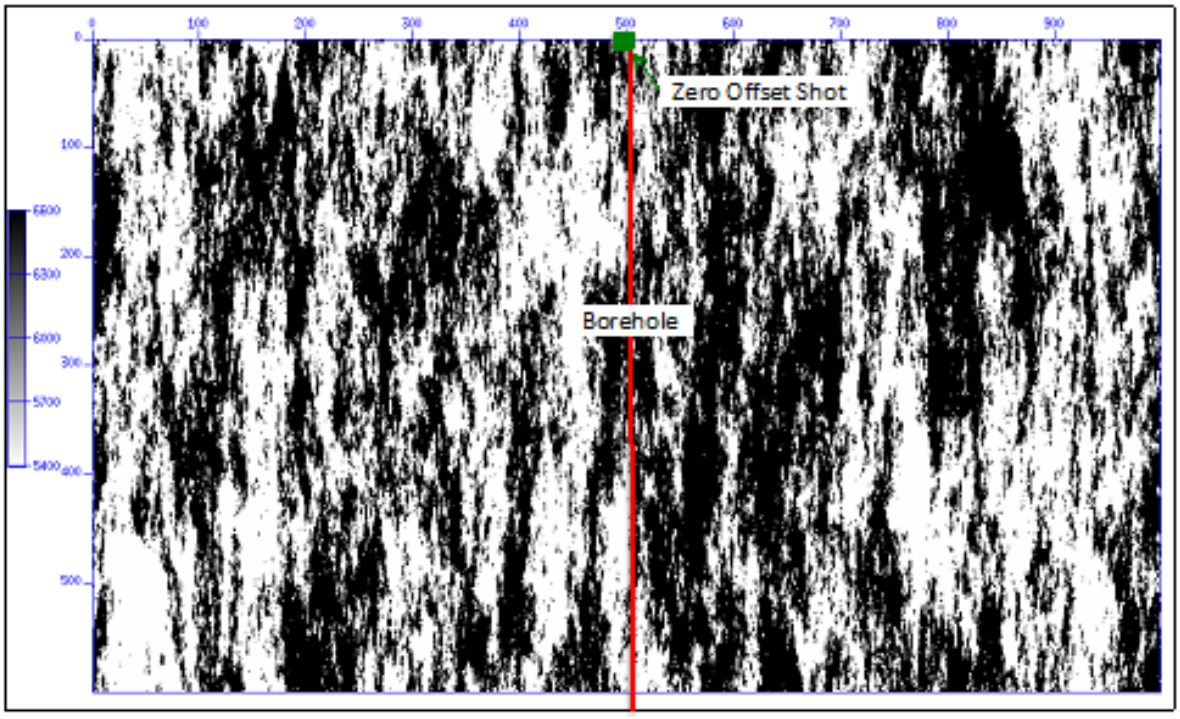

Figure 4.20 Vertically Dipping Bimodal Velocity Model
60 m X correlation length, **300 m** Z correlation length and **0.067** reflection coefficient.

are different. The FK spectrum of the horizontal case produces high amplitudes in the positive wavenumber domain, opposite to the direct wave (figure 4.21), which represents upgoing waves. The apparent velocities of the upgoing waves are very similar to the velocities of the direct wave. In figure 4.22 the FK analysis performed on the vertically dipping case, which demonstrates that the larger amplitudes from the scattered wavefield are contained within the negative wavenumber domain, representing the downgoing wavefield. These downgoing-scattered waves are recorded with a number of apparent velocities (figure 4.22), meaning the range of illumination angles created by the heterogeneities has increased. These increased travel angles of the scattered wavefield are seen within the first 300 receivers (figure 4.23 A), but the scattered wavefield records similar travel angles to the direct wave in the last 300 receivers (figure 4.23 B). Since the shot location is at zero offset with respect to the borehole, some of the ray paths that are recorded by the shallow receivers have high angles with respect to the vertically layering, while the deeper receivers record ray paths that are closer to parallel to the vertical layering (figure 4.24). Which results in the down-going wave front providing high angle ray paths at the shallower receivers because the point source has not spread much. By the time the down-going wave front reaches the deeper receivers it has spread considerably, so that the wave front is starting to approximate a plane wave for the deeper receivers and thus not able to record increased illumination angles.

The results for the horizontally and vertically dipping models have interesting implications on the benefits of the scattered wavefield when processing data via the virtual source method. The horizontally oriented layers (figure 4.19) display coherence

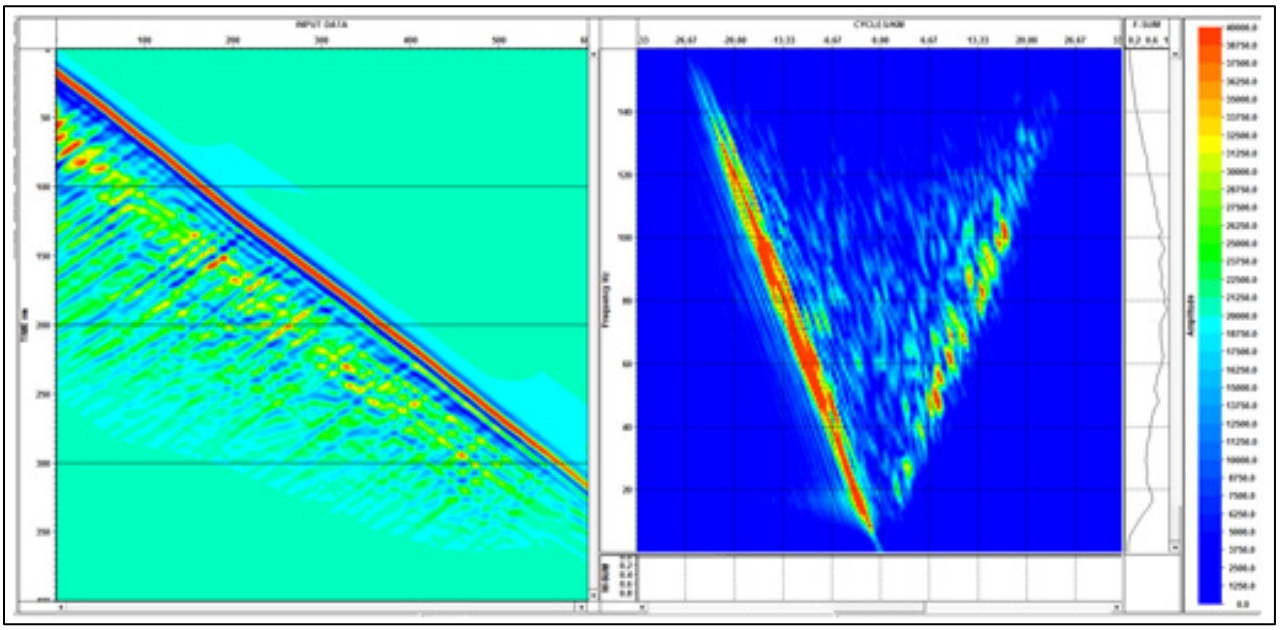

Figure 4.21 FK analysis of a zero offset VSP of a horizontally dipping velocity model (figure 4.19): 300 m X correlation length, 60 m Z correlation length and a 0.067 reflection coefficient.

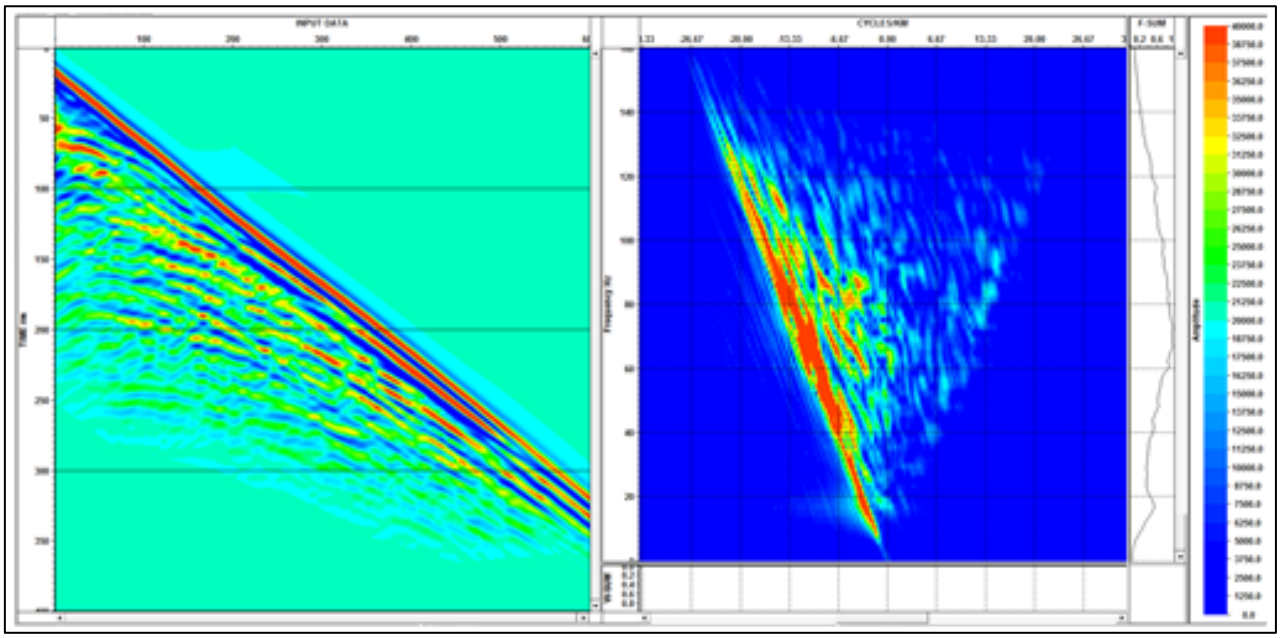

Figure 4.22 FK analysis of a zero offset VSP of a vertically dipping velocity model (figure 4.20): 60 m X correlation length, 300 m Z correlation length and a 0.067 reflection coefficient.

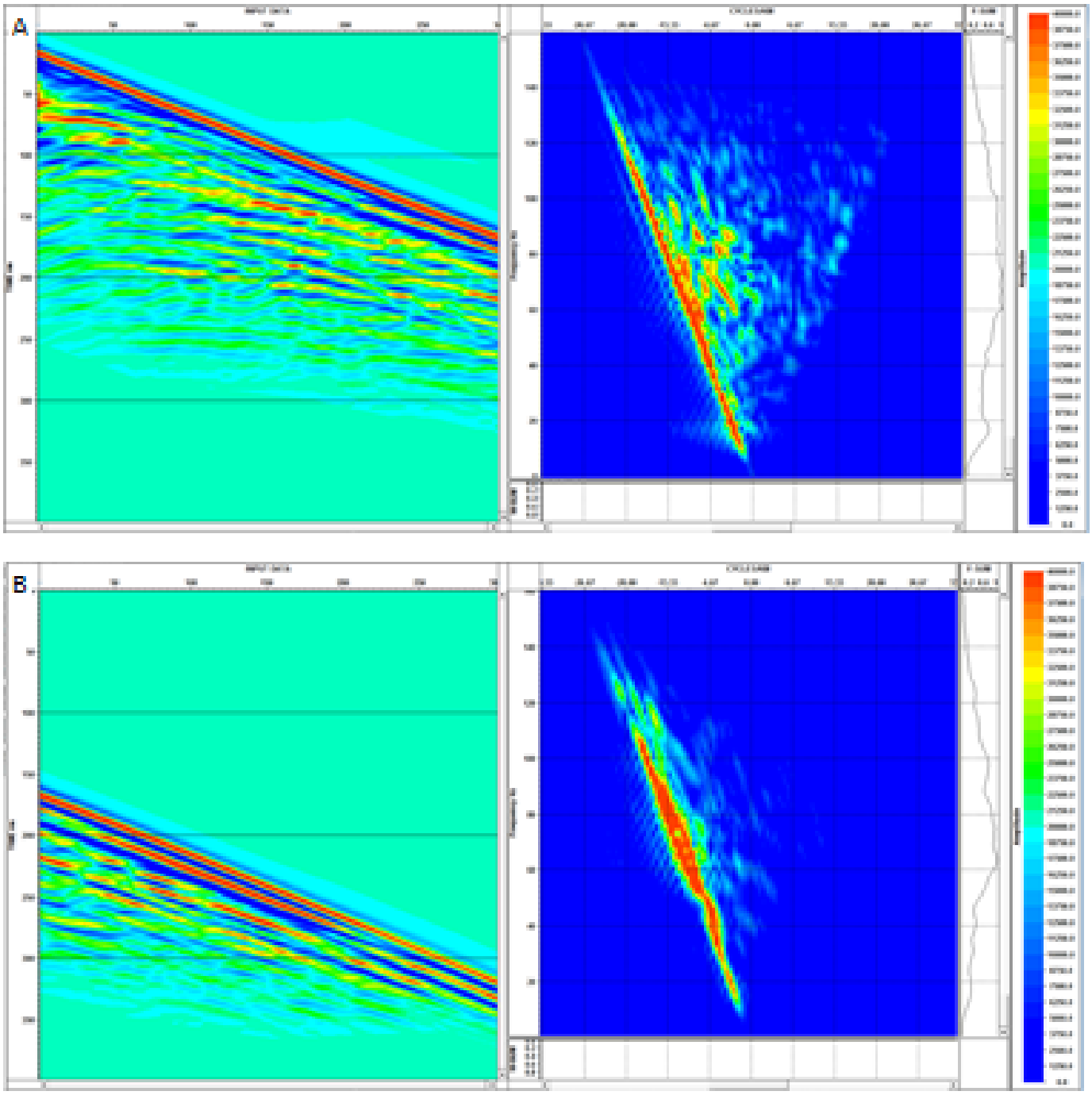

Figure 4.23 FK analysis of a zero offset VSP on a vertically dipping velocity model (A) FK analysis of the seismic data recorded by the shallowest 300 receivers in the borehole and (B) is the FK analysis of the seismic data recorded by the deepest 300 receivers in the borehole.

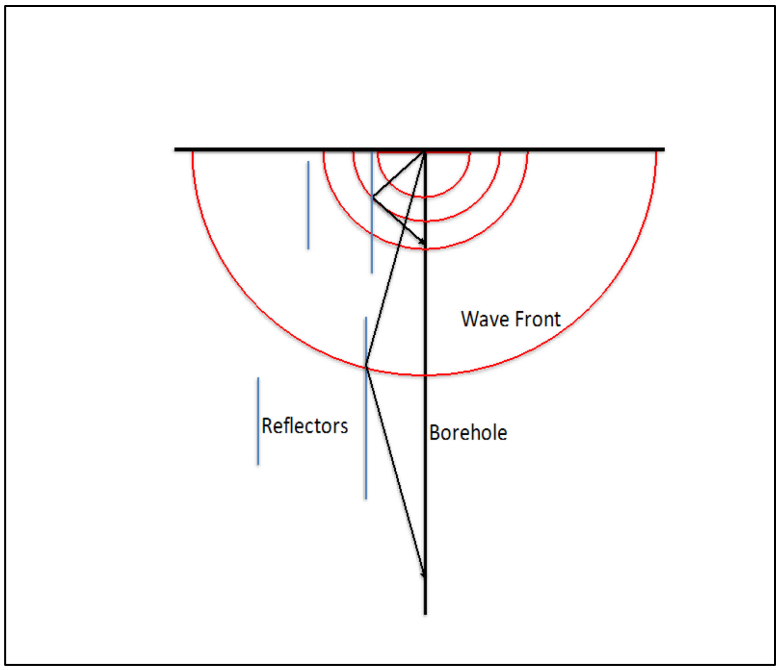

Figure 4.24 Simplistic Diagram of Vertically Dipping Reflectors

in the scattered upgoing wave field seen in the FK spectrum (figure 4.21). This indicates that the upgoing-scattered wave might increase kinematically correct virtual source – receiver pairs with receivers shallower in the borehole than the virtual source. However, when the beds within our model are dipping vertically the shallower receivers in the borehole primarily record the increased illumination angles from the scattered wavefield (figure 4.22). So, the largest difference between the two models is the amount of energy partitioned from the direct wave to upgoing-scattered waves with horizontally oriented layers compared with vertical layers. The upgoing-scattered waves are so prevalent, because the reflections from the horizontal orientation of the beds/foliations will create upgoing waves that can be recorded by receivers due to the geometry of the VSP survey, where as the reflections from vertical layers will still be recorded as downgoing-scattered waves. However, both end-member anisotropic models displayed that the scattered wave

field will increase the range of illumination angles on a target, thus increasing the ray paths that could create stationary phase events.

4.4 Virtual Source Method applied to a Vertical Reflector

Section 4.3 examined the nature and strength of a scattering wave field in a number of different heterogeneous fields. The results illustrate that the nature of geologic heterogeneity plays a significant role in determining the contribution scattering has on increasing the angels of illumination. In the next section I apply the virtual source technique with a heterogeneous model and a simplistic target, to test these results. Section 4.4 tests if the increased angles caused by the heterogeneous field will benefit the imaging capabilities of the virtual source technique. The first step in the analysis is to create a homogeneous reference model, in order to analyze any differences introduced by the geological heterogeneity. The virtual source gathers, NMO corrected CMP gathers and the final stacked seismic section will be fully interpreted on the reference model. The final step will be to introduce heterogeneities to the same model to determine if the scatted waves improve the imaging capabilities, when using the virtual source method.

4.4.1 Generating 2D Synthetic Data

As discussed in section 4.2, synthetic generation of seismic data for each of the models was performed using a 2^{nd} order finite difference algorithm. A VSP walk away

# of Receivers	Receiver Spacing	# of Sources	Surface Source Spacing	Virtual Source Spacing	Grid Size in X-dir	Grid Size in Y-dir
300	6 m	150	10 m	6 m	1800 m	3000 m

Table 4.2 Acquisition parameters for 2D synthetic model of the Vertically Dipping Dyke.

Velocity Model	Country Rock Average Velocity (m/s)	Reflection Coefficient	Correlation Length (m)	Dyke Velocity (m/s)
Homogeneous	6000 m/s	N/A	N/A	4500 m/s
Heterogeneous	6000 m/s	0.067	60 m	4500 m/s

Table 4.3 Velocity values for 2D synthetic model of the Vertically Dipping Dyke and Country Rock.

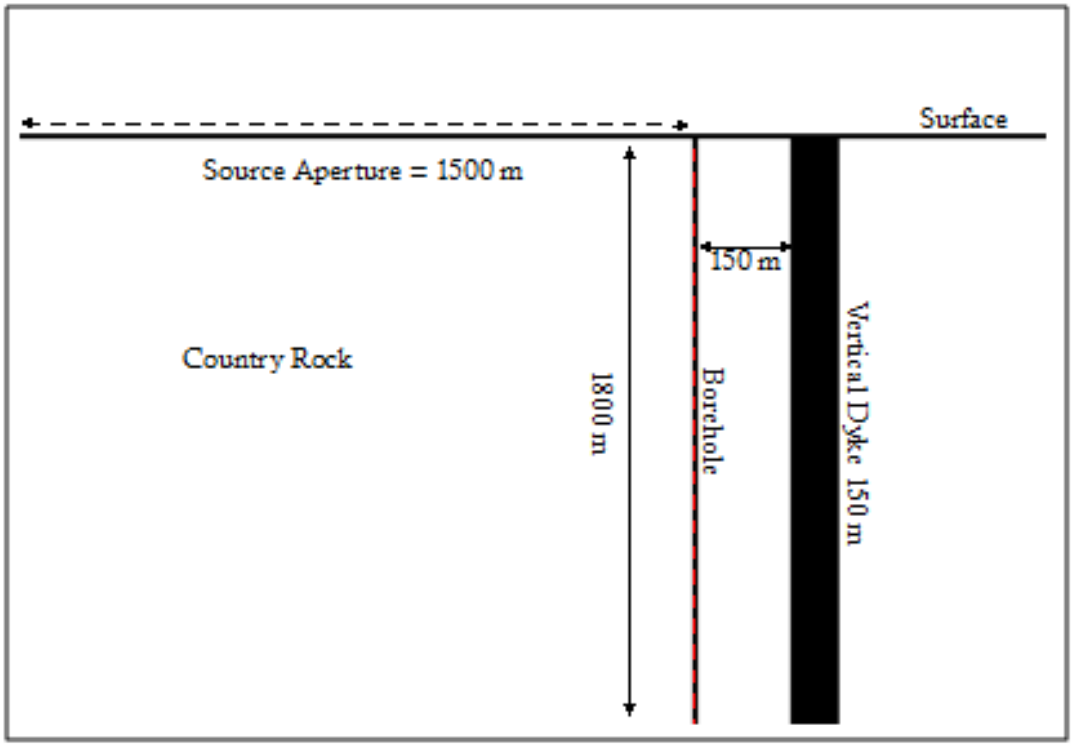

Figure 4.25 Vertically Dipping Model and Survey Parameters

survey was utilized to image a 150 m wide vertically dipping target (table 4.2 and figure 4.25). The velocities and densities for the synthetic modeling were chosen to coincide with Brand (2011), and can be seen in table 4.3. Brand (2011) used seismic velocities based on the granites and gneisses from the Reid Brook and Eastern Deep Zones for the country rock, and the massive sulfides from the Voisey's Bay Mine were used for the vertically dipping dyke Duff, (2007). All the synthetic models created for this section used the mean velocities from these zones.

4.4.2 Homogeneous Model

In order to fully understand the impacts scattering will have on the imaging capabilities of the virtual source method, a reference model with a homogeneous background was constructed. The seismic parameters for the reference model can be seen in table 4.3. Since, the model is homogeneous only signal produced from the target, and artifacts associated with the edge of the synthetic model will be recorded by the receivers. The homogeneous model provides a basis for comparison of the affects that heterogeneity will have at each of the virtual source method processing steps.

The first step in this sequence is to create, and run a VSP walk away survey, which includes 150 surface sources spaced at 10 m, and 300 receivers in the borehole spaced at 6 m (figure 2.24). Next, the cross correlation between two seismic traces from two different receivers that record the same surface source is completed (figure 1.2.). This process is repeated for the 150 surface sources with each receiver pair from the 300

Correlation Gathers						Virtual Source Gather
Source #1		Source #2		Source #150		
R1 X R1 R1 X R2 ↓ R1 X R300	+ + +	R1 X R1 R1 X R2 ↓ R1 X R300	+ + +	R1 X R1 R1 X R2 ↓ R1 X R300	= = =	VS1R1 VS1R2 ↓ VS1R300
R2 X R1 R2 X R2 ↓ R2 X R300	+ + +	R2 X R1 R2 X R2 ↓ R2 X R300	+ + +	R2 X R1 R2 X R2 ↓ R2 X R300	= = =	VS2R1 VS2R2 ↓ VS2R300
↓		↓		↓		↓
R300 X R1 R300 X R2 ↓ R300 X R300	+ + +	R300 X R1 R300 X R2 ↓ R300 X R300	+ + +	R300 X R1 R300 X R2 ↓ R300 X R300	= = =	VS300R1 VS300R2 ↓ VS300R300

Table 4.4. Generation of Virtual Source Gathers
Explaining how to generate Correlation Gathers as well as the summation procedure that creates Virtual Source Gathers.

receivers, too create each correlation gather (table 4.4). Each correlation gather is then summed together, creating one trace in a virtual source gather, where the non-stationary phase events are summed destructively and kinematically correct events are summed constructively. The process of generating correlation gathers into virtual source gathers generates artifacts in the data, which need to be interpreted. By this stage the surface sources are redatumed to act as virtual sources in the borehole. Since, the virtual sources and receivers are in the same plane the survey can be processed using standard CMP techniques, taking advantage of CMP based noise suppression. Some examples of the CMP processing techniques would be normal moveout correction, stacking and migration.

4.4.2.1 Analysis of Correlation and Virtual Source Gathers

In this section, a detailed analysis of the virtual source gathers and correlation gathers is performed to understand how well the virtual source technique images the vertically dipping reflector in a homogeneous model before CMP processing. The Cross-correlation measures the similarities between two different signals. The cross-correlation comprises two sections, which are known as the leads and the lags (figure 4.26 A and B). The lags, or the causal section of the cross-correlation is the portion of the data that produces a seismic source at the virtual source location that is recorded at the borehole receivers. The leads, or acasual part of the cross-correlation represents the time reversal

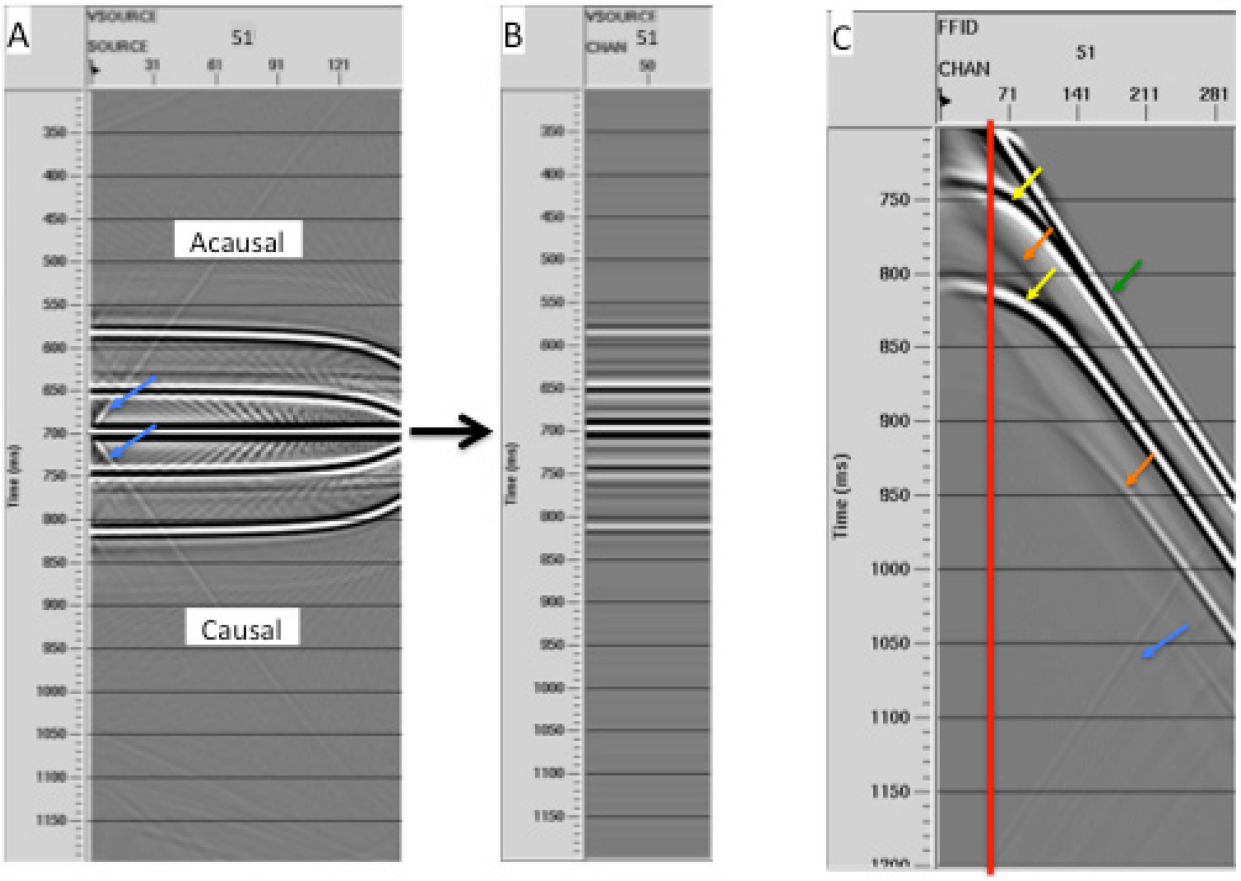

Figure 4.26 Correlation and Virtual Source Gathers
Virtual source 51. A and B display the summation process of each correlation gather into a single virtual source trace. In C the red line represents the location of virtual source 51. Due to the geometry between the borehole and target any receivers located shallower than virtual source 51 will not produce stationary phase, thus being removed from the dataset. The yellow and green arrows represent the reflections and the direct wave respectively. Two artifacts are identified by (i) the blue arrows, which point out the side reflections of the direct wave and reflections, and (ii) the orange arrows that point to the multiples of the front and back reflections.

of the virtual source or an exchange in locations of the virtual source and receiver. In our application of the virtual source method only the causal section of the cross-correlation is of interest. After summing each correlation gather into a virtual source trace the acasual section of the cross-correlation is removed (table 4.4 and figure 4.25 C). This process of removing the acausal section and summation of the causal section happens in each correlation gather resulting in one trace of the virtual shot gather.

A key point to note is the geometric relationship between the borehole and the vertically dipping reflector (figure 4.25) cause receivers above the virtual source too not be able to produce stationary phase during the cross correlation process (Brand, 2011). In figure 4.26 C the vertical red line represents the location of virtual source 51, to the right are receivers located deeper in the borehole and to the left are receivers located shallower in the borehole. Since shallower receivers than the virtual source are unable to produce kinematically correct events all of those traces can be removed from the data. Removing those events decreases the amount artifacts located in the data. In other circumstances of unknown dip, receivers located shallower than the virtual source in the borehole may produce stationary phase events. So, in circumstances of unknown dip non-stationary phase contributions will have to cancel out during summation.

Another factor that limits the number of kinematically correct events in the correlation gathers is the surface source aperture. As discussed in chapter 3, the surface source aperture limits the number of far offset traces in the virtual source gather that can

produce stationary phase events. So, the shorter the source aperture the greater chance of creating artifacts in the virtual source gathers (figure 4.26 C).

Figure 4.26 C highlights a number of events in virtual source gather 51. The reflections from front and the back of the target are labeled with yellow arrows and the direct wave is highlighted in green. It is clear that the cross-correlation and summation process is able to image events similar to a traditional surface survey. However, in the virtual source gathers there are a number of artifacts evident throughout the shot record. Some of these events have no apparent physical meaning, and were summed into the virtual source gathers as a result of the survey geometry, and limited modeling space. One artifact, highlighted in blue, that shows up in the correlation gather and virtual source gather (figure 4.21 C) is the side reflections of both the direct wave and the reflections. This occurs because our model does not have infinite space, and has limited model dimensions. A taper applied to the final few traces in each correlation gather, prior to summation, could reduce the appearance of these artifacts in the virtual source gathers. Another artifact, highlighted with orange arrows, in figure 4.21 C is multiples of the front and back reflections.

4.4.2.2 NMO and Stack Analysis

Once the summation and pre processing is complete this model can be processed with all the noise cancelling capabilities of a traditional CMP seismic survey. The virtual source gathers must be reorganized into Common Midpoint (CMP) Gathers, allowing for

multifold coverage of the target. The multifold coverage, given by the CMP gather, enhances the signal to noise ratio after the traces in each CMP gather are summed. In a traditional surface seismic survey the reflections in each CMP gather displays a hyperbolic response due to the increased offset between source-receiver pairs. The observed reflections recorded from the virtual source method have variant results: (i) The reflection recorded from the front of the target does produce a hyperbolic response until it becomes tangential with the direct wave, as would a reflection from a traditional seismic survey (figure 4.27 A). (ii) The reflection from the back of the target however, produces a similar hyperbolic response as the front reflection in the near offset virtual source – receiver pairs. But, in the far offset virtual source – receiver pairs the theoretical hyperbolic response is not correctly recovered (figure 4.27 A). The lack of hyperbolic moveout is thought to be a direct result of a limited kinematically correct events created for the virtual source method for these far offset virtual source – receiver pairs. However, there is no diagnostic test to prove this theory to be correct. Another point to note is there are a number of non-physical events, highlighted with green arrows, in figured 4.27 A. Some of the non-physical events do not cancel out in the summation process, because the integration limits of each correlation gather are truncated by the limited source aperture.

The next step in the processing sequence is to apply a normal moveout correction (NMO). The NMO correction is designed to remove the time delay associated with the increasing offset of the source–receiver pairs in each CMP gather. The normal moveout correction used a constant velocity model of 6000 m/s because it was the average velocity

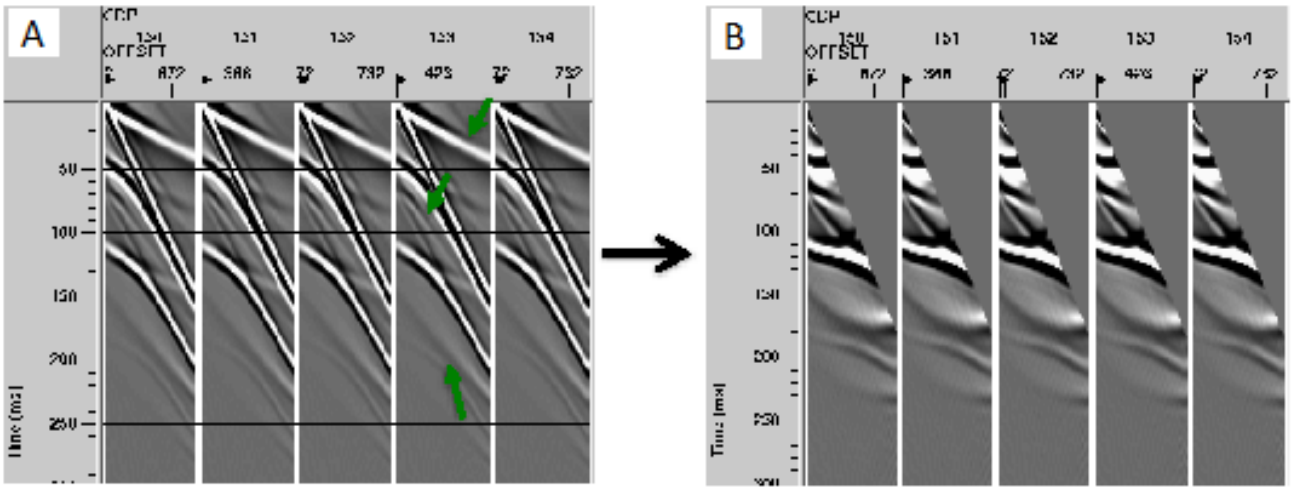

Figure 4.27 CMP Gather 150-154
(A) CMP 150-154 images the front and the back of the vertical dipping reflector, however the reflections do not produce the typical hyperbolic response seen in traditional seismic surveys. The green arrows represent artifacts in the data. (B) The NMO corrected CMP gathers of 150-154 images both reflections, but are not flattened due to the non hyperbolic response seen in the CMP gathers

chosen for the reference model. When the NMO correction is applied to the data the CMP gathers do not produce flat events, which is due to the lack of hyperbolic moveout in the two reflections (figure 4.27 B). However, Brand (2011) was able to prove that if a wave is within half a wavelength of each other that they will sum constructively. Given that most of the amplitudes for each reflection are within half a wavelength (figure 4.27 B), the final stacked seismic section is able to image both the front and back of the target (figure 4.27 B).

When the NMO correction has been applied the next step in the processing workflow is stacking each NMO corrected CMP gather into one trace. The stacking process is used to increase the signal to noise ratio in the seismic profile by the fold of the data (figure 4.27). The CMP stacking process also removes non-stationary contributions from the virtual source, as they do not satisfy the CMP hyperbola. The final stacked image of the vertically dipping reflector is compared to the original velocity model in figure 4.27. Even though there is a limited source aperture the virtual source method is able to produce a seismic image of both the front and the back reflector, where the fold of the data was sufficient enough. At the bottom and top of the model not all of the non-stationary phase contributions are removed causing a number of artifacts to occur in the dataset.

Another key comparison in figure 4.28 is between the seismic stack and graph depicting the fold of stationary phase points with respect to depth in the borehole. It is quite evident in the stacked seismic section that more artifacts appear close to the surface

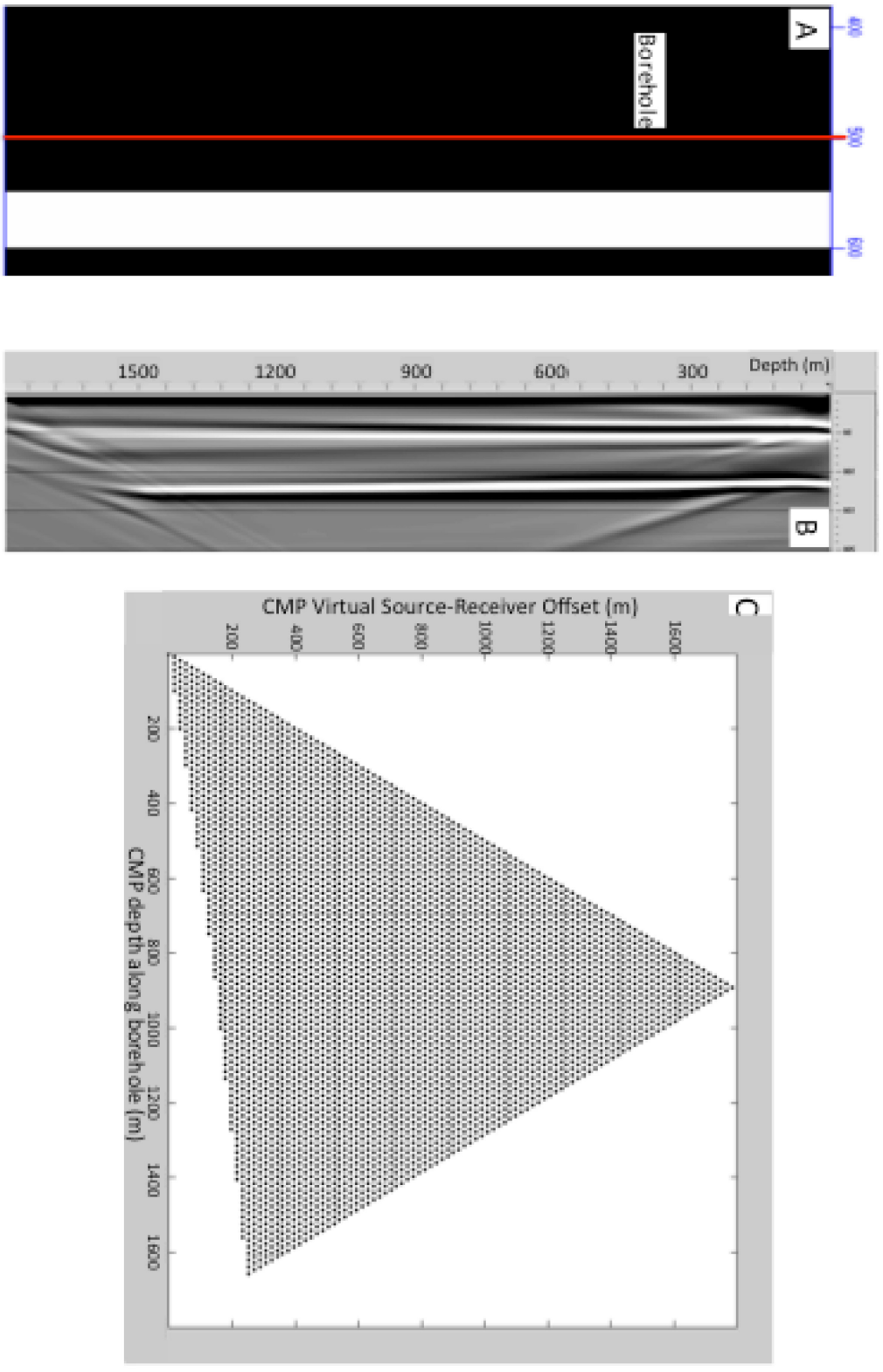

Figure 4.28 Stacked homogeneous vertically dipping model
This is a comparison between the input model (A) and the final stacked image (B) and the CMP fold represented by the graph CMP Virtual Source – Receiver Offset vs CMP depth along borehole (C).

and deep in the borehole (figure 4.28 B). After interpreting figure 4.28 C the amount of stationary phase points is limited both near the surface as well as deep in the borehole. So, it is expected that non-stationary phase events would be summed into the seismic stack creating artifacts because of the lack of stationary phase events at both the beginning and end of the seismic section.

4.4.3 Heterogeneous Models

This chapter has developed an understanding of the strength and nature of different scattering fields (section 4.3), as well as the imaging capabilities of the virtual source method when using a homogeneous model (section 4.4.2). The next step is to determine if there are conditions in which the virtual source method can take advantage of seismic scattering, and improve imaging capabilities of steeply dipping reflectors. The heterogeneous fields applied to the country rock were designed to test the affects of the virtual source technique, in both a strong scattering and a weak scattering regime. The variations of the velocity, and the correlation lengths are based on the work completed in section 4.3. To insure that changes in the final stacked image are strictly due to the introduction of heterogeneities the same survey parameters used in section 4.4.2 were used for these models.

4.4.3.1 FK Filter

Before analysis can be performed, by comparing the virtual source technique in a homogeneous model to a heterogeneous model, there must be pre-processing applied to the heterogeneous model. The seismic wavefield scatters in all directions when introduced to the heterogeneities. The waves that have been reflected by the heterogeneities of the model and are travelling up-wards in the shot gathers, known as up-going waves, produce artifacts in the virtual source gathers. Due to the orientation of the vertical target and acquisition geometry the up-going waves cannot produce stationary phase. In order to remove the influence of the up-going waves an FK filter was applied to the VSP shot gathers (figure 4.29) before cross-correlation. Figure 4.30 displays two correlation gathers, one with an FK filter applied (A) and the other without an FK filter applied (B). The noise produced by the up-going wavefield is diminished when the FK filter is applied because there are fewer artifacts in the correlation gathers (figure 4.30). Figure 4.31 compares virtual source gather 51 with no up-going waves (A) and with up-going waves (B). It is clear that the FK- filter is able to remove a sizeable portion of the unwanted up-going waves, allowing fewer artifacts to be summed into the data.

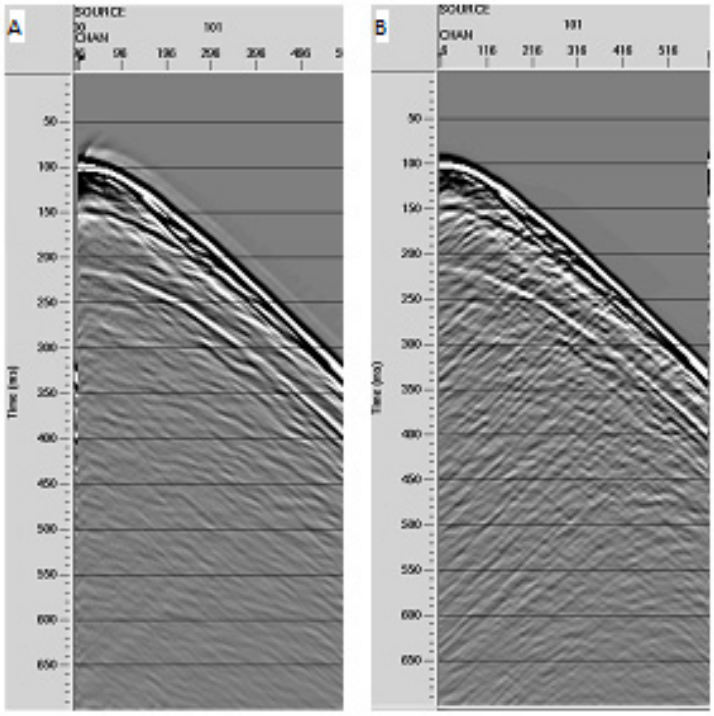

Figure 4.29 Testing FK filter results using VSP shot gather
VSP shot gathers from surface source 101. (A) VSP shot gather with F-K filter applied, which remove the upgoing waves, (B) VSP shot gather with no F-K filter applied

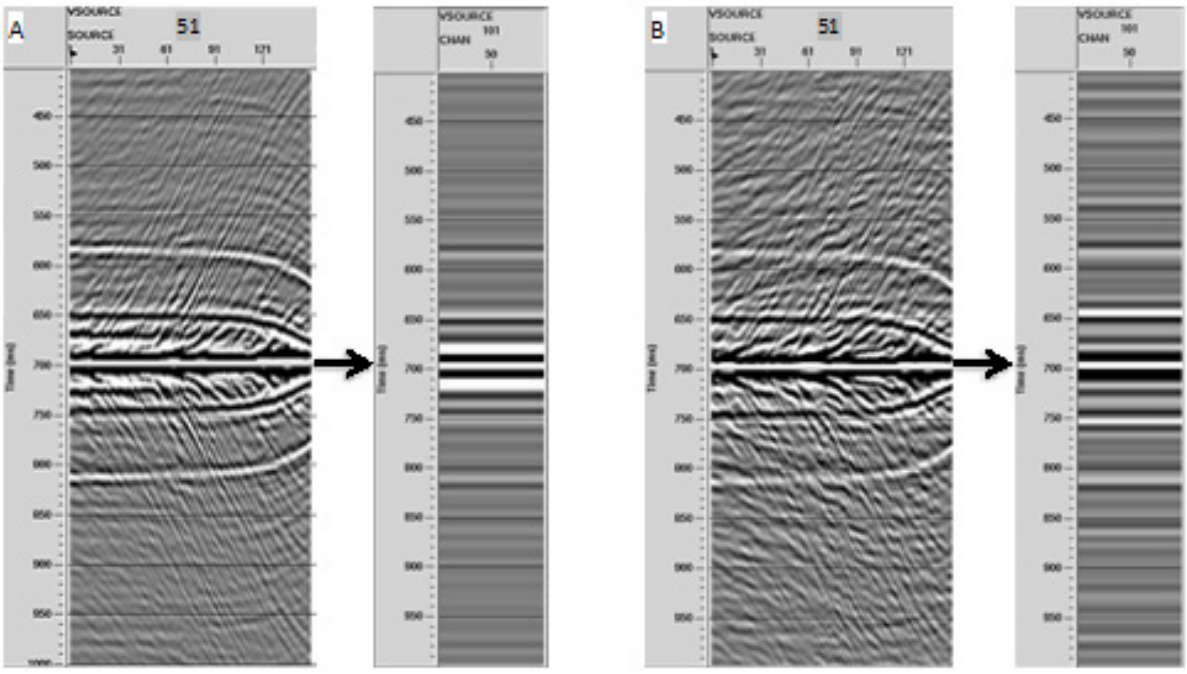

Figure 4.30 Testing FK filter results with Correlation Gathers
Correlation Gather from virtual source 51 and receiver 51. (A) Correlation gather with an F-K filter applied, removing upgoing waves in the VSP shot gathers, (B) Correlation gather without an F-K filter applied.

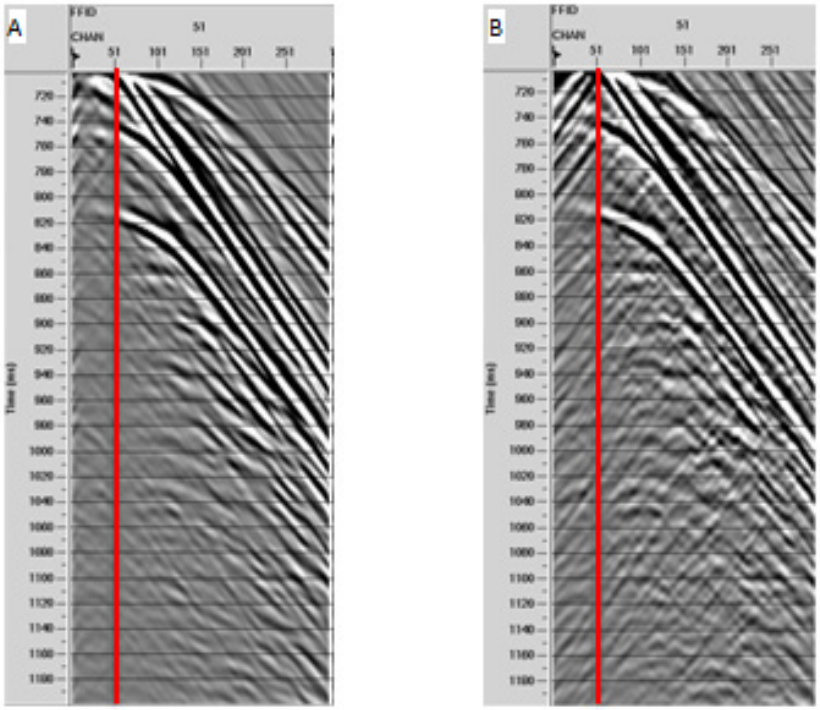

Figure 4.31 Testing FK filter results using Virtual Source Gathers
Virtual Source Gather 51. (A) Virtual source gather with an FK filter applied, removing an upgoing waves and (B) Virtual source gather with no FK filter applied.

4.4.3.2 Analysis of Virtual Source Method.

Introducing scattering to any model will increase the amount of semi coherent noise in the data, as well as potentially useful signal. Due to the increased complexity of the model, care must be taken during the cross-correlation and summation stage of the virtual source method. So, to further understand how to utilize the signal created by scattering, three different mutes were applied to the seismic trace, which represents the virtual source during the cross-correlation process (figure 4.32). The three different mute lengths were chosen using two end members of the dataset and another that utilizes the scattering wavefield without adding excessive noise during cross-correlation (figure

4.33). The three mute lengths were: (i) the direct wave only (figure 4.33 A), (ii) the direct wave + coda (figure 4.33 B) and (iii) all of the data (figure 4.33 C).

Determining which data set produces the highest quality post-stack image requires a detailed examination of the CMP gathers and NMO corrected CMP gathers (figure 4.34 and 4.35). The CMP gathers of the direct wave only case (figure 4.34 C) and the entire dataset (figure 4.34 A) are almost identical, but in the direct wave + coda case (figure 4.34 B) there are significant differences noted. The main difference is the amplitude decrease from the reflections in the further offset virtual source-receiver pairs for the direct + coda case (figure 4.34 B). The amplitude decrease happens approximately at

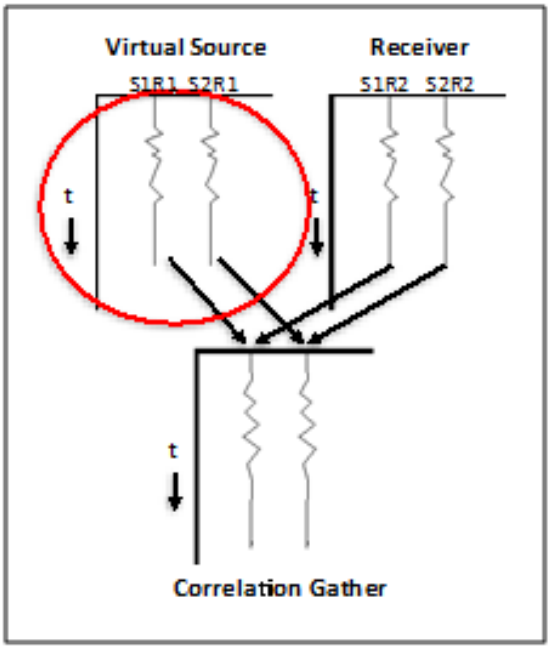

Figure 4.32 Creation of Correlation Gathers
Highlighting the seismic trace that acts as a virtual source during the cross-correlation of the virtual source method. Modified image from Mehta, 2008.

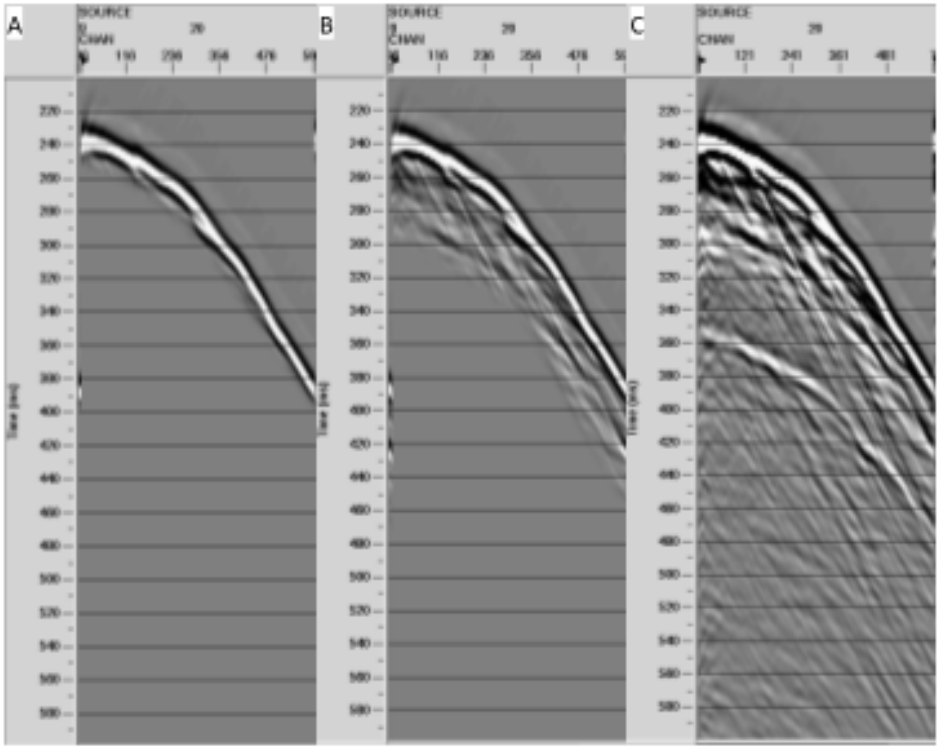

Figure 4.33 Mutes applied to the reciever acting as a virtual source during cross-correlation
(A) all coda is muted leaving the direct wave, (B) excess coda is muted leaving the direct wave and trailing coda, (C) no mute applied leaving all the data.

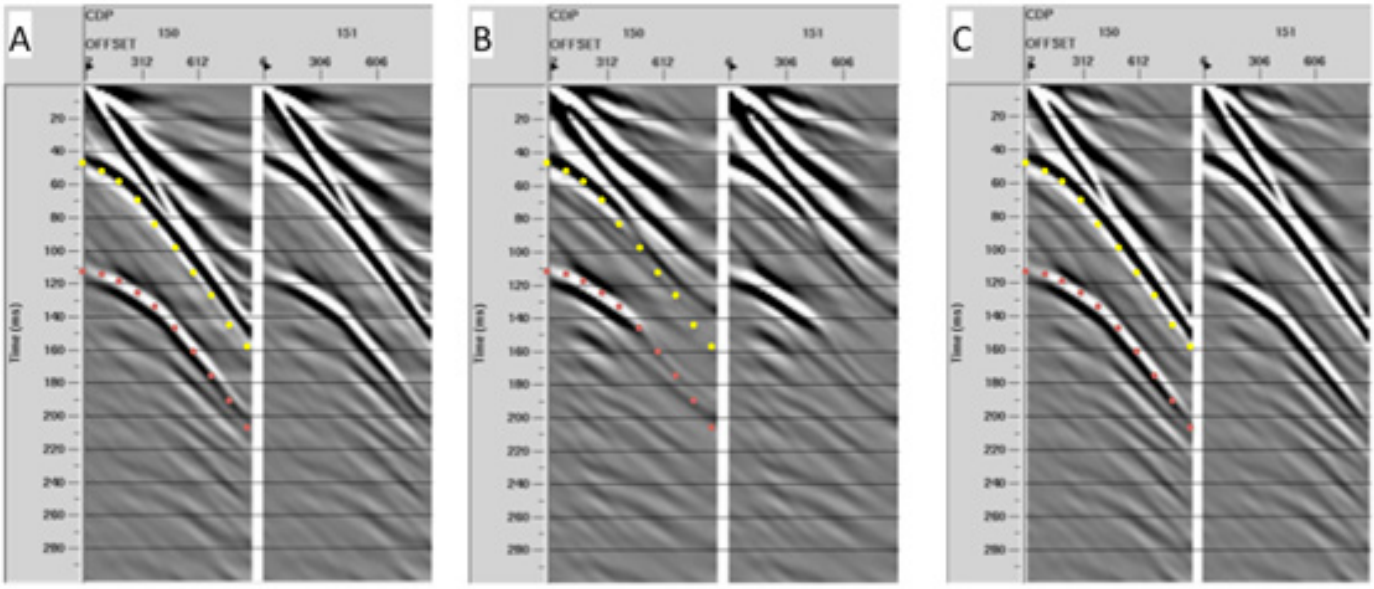

Figure 4.34 CMP Gathers from Heterogeneous Model
CMP gather 150-151. The cross-correlation process: (A) using only the direct wave for the virtual source, (B) using the direct wave and some trailing coda for the virtual source and (C) using all the data. The yellow dots represent the calculated hyperbolic response of the front reflection and the red dots represent the back reflection using the NMO equation and the same geometric parameters.

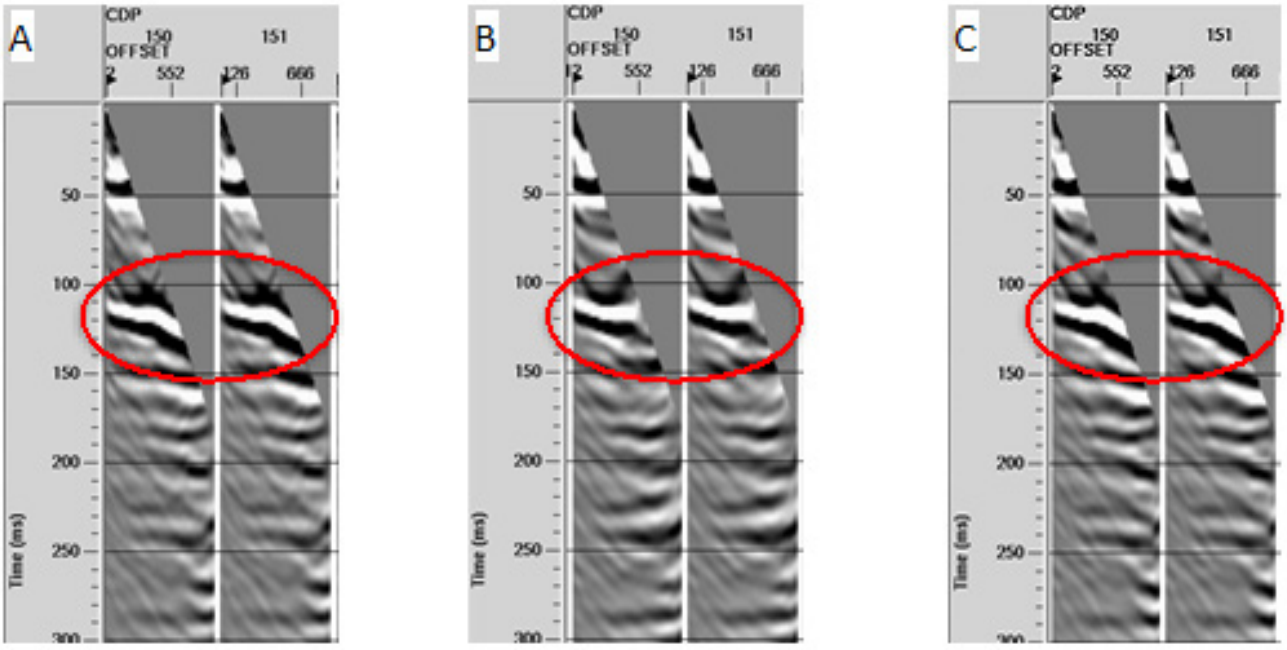

Figure 4.35 NMO corrected CMP Gathers from Heterogeneous Model
NMO corrected CMP gather 150-151. The cross-correlation process: (A) uses only the direct wave for the virtual source, (B) uses the direct wave and some trailing coda for the virtual source and (C) uses all the data.

400 m offset, which is the offset at which the reflections change from a hyperbolic shape to a linear shape in the direct only and the entire dataset case. For further analysis, the hyperbolic shape of both reflections was calculated using the NMO equation. The calculated reflections were then superimposed onto the CMP gather from figure 4.33, where the yellow dots represent the front reflection, and red dots represent the back reflection. The calculated theoretical reflections do have a similar response to the actual CMP reflections, at first glance. If the results from figure 4.34 (A) and (C) are examined with more detail it is evident that there is a mismatch between the theoretical and actual CMP reflection results once the reflections change from a hyperbolic to linear response. After the NMO is applied to the CMP gathers this mismatch between the theoretical and actual results causes the reflections to overcorrect in both the direct wave and entire

dataset cases, but the coda + direct wave case produces flatter reflections (figure 4.35). The evidence produced from the CMP gathers and NMO corrected gathers is not conclusive, but leads us to believe that the coda could be increasing the destructive interference and cancellation of non-stationary phase events.

The final stacked seismic section images both reflections with each model, since the vertically dipping model is simplistic (figure 4.36). However, there are slight differences seen in each heterogeneous model. Around CDP 350 in figure 4.36, highlighted with orange arrows, the front reflector still has strong amplitudes in (C), where as in (B) and (D) the amplitudes are significantly lower. A similar response happens in the back reflector, but is not as obvious. This is an interesting result because the coda + direct case is causing stronger amplitudes to emerge, which could be due to greater cancellation of non-stationary phase events or increased stationary phase events created during cross correlation. Another point to note is when the NMO corrected CMP gathers were stacked the deeper portion of the reflector was poorly imaged in all three datasets, which is highlighted in figure 4.36 with a blue oval. This result of improper imaging of the deepest segment of the target also occurs to the homogeneous reference model (figure 4.36 A).

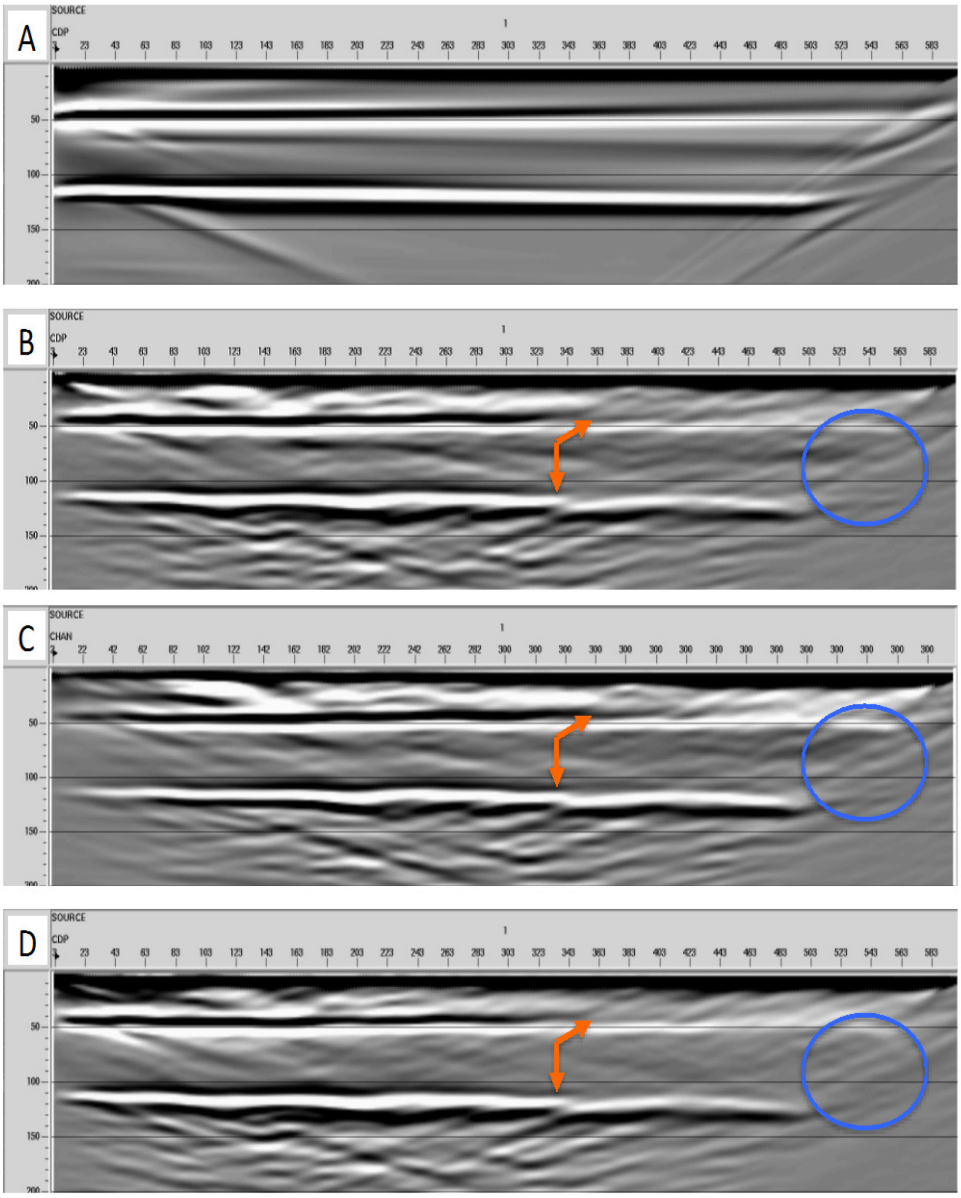

Figure 4.36 Final Stacked Images of Vertically Dipping Model
A comparison of the four Stacked Vertically Dipping Reflector images. (A) Homogeneous reference model, (B) using entire data window during cross-correlation, (C) using direct + trailing coda during cross-correlation and (D) using only direct wave during cross-correlation.

4.4.3.3 Analysis of correlation gathers

All three heterogeneous models produced a similar stacked seismic image, so further investigation was needed to see if there could be advantages to using the coda when imaging a more complex target. The CMP gathers and the final stacked image provide evidence that the coda helps during cross-correlation a higher quality image could be produced. But, to see how the virtual source method takes advantage of the scattered waves a detailed analysis of the correlation gathers was carried out. After examining the correlation gathers is it clear that determining differences from the three datasets is difficult. Differencing the correlation gathers from the direct + coda and the direct wave only case could demonstrate what was added to the data by the scattered wavefield.

Before differencing the two datasets the average absolute amplitude of the direct wave from the correlation gathers of each dataset was extracted. The average absolute amplitude of the direct wave was obtained so both datasets could be differenced without any bias towards one heterogeneous model. Figure 4.37 indicates that the amplitudes are greater for the direct wave dataset so a scaling factor was applied. Calculating the average from each graph determines that a 0.68 scaling factor should be applied to the direct wave dataset before differencing the correlation gathers. Next the direct wave case was polarity flipped by multiplying the dataset by -1 for easy interpretation between each correlation gather set, seen in figure 4.38 (B) and figure 4.39 (B). Once this is complete the polarity flipped direct wave case and the direct wave + coda case were summed

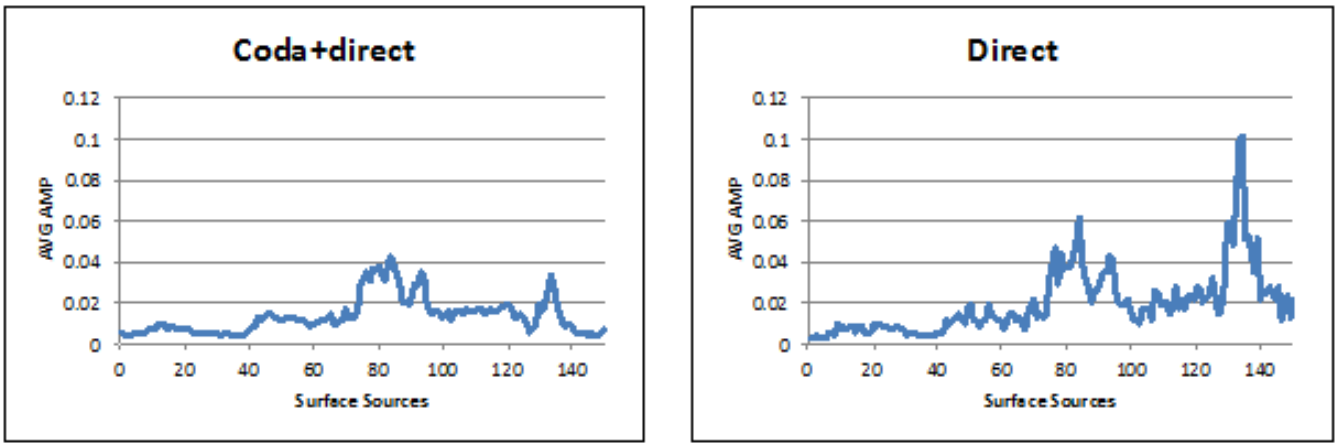

Figure 4.37 Average Absolute Amplitude of the direct wave from the correlation gathers

together (differencing the original datasets). An important point to note is that in Promax each seismic window is scaled individually for easiest viewing of each seismic section. Meaning that differencing of each dataset is still valid even if the datasets (figure 4.38 A and B, figure 4.39 A and B) appear to have similar amplitudes after differencing the two dataset.

The results of the differencing between the two datasets are not definitive, however are still instructive. Figure 4.38 shows the correlation gather from virtual source 51 and receiver 100, where the direct + trailing coda (A) is differenced from the direct wave only case (B). The second reflectors (representing the back of the vertically dipping target) stationary phase contribution is highlighted with a blue oval, and the non-stationary phase contribution is highlighted with a red oval (figure 4.38). The stationary phase component of the correlation gather was identified in figure 4.38 as the portion of the correlation gather that will sum constructively and the non-stationary phase

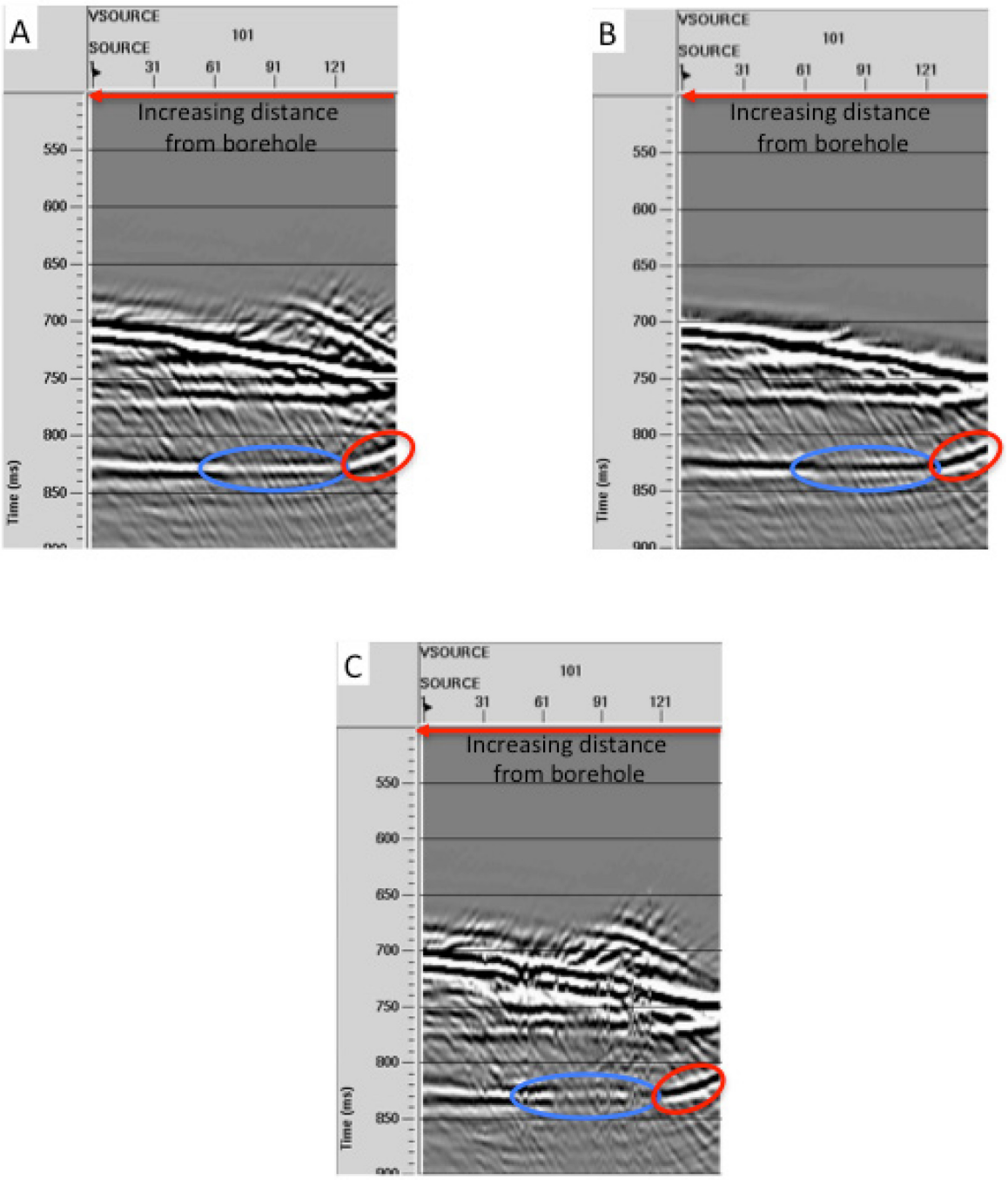

Figure 4.38 Differencing Near Virtual Source – Receiver Pairs
Correlation Gather of Virtual source 51 and receiver 100. (A) Direct and trailing coda, (B) normalized direct wave only case by multiplying the correlation gather by -0.68 and (C) the difference between A and B. The blue oval highlights stationary phase contribution and the red oval highlights the non-stationary phase contributions.

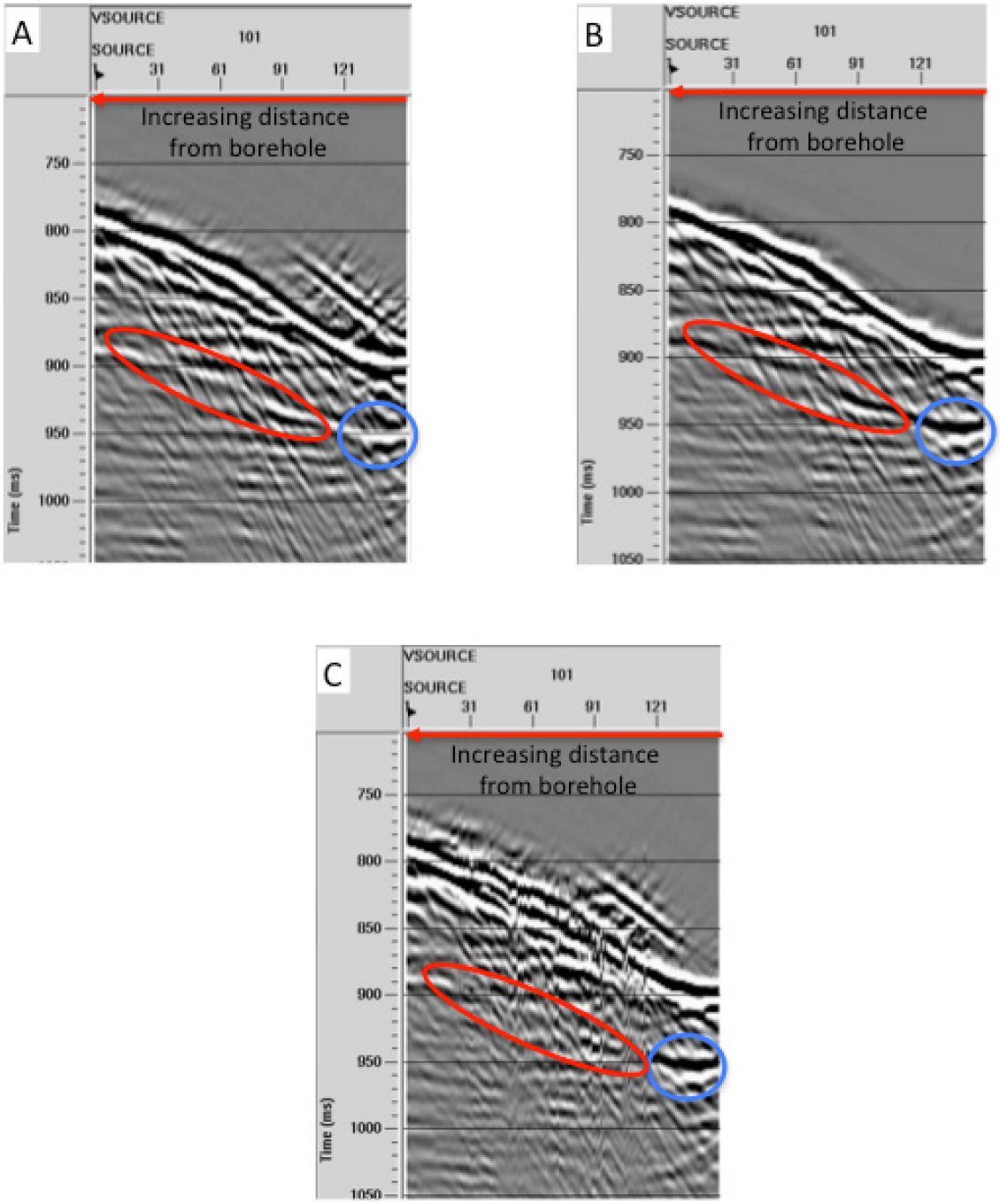

Figure 4.39 Differencing Far Offset Virtual Source – Receiver Pairs
Correlation Gather of Virtual source 51 and receiver 250. (A) Direct and trailing coda, (B) normalized direct wave only case by multiplying the correlation gather -0.68 and (C) the difference between A and B. The blue oval highlights stationary phase contribution and the red oval highlights the non-stationary phase contributions.

contribution as the area that will sum destructively. The result of the differencing (C) suggests that the stationary phase portion of the direct + coda case is dominant but in the non-stationary phase component is dominated by the direct wave only contribution. The same differencing procedure was also completed on the correlation gather from virtual source 51 and receiver 250 to examine a larger offset virtual source – receiver pair (figure 4.39). The outcome after differencing the two datasets is different as the direct wave case is dominant in stationary phase component for this set of correlation gathers (figure 4.39 C) suggesting that the coda is not contributing sufficient stationary phase in further offset virtual source receiver pairs.

Differencing the two virtual source - receiver pairs produced varied results, so further investigation is needed. Virtual source – receiver pairs that create kinematically correct reflector locations are different in each correlation gather as seen in figures 4.38 and 4.39, highlighted with blue ovals. The second reflector shows that near offset virtual source – receiver pairs have more constructive interference from the surface sources located farther from the borehole (figure 4.38). Where as, the far offset virtual source – receiver pairs have more constructive interference from surface sources located close to the borehole (figure 4.39). If the differencing does gives us definitive results then it indicates that more energy is partitioned from the direct wave to the coda as the surface sources have longer offsets from the borehole. Since, the energy partitioned to the coda travels at different angles it potentially provides more angles of illumination, which creates more ray paths that could produce kinematically correct events. However, more energy is contained within the direct wave at surface sources

located close to the borehole since the seismic wave travels less distance in the subsurface. So, at near offset surface sources coda will have less influence and the direct wave will have more influence when creating stationary phase points. If proven correct these results would be very instructive into how coda affects the imaging capabilities of the virtual source method.

4.4.3.4 Weak Scattering Heterogeneous Model

A strong scattering field was originally investigated because the variation in impedance created high amplitude events in the coda. Transferring a significant amount of energy to the scattered wavefield will generate more illumination angles to benefit the virtual source techniques processing workflow (figure 4.40). The next step in this work is a comparison of the strong scattering results of the same experiment in the weak scattering regime (figure 4.41). The heterogeneous model used to created the weak scattering heterogeneous field was designed geometrically the same to the previous heterogeneous models in section 4.4.3. The only difference is that the reflection coefficient was decreased from being 0.067 to 0.033. The decrease to a reflection coefficient of 0.033 gives a velocity variation of 5800-6200 m/s.

Before evaluating the final processed stacks, a zero offset VSP shot gather of the strong scattering and weak scattering regime was examined (figure 4.40, 4.41). The two shot gathers are transferred to the FK domain to interpret the energy in each scattered wavefield. The FK domain illustrates that there is more energy partitioned from the

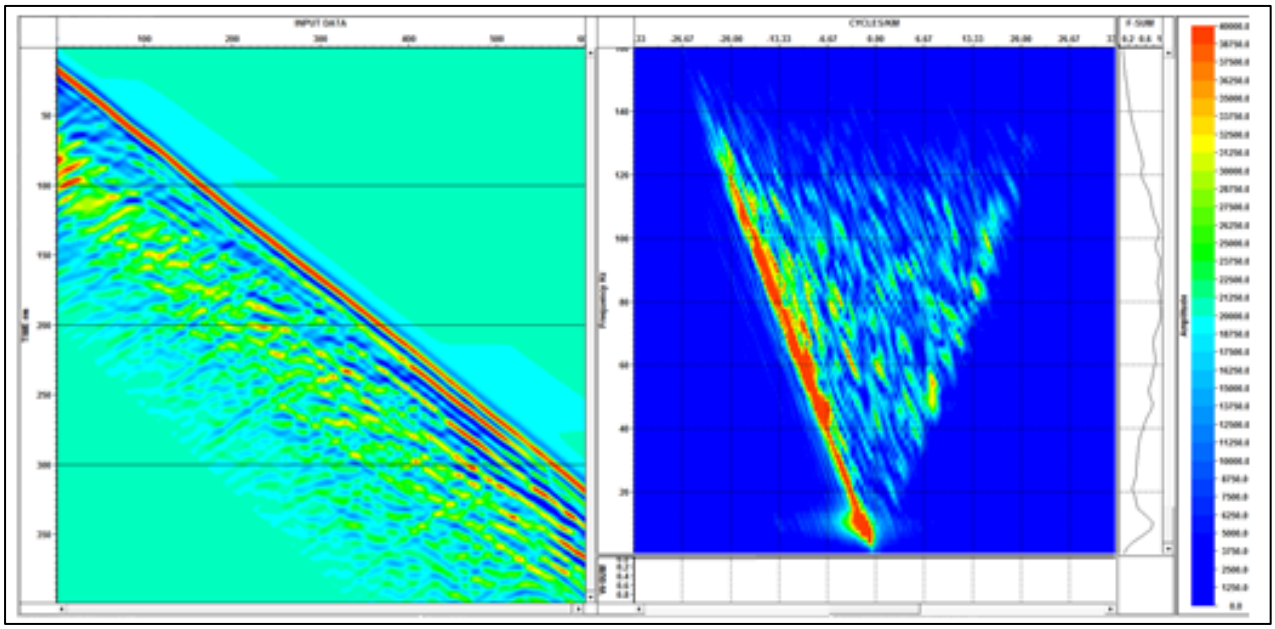

Figure 4.40 FK Analysis in Strong Scattering Regime
A Zero Offset VSP completed on a heterogeneous field with a correlation length of 60 m and a bimodal reflection coefficient of **0.067** causing this heterogeneous medium to be in the strong scattering regime. The spectrum of energy represents the apparent velocity range of the direct wave and trailing coda.

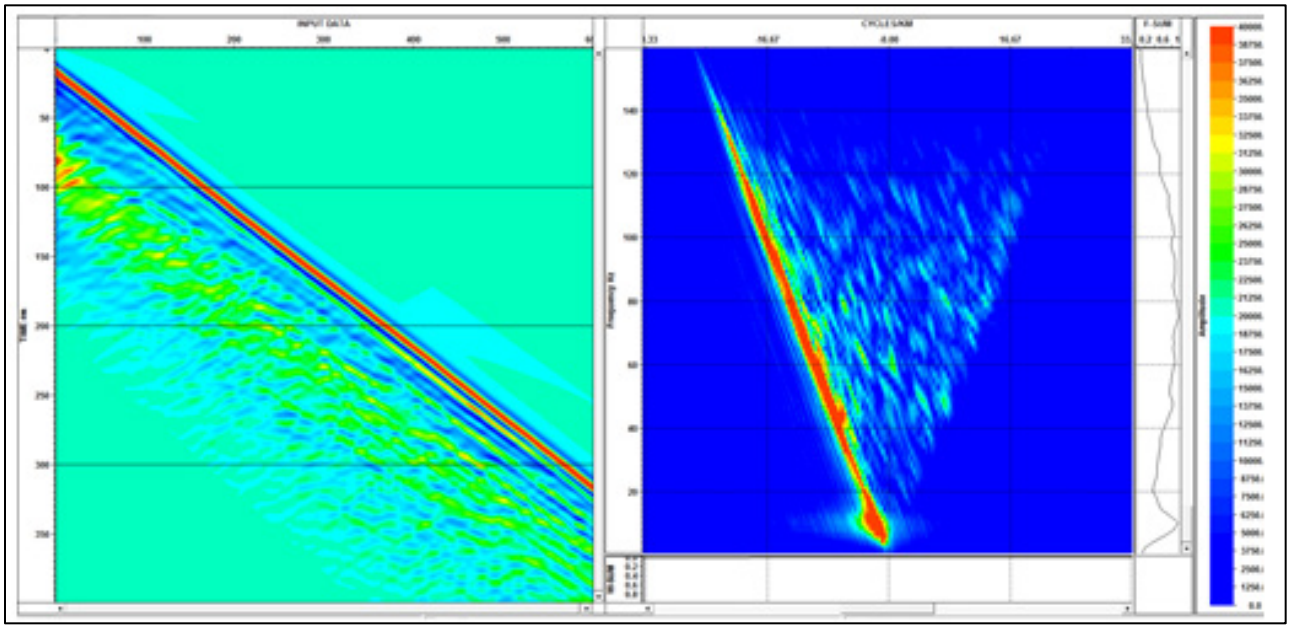

Figure 4.41 FK Analysis in Weak Scattering Regime
A Zero Offset VSP completed on a heterogeneous field with a correlation length of 60 m and a bimodal reflection coefficient of **0.033** causing this heterogeneous medium to be in the weak scattering regime. . The spectrum of energy represents the apparent velocity range of the direct wave and trailing coda.

direct wave to the scattered wavefield in the strong scattering regime, which is expected. Although, the amplitudes within the weak scattering wavefield are not as strong, the wavefield still contains increased illumination angles.

Using the same processing method as discussed in section 4.4.3, a comparison between no scattering, weak scattering and strong scattering is made. Making this comparison tests if the strength of energy being partitioned to the scattered media affects the seismic imaging capabilities (figure 4.42). The weak scattering case (figure 4.41 B) images the vertically dipping target with similar quality seen throughout chapter 4. However, deeper in the borehole there is an artifact, highlighted with a red rectangle, in both the no scattering and weak scattering cases (figure 4.42 A and B). In the strong scattering case the artifact is cancelled out. Referring back to section 4.3.1 could give some insight into why this artifact is cancelled out in the strong scattering model. The 1000 m offset VSP proved that by increasing the seismic waves travel time in a heterogeneous media more energy would be partitioned to the scattered wavefield. The artifact is located close to the bottom of the borehole, suggesting that the strong scattering model partitioned enough energy from the direct wave to the scattered wavefield to cancel the non-stationary phase event. The weak scattering model did not partition enough energy to the scattered wavefield to have the same impact on the non-stationary phase event.

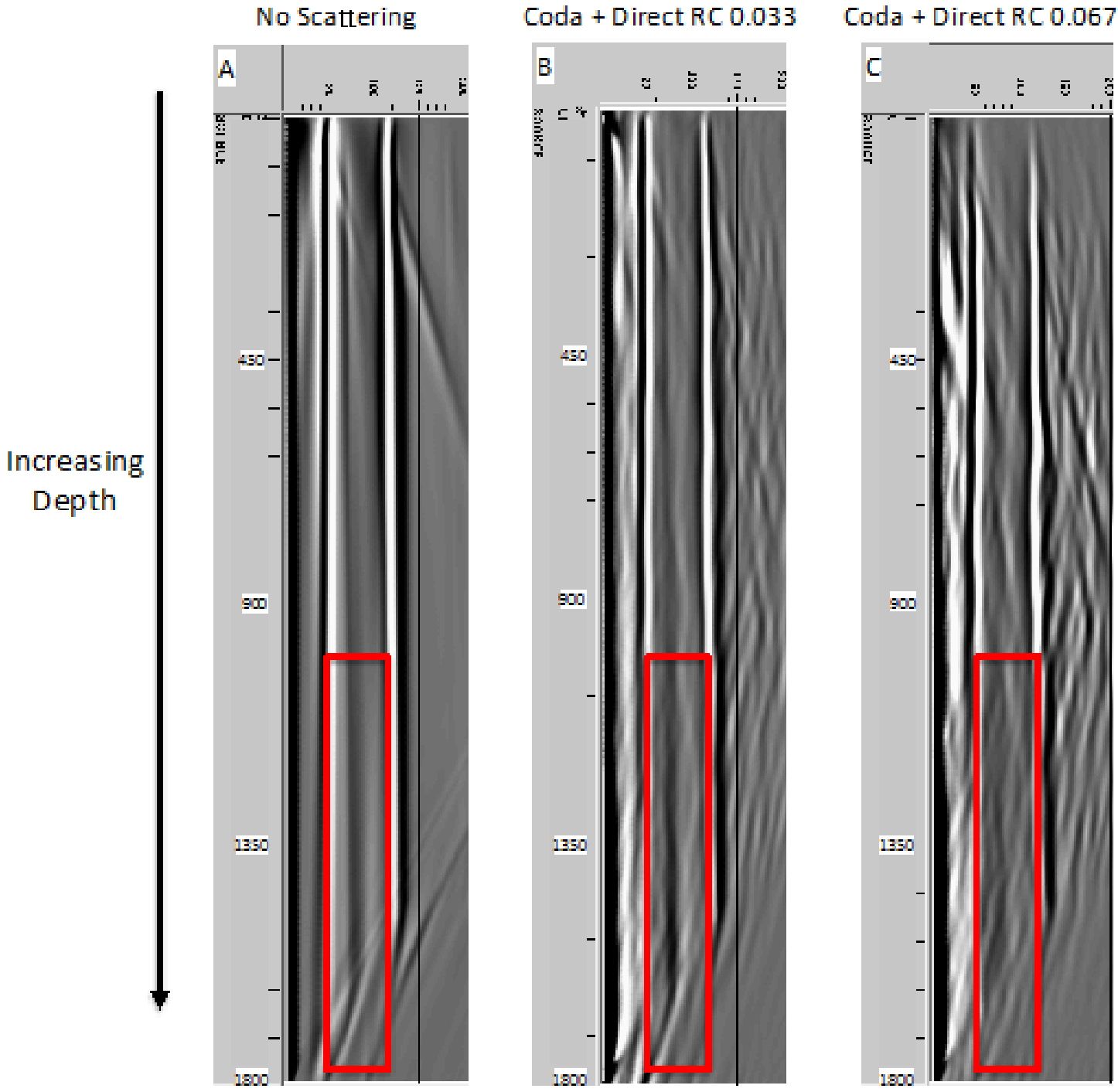

Figure 4.42 Final Stacked Image of Strong vs Weak Scattering
A comparison between three Final stacked seismic images where (A) is the homogeneous case, (B) is the weak scattering case and (C) is the strong scattering case.

4.5 Concluding Remarks

Chapter 4 presented a number of experiments that exhibited practical seismic imaging uses for the virtual source method in a heterogeneous environment. The experiments included testing various stochastic fields within reasonable geological parameters and imaging a vertically dipping dyke in both a homogeneous medium and a heterogeneous medium.

Varying the parameters of the scattering fields within realistic geological conditions identified heterogeneous mediums that will produce greatest impact when using the virtual source method. The experiments demonstrated that heterogeneous mediums created the greatest illumination angles when a two-phase velocity distribution, with a large reflection coefficient, and a correlation length close to the dominant seismic wavelength of the model were used. Under those scattering conditions large amounts of energy are transferred from the direct wave to the trailing coda, which increased the amount of travel paths. The increased ray paths of the coda have the potential to produce constructive interference of stationary phase points and destructive interference of artifacts during the cross-correlation and summation portion of the virtual source method.

The simplistic vertically dipping model suggests that the coda is helping in both constructive and destructive interference, however the results were not conclusive. When comparing the CMP gathers and the NMO corrected CMP gathers of each dataset it suggests that the heterogeneous medium perturbs the kinematically incorrect portion of

each reflection causing destructive interference of non-physical events in the direct + coda case. Another important section of chapter 4 is the examination of the correlation gathers. Differencing the correlation gathers in the coda + direct wave and the direct only case showed that the further offset surface sources partition more energy from the direct wave to the coda, allowing for greater angles of illumination, and thus more ray paths that could create stationary phase points. If proven that differencing the correlation gathers produces a legitimate result the conclusions would be very instructive in showing that coda can increase the amount of kinematically correct events. Unfortunately, this chapter was unable to definitively prove that coda produces a better result through cancelation of non-physical events, or creation of more kinematically events. But, chapter 4 definitely hints that the coda is able to provide cancellation and creation of events that are beneficial to the final seismic result.

Chapter 5. Complex Geological Models and the Virtual Source Method

5.1 Introduction

The research for this master's project was designed to investigate the influences geological scattering can have on imaging steeply dipping structures, while using the virtual source technique. Chapter 3 used straight ray tracing to examine the affects acquisition parameters have on the virtual source method. In Chapter 4 I developed an understanding of the nature of scattering, and applied that knowledge in an attempt to improve imaging on a vertically dipping target. However, due to the simplicity of the model an adequate amount of stationary phase points were acquired for all datasets, making it difficult to determine the effect scattering has on the image quality. Chapter 5 will provide a more challenging implementation of the virtual source method by testing a corrugated model (figure 5.1). The increased complexity of this model is meant to provide a more diagnostic result by introducing a target, which is more sensitive to increased illumination angles.

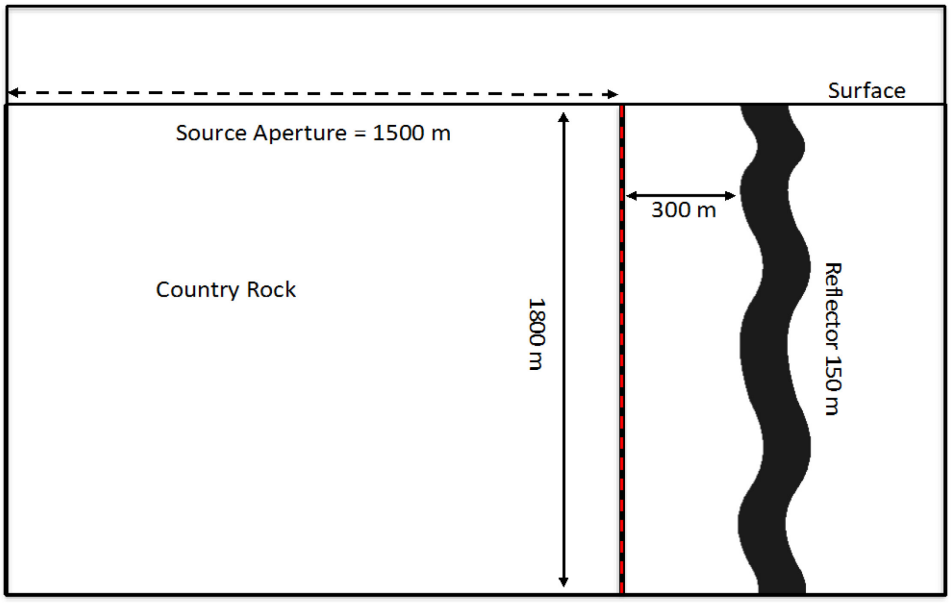

Figure 5.1 Geometry of Corrugated model
The size of the model is 3000 m in the x-direction and 1800 m in the z-direction. The borehole is placed in the middle of the model in order to minimize edge effects.

5.2 Synthetic Modeling

The corrugated model represents a more complex scenario than the planar, vertically dipping model and was created in order to test Baulkin and Calvert's (2006) assertion that strong scattering in the near surface may help virtual source data by simulating wider surface source offsets. Broadening of the surface source offsets effectively increases the range of illumination angles that have the possibility to create stationary phase rays or allow for more cancellation of non-stationary rays. Too understand how scattering contributes to the virtual source method a comparison between the contribution of the scattered wavefield and the direct wave must be made. The generation of three synthetic datasets with different mutes applied before cross correlation will be utilized in order to complete this comparison.

The set of experiments used the same finite difference algorithm as in Chapter 4, to generate the seismic data. The seismic survey used was a VSP walk away survey in order to image the corrugated model. The synthetic seismic source produces a zero phase Ricker wavelet, which emanates from 150 surface sources that are spaced 10 m apart creating a source aperture of 1500 m. The surface sources are then recorded by 300 receivers spaced 6 m apart, which are placed in the borehole 300 m away from the target (table 5.1). The only difference between this geometric set up and the one in chapter 4 is the borehole is 300 m away from the target rather than 150 m. Increasing the distance between the borehole and the target reduces the amount of overprint the direct wave has on the front of the target. The velocity gradient, reflection coefficient and correlation

length were chosen based on the observations made in section 4.3 (table 5.2). The seismic velocities were based on the granites and gneisses from the Reid Brook and Eastern Deep Zones for the country rock, and the massive sulfides from the Voisey's Bay Mine were used for the vertically dipping dyke (Duff, 2007).

# of Receivers	Receiver Spacing	# of Sources	Surface Source Spacing	Virtual Source Spacing	Grid Size in X-dir	Grid Size in Y-dir
300	6 m	150	10 m	6 m	1800 m	3000 m

Table 5.1 Model and Survey Geometry of Corrugated Model

Velocity Model	Country Rock Average Velocity (m/s)	Reflection Coefficient	Correlation Length (m)	Dyke Velocity (m/s)
Homogeneous	6000 m/s	N/A	N/A	4500 m/s
Heterogeneous	6000 m/s	0.067	60 m	4500 m/s

Table 5.2 Velocity values for 2D synthetic model of Corrugated Target and Country Rock

5.3 Imaging the Corrugated Model

In Chapter 4 the direct wave + coda case provided a final stacked image that was imaged marginally better than the direct wave only and whole data case. The direct + coda case in Chapter 4 did suggest: (i) that there could be greater cancellation of the non-stationary phase portion of the reflections when compared with the other two datasets, (ii) there is more contribution from the stationary phase portion of the near offset virtual source – receiver pairs when compared to the direct wave only case. The vertically dipping model was a simplistic model and adding more complexities in the corrugated model helps to further understand the issues that were not resolved in Chapter 4. The added complexities of this model will try to determine if the greater angles of illumination from the scattered wave field offer more cancellation of non-stationary phase points, or addition of ray paths that have the geometry to create stationary phase points. To test this theory three mutes are applied to the trace acting as the virtual source during cross-correlation: (i) the direct wave only (figure 5.2 A), (ii) the direct wave + coda (figure 5.2 B) and (iii) the coda only (figure 5.2 C). A comparison is made between the three datasets once processing has been completed, to investigate how the scattered wave field affects the final migrated image.

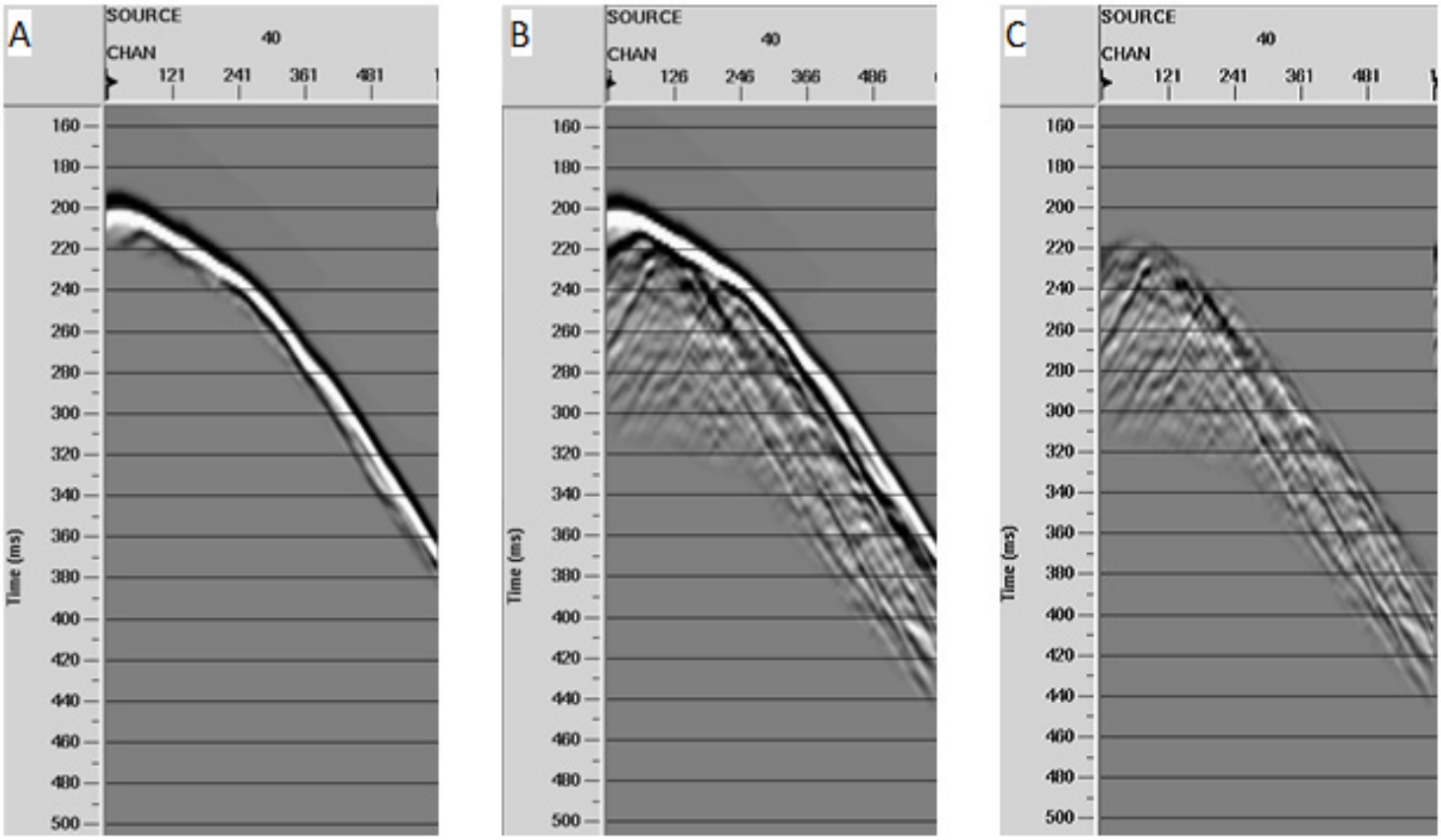

Figure 5.2 Mutes applied to VSP shot gathers
Mutes applied to the reciever acting as a virtual source during cross-correlation. (A) all but the direct wave is muted, (B) excess coda is muted leaving the direct wave and trailing coda, (C) the direct wave and excess coda is muted.

5.3.1 Analysis of Processed Corrugated Model

Similar processing techniques, as discussed in Chapter 4, will be applied to all the models in Chapter 5. Once the cross-correlation and summation process was completed a NMO correction of 6000 m/s was applied to the CMP gathers, to generate a virtual source stacked image. Although there are benefits when applying CMP processing techniques in the virtual source method, there are also issues. The reflections in the virtual CMP gathers do not have the same hyperbolic response as seen in a traditional surface seismic survey (figure 5.3). It has not been diagnostically proven, but the reflections non-hyperbolic response is thought to be due to insufficient stationary phase points contributing to the virtual CMP gathers. This poses a problem when applying a NMO correction as it is designed to flatten reflections with a hyperbolic response (figure 5.4). This issue is overcome because an adequate amount of the seismic traces associated with the front and back reflection flattens to within half a wavelength, allowing for constructive interference of each reflection.

Having demonstrated that each reflection will properly stack into the data, a final migrated seismic image of each model will be examined. An effective migration technique that is used during this processing sequence is a Post-stack Kirchhoff Time Migration. A Post-stack Kirchhoff Time Migration is able to migrate any of the structural highs and lows in the model into the proper position in the seismic profile, as the data previously assumes arrivals are parallel with respect to the borehole. When the data is migrated a comparision is made between the direct wave + coda dataset (figure 5.5

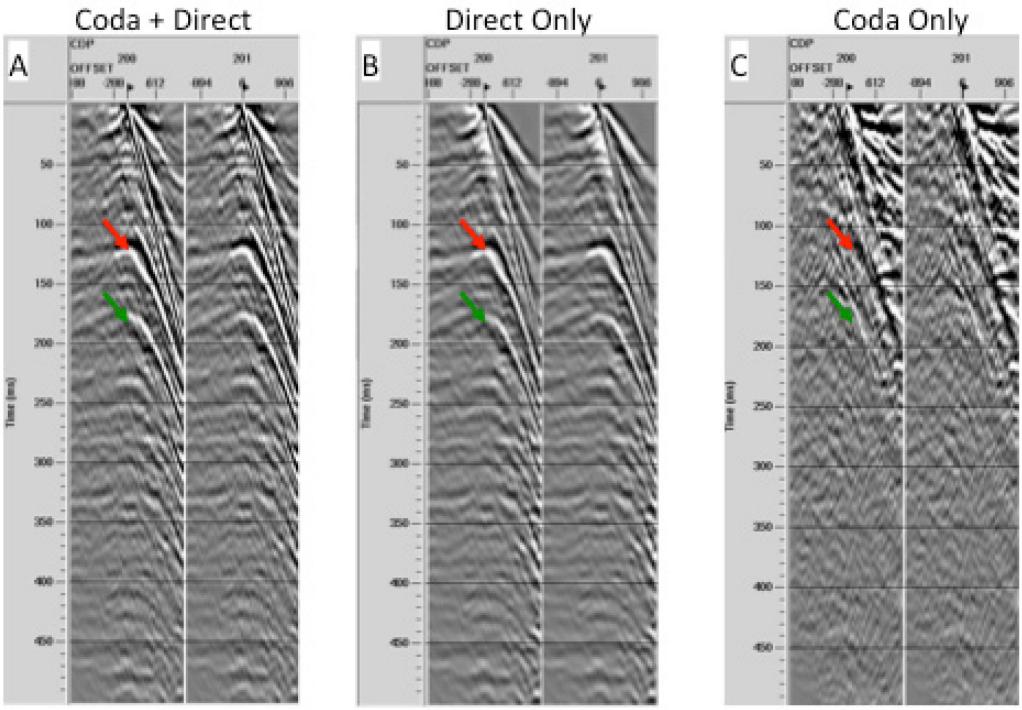

Figure 5.3 CMP Gathers from Coregated Model
CMP Gather 200-201. (A) the coda + direct case, (B) Direct only case and (C) Coda only case.

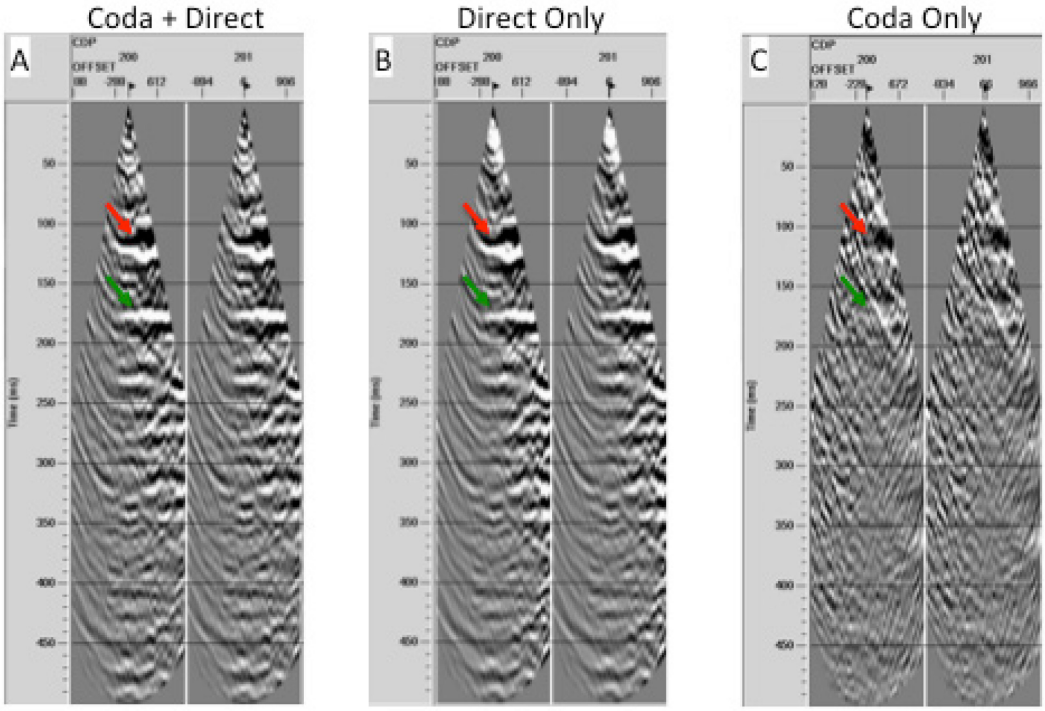

Figure 5.4 NMO corrected CMP Gathers from Coregated Model
NMO corrected CMP Gather 200-201. (A) the coda + direct case, (B) Direct only case and (C) Coda only case.

B) and the direct wave dataset (figure 5.5 C). The image quality is slightly improved in the direct wave + coda case, highlighed by the arrows in figure 5.5 B. The migrated data is most noteably improved in the portions of the target that are dipping toward the borehole. However, this comparison does not diagonstically prove how the scattered wavefield contributes to improving the processed image. To examine how the coda is contributing to the virtual source technique a mute that removes the direct wave and leaves just the coda was applied to the trace acting as the virtual source during cross-correlation (figure 5.2 C). The final migrated image of the coda only dataset (figure 5.5 D) demonstrates that the coda is able to generate the front and back reflection of the target of interest. The coda does not create stationary phase for the length of the borehole (figure 5.5 D), but it is still beneficial to the image quality when using virtual source technique.

To determine how the scattered wavefield affects the final migrated image a detailed analysis of the CMP gathers and NMO corrected CMP gathers is required. Both reflections are highlighted in figure 5.3 and 5.4, with some noteworthy results. Although the reflections have a similar response in both the direct and the direct + coda cases the far offset virtual source – receiver traces in the CMP gathers of the direct + coda case has a slight decrease in amplitude (figure 5.3 A and B). This result, despite not being as evident as the decrease of the non-hyperbolic portion in the CMP gathers seen in the direct wave + coda case from section 4.4.3.2, still occurs. The real differences are obvious in the coda only case. The CMP gathers appear to be nothing more than incoherent random events (figure 5.3 C), but the NMO corrected CMP gathers do image

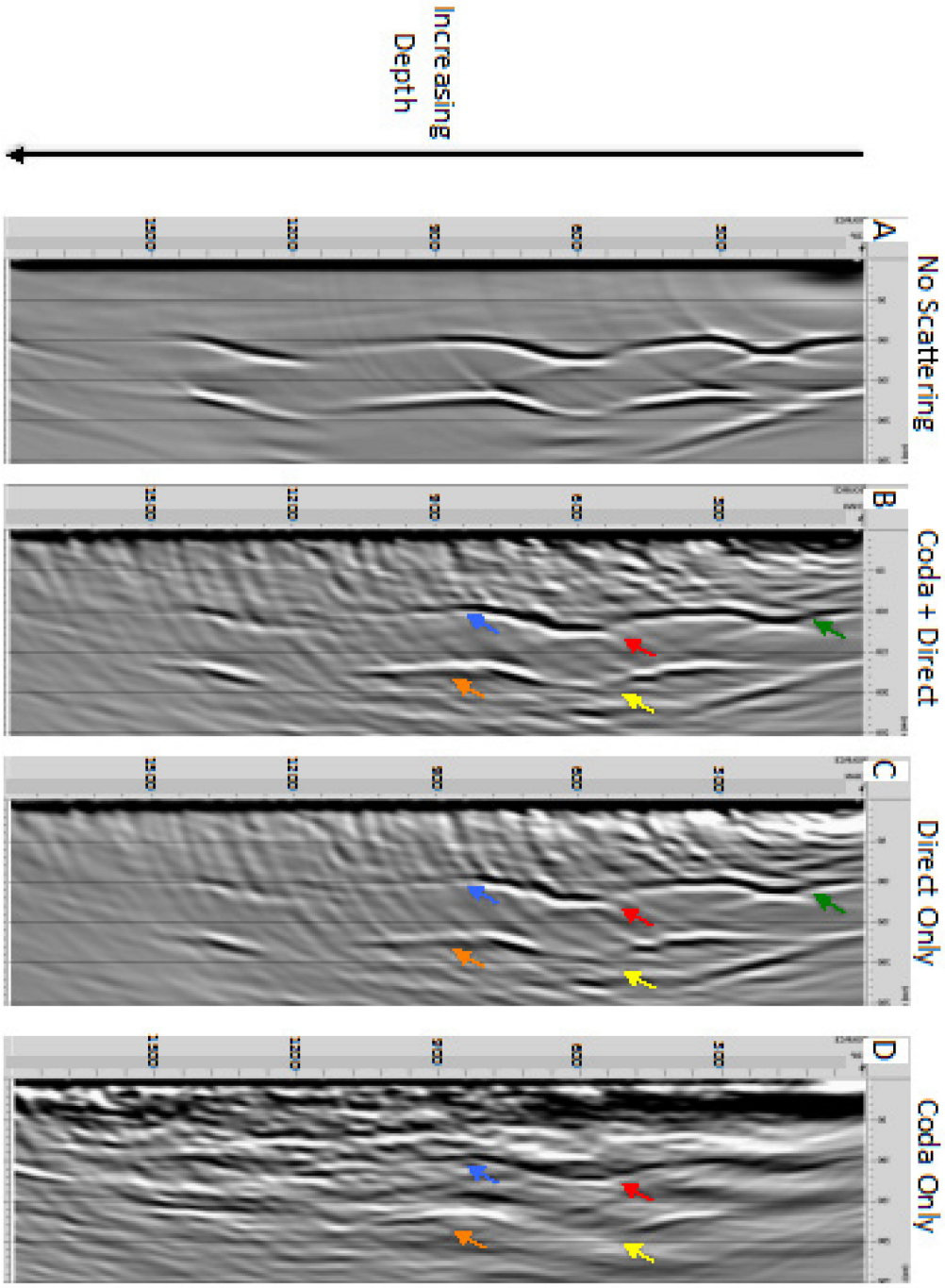

Figure 5.5 Migrated Corrugated model
(A) The virtual source method completed with direct + coda, (B) The virtual source method using direct + coda during cross-correlation process with heterogeneities in country rock, (C) The virtual source method using direct during cross-correlation process with heterogeneities in country rock, (D) The virtual source method using only coda during cross-correlation process with heterogeneities in country rock.

the front and back reflections as somewhat flat events (figure 5.4 C). The reflections are low amplitude compared to the other artifacts in the data, which gives evidence that the scattered wavefield does contribute stationary phase as well as cancellation of non-stationary phase components.

Further investigation into the FK spectrum similar to section 4.3 is needed to better understand the benefits from the increased angles caused by the scattered wavefield (figures 5.6 and 5.7). Two VSP shot gathers were collected from two different surface shot locations: i) 1000 m offset (figure 5.6) and ii) zero offest (figure 5.7). FK analysis is performed to determine how much scattering occurred in the data. In the zero offset VSP many of the strong amplitudes are still contained in the direct wave, however in the 1000 m offset VSP a lot of those amplitudes are partitioned to the scattered wavefield. The scattered wavefields are travelling with higher aparent velocities and greater amplitudes in the 1000 m offset VSP survey. Since the scattered wavefields are traveling with more angles of illumination, and higher amplitudes it effectivly increases ray paths that could create stationary phase rays as well as for cancellation of kinemtatically incorrect events. Another point to note is that the far offset surface sources primarily contribute to near offset virtual source – receiver pairs, so most of the increases in image quailty should be produced in the near offsets.

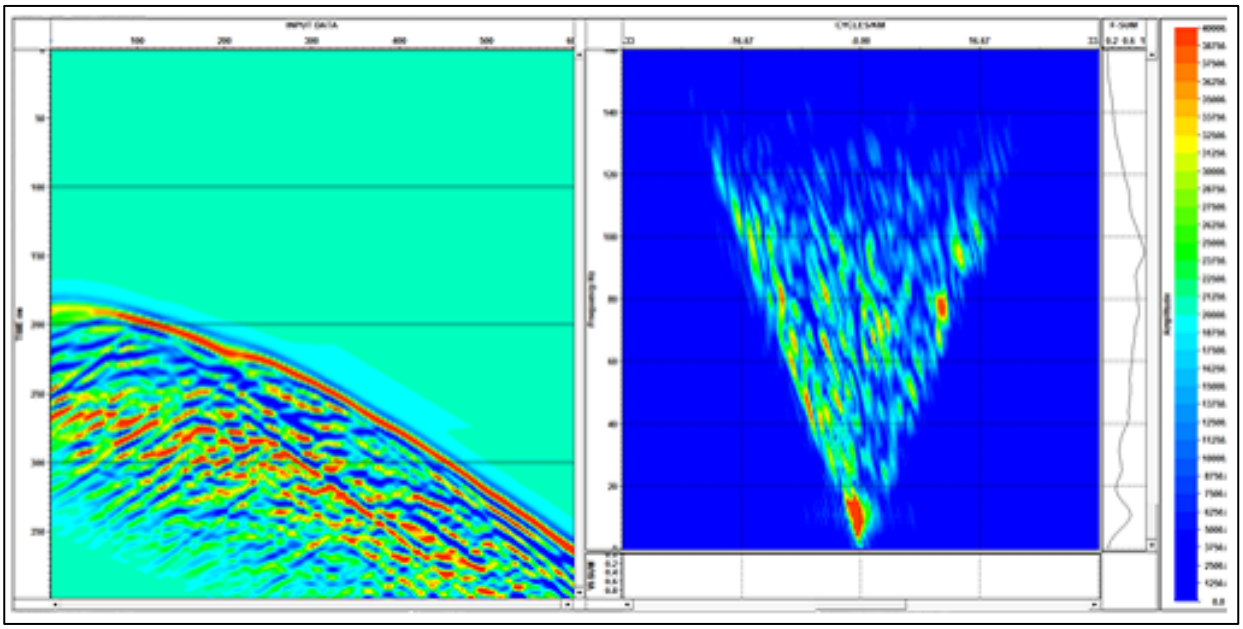

Figure 5.6 1000 m Offset VSP in a heterogeneous field with a correlation length of 60 m and a reflection coefficient of 0.067

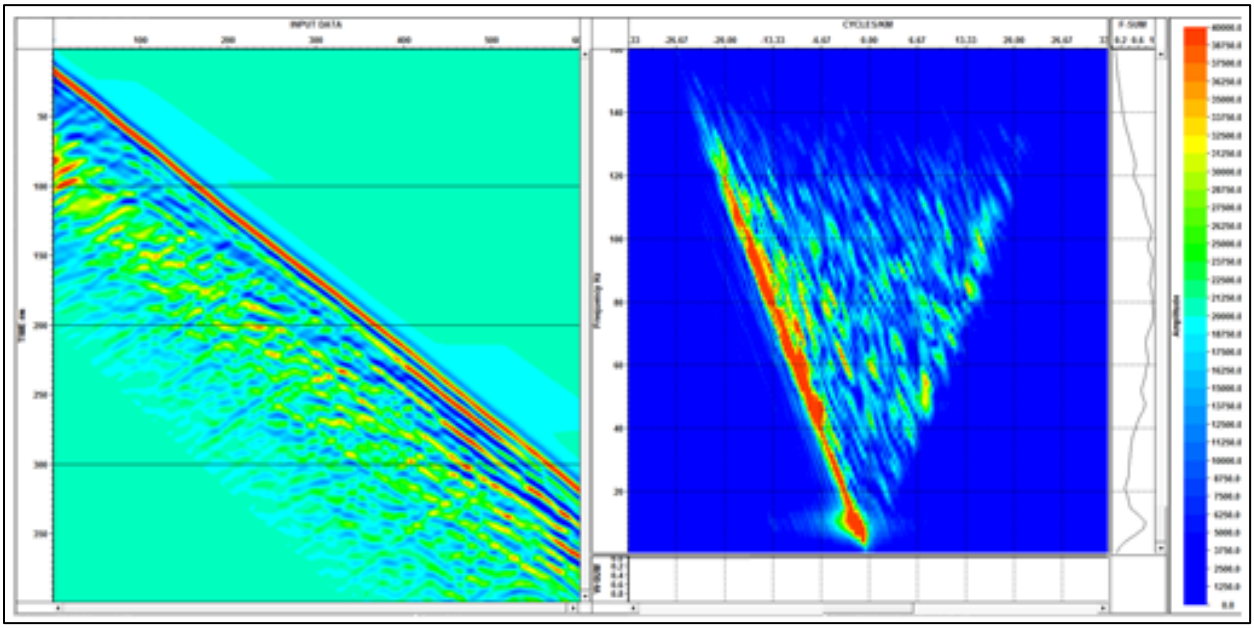

Figure 5.7 Zero Offset VSP completed on heterogeneous field with a correlation length of 60 m and a reflection coefficient of 0.067

5.3.2 Pre-stack Imaging

Stacking the data before migration can potentially have damaging effects to the seismic image quality because it can remove tails of diffractions, as well as remove important reflections near the edges of the survey due to low CMP fold. Pre-stack migration mitigates the effects that stacking can place on the data, thus "provides a solution to the problem of conflicting dips with different stacking velocities" (Yilmaz, 2001). The petroleum industry has to search for oil and gas in geological environments with complex geometries making pre-stack migration a very appealing imaging technique. The corrugated model in figure 5.1 has a complex geometry that could be affected by NMO stacking, so a pre-stack migration could be appropriate for imaging this model.

A Kirchhoff Pre-stack Depth Migration was completed on the homogenous corrugated model and the direct + coda heterogeneous model (figure 5.2 B). The pre-stack depth migration does well when imaging the corrugated reflector in the homogenous case because the dataset is all signal (figure 5.8 A). However, when the model included heterogeneities, the pre-stack depth migration images high amplitude events in the area between the receivers and the target, causing the final result to contain unwanted noise (figure 5.8 B). These events are thought to be either, artifacts from the pre-stack depth migration, or reflectors due to the heterogeneities within the model. The post-stack migration does not migrate as many of the events between the receivers and

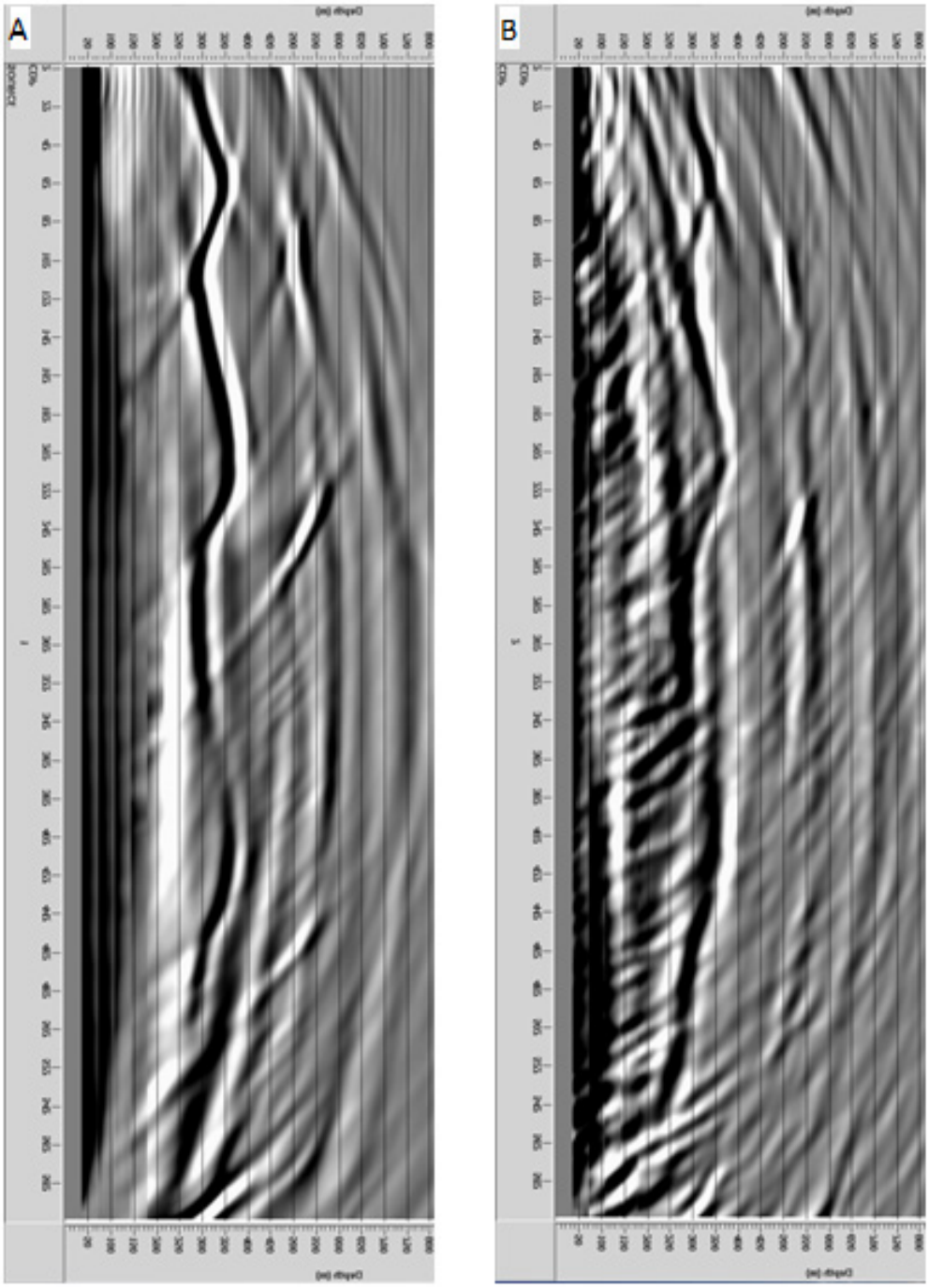

Figure 5.8 Kirchhoff Prestack Depth Migration of corrugated model
(A) Virtual source method completed with a homogenous country rock, (B) The virtual source method using direct + coda during cross-correlation process with heterogeneities in country rock

the borehole, because they are stacked out in the CMP stacking process (figure 5.5 B). So, by stacking the data before migration in the heterogeneous case provides a lot of benefits to the final image quality of the data.

5.4 Reducing the Surface Source Aperture

In chapter 4 and chapter 5, the results suggest that the coda is providing benefits when using the virtual source technique. By decreasing the surface source aperture on a VSP walk away survey the boundaries of the coda's influence on the vritual source method will be studied. To test the significance of decreasing the surface source aperture when applying the virtual source method, a straight ray analysis was completed using the same MATLAB code used in chapter 3. The experiment included two VSP walk away surveys with surface source apertures of 1500 m (model 1) and 500 m (model 2) (table 5.3). For symplicity, and general orientation of the corrugated model a vertically dipping target in a homogeneous medium was most appropriate. The survey geometries are the same as seen thoroughout chapter 5, for consistency and so that direct comparisons can be made. However, the receivers located in the borehole were decimated from 300 to 100 receivers and are spaced 18 m apart to decrease the clutter in the graphs, allowing for easier interpretation. Conducting a straight ray analysis will determine the difference in the amount of stationary phase rays created by each source aperture.

Model Number	Receiver Spacing (m)	Number of Receivers	Borehole Depth (m)	Distance to Reflector (m)	Source Aperture (m)
1	18	100	1800	300	1500
2	18	100	1800	300	500

Table 5.3 Straight ray analysis testing the ability for a 1500 m vs 500 m source aperture to create stationary phase rays

The VSP walk away survey in model 1 used an extended source aperture of 1500 m. The source aperture produces stationary phase rays at a maximum approximate depth of 1300 m in the borehole leaving the deepest 500 m without any kinematically correct virtual sources (figure 5.9, 5.10). The deepest part of the target is going to be poorly imaged, which are similar results seen thoughout this thesis project. Model 2 used the same survey geometry except there was decrease in the surface source aperture by a third to 500 m. Decreasing the source aperture creates virtual sources at a maximum depth of 850 m depth (figure 5.11). The decimated source aperture reduces the maximum depth of a kinematically correct virtual source by 450 m. There is also a significant decrease in the fold of the data caused by reducing the source aperture (figure 5.10 and 5.12). The decrease in fold primarily comes from the near virtual source – reciever offsets, which are contributed from the far offset surface sources. To further back up this result, in figure 5.9 it is clear that surface sources locacted between 500 m to 1500 m produce a significant amount of kinematically correct virtual sources.

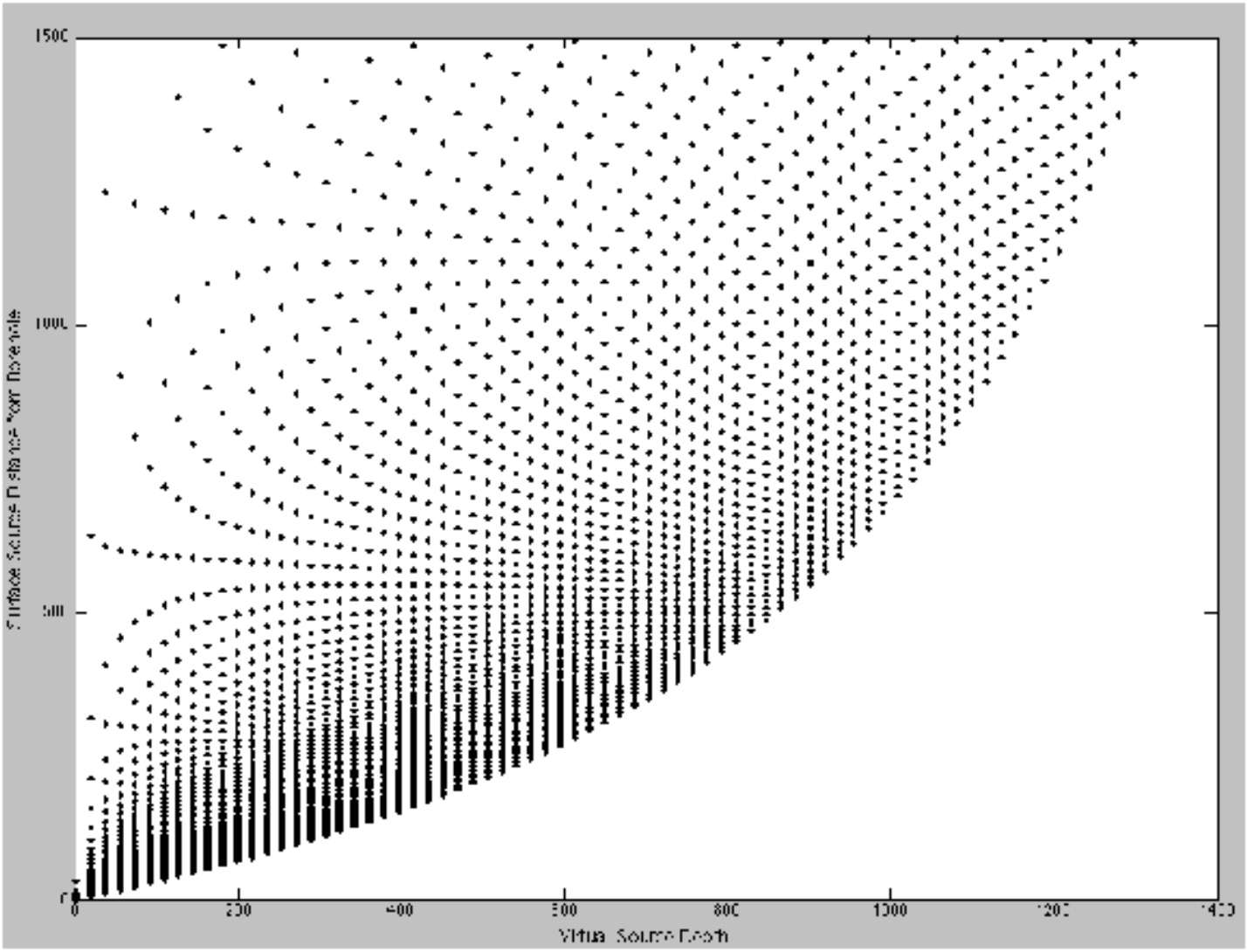

Figure 5.9. Model 1 creates kinematically correct virtual sources down to a depth of 1300 m.

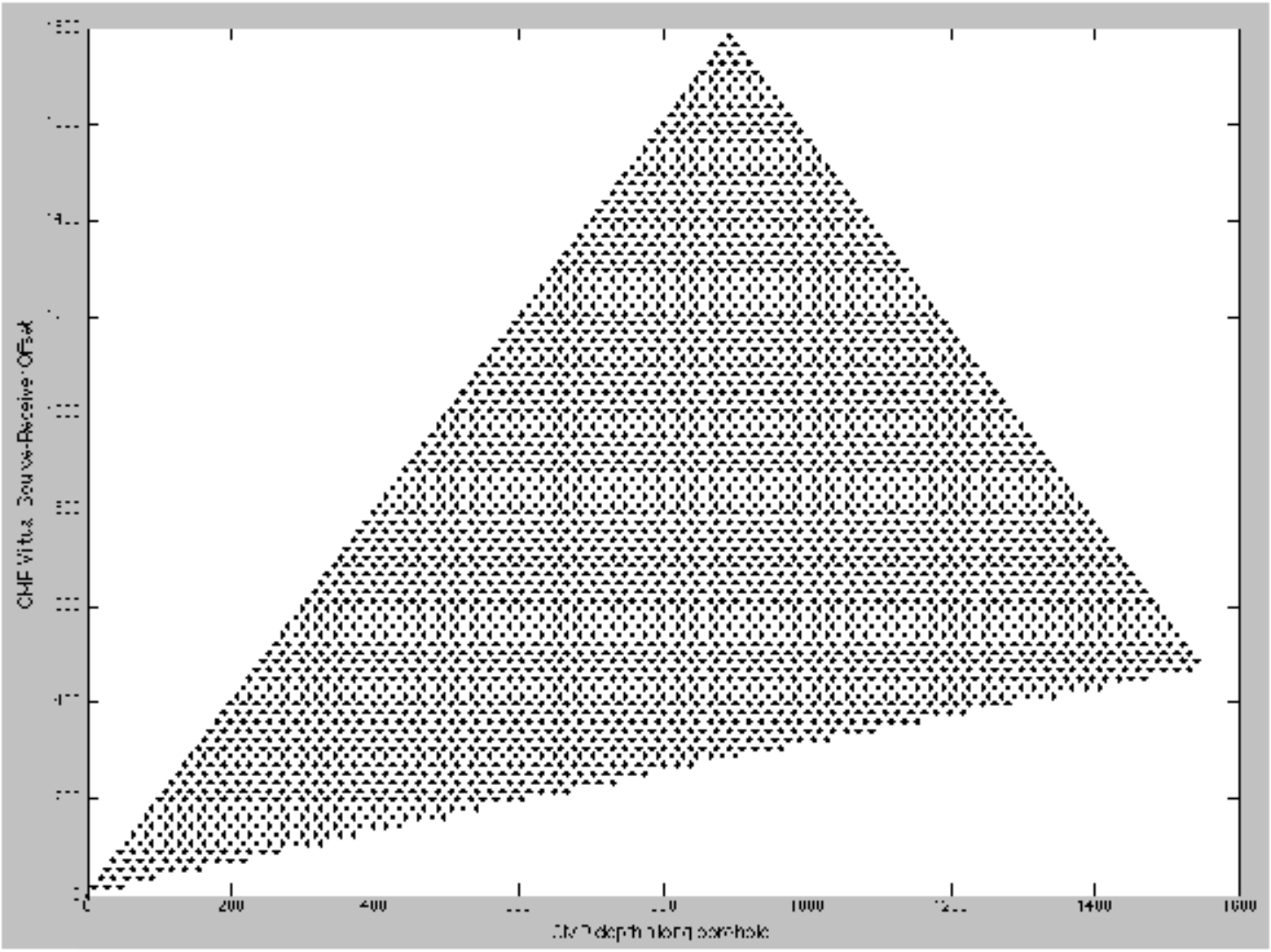

Figure 5.10 CMP depth along borehole vs. CMP Virtual Source – Receiver Offset for Model 1

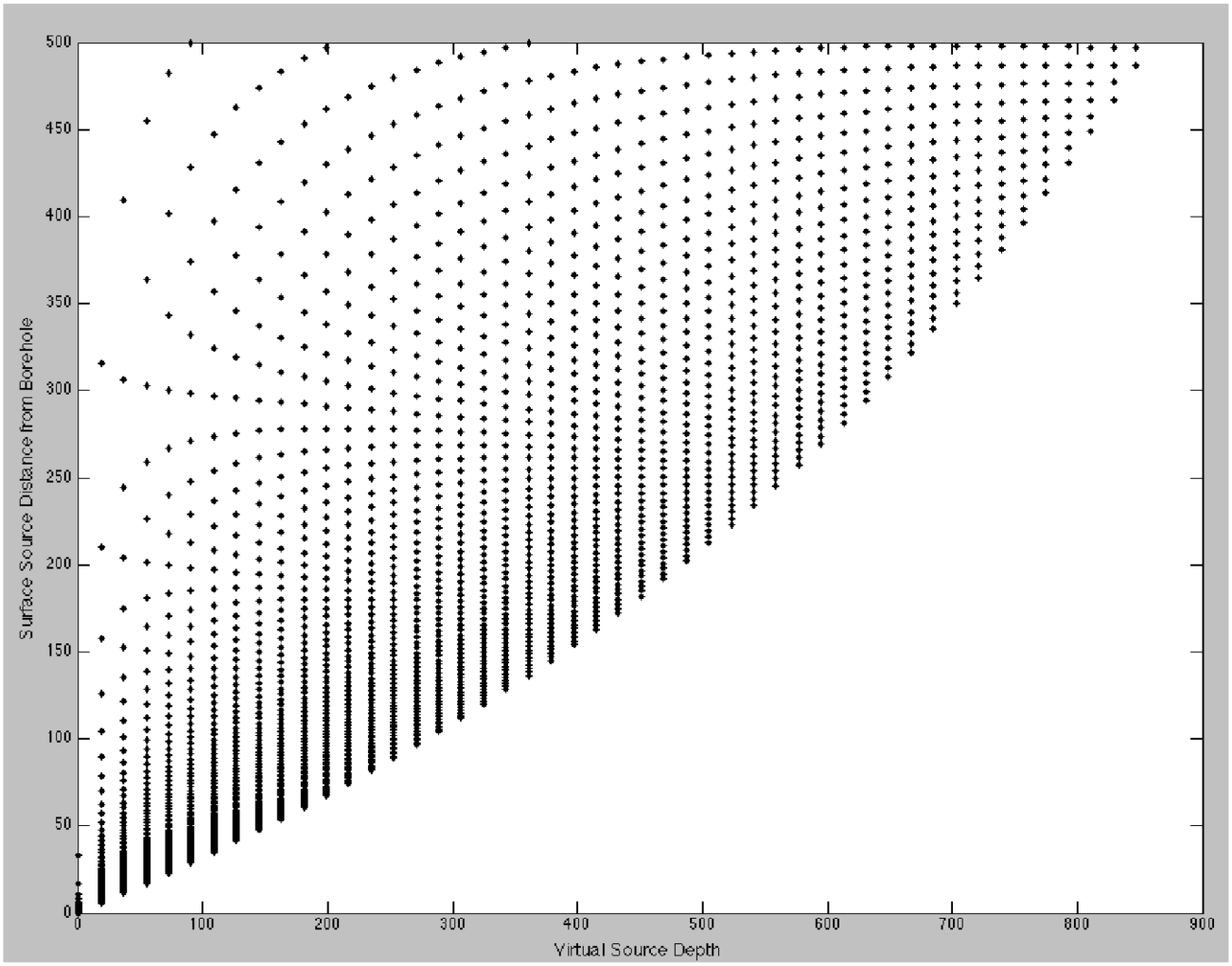

Figure 5.11. Virtual Source Depth vs. Surface Source Distance from Borehole for Model 2

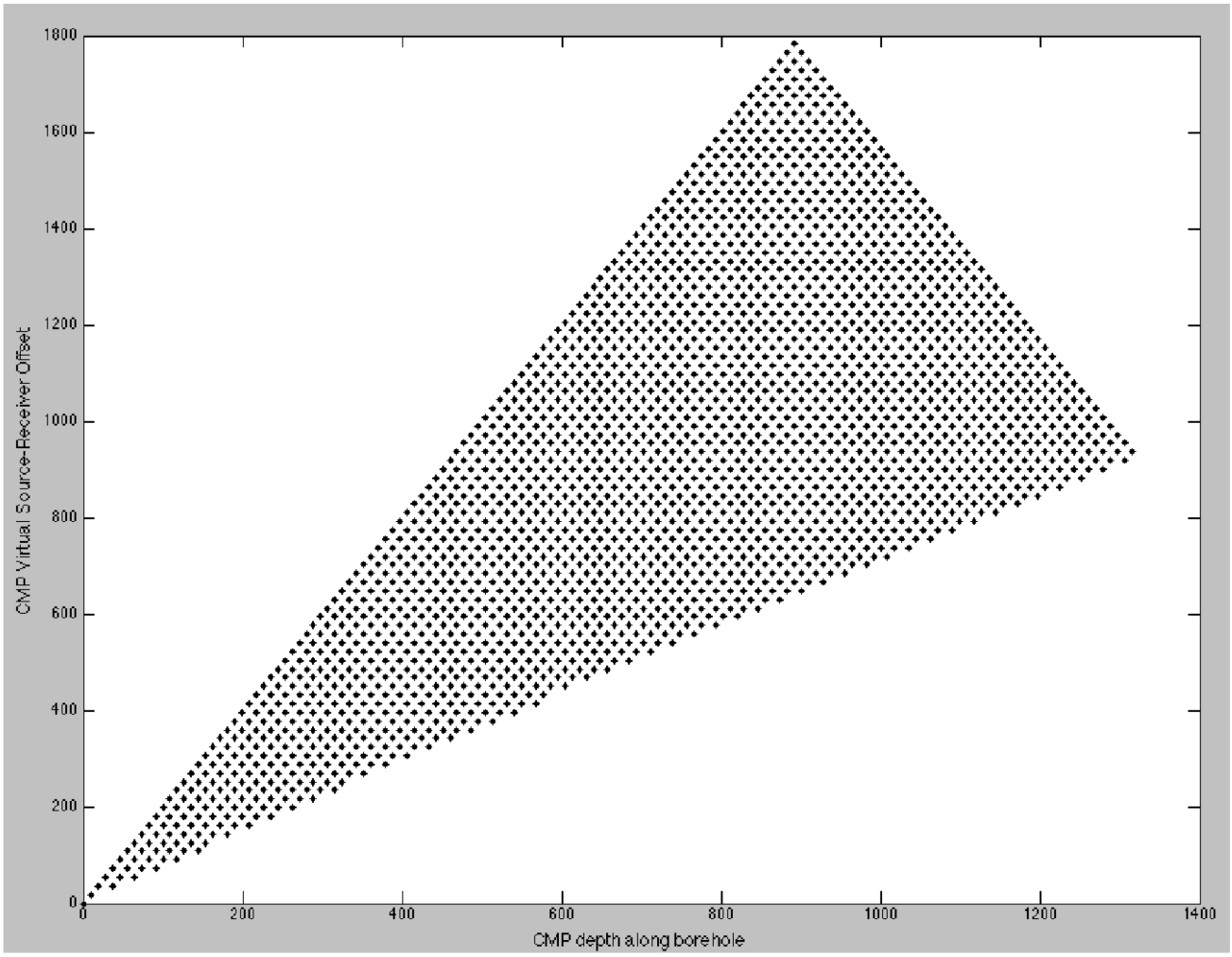

Figure 5.12 CMP depth along borehole vs. CMP Virtual Source – Receiver Offset for Model 2

5.4.1 Practial Application of Reducing Source Aperture

When completing onshore seismic surveys the source aperture and source density is often limited by many different enviormental constraints (forest, lakes, ect), as well as the cost of the survey. Being able to decrease the amount of sources needed, while still being able to image the target of interest will significantly reduce environmental effects and the cost of the survey. To practically test the affect of decreasing the surface source aperture and density the surface source aperture was decreased from 1500 m to 500 m and source spacing was increased from 10 m to 20 m. This surface source geometry was run on two models: (i) the bimodal velocity model seen in section 5.3 and (ii) a homogeneous model. These models will establish if including the scattered wave during cross-correlation can replace surface sources. The target and receiver geometry are the same as the previous models in chapter 5, as seen in table 5.1.

This decimiated model was processed with the same processing workflow as the other models in chapter 5 to keep consistentcy between them. It is obvious that the imaging capibilities have been significantly reduced in the decimated models (figure 5.13), giving similar results as seen in the ray tracing analysis. In both decimated cases (figure 5.13 B and D) the decrease in image quality is most noteable in the deeper portions of the target as well as the portions that are dipping away from the borehole. Deeper than approimately 400 m, both reflections are either placed in kinematically incorrect positions or the amplitude is so low that they are not visable over the artifacts in the heterogenous case (figure 5.13 B). In the homogenous decimated model the

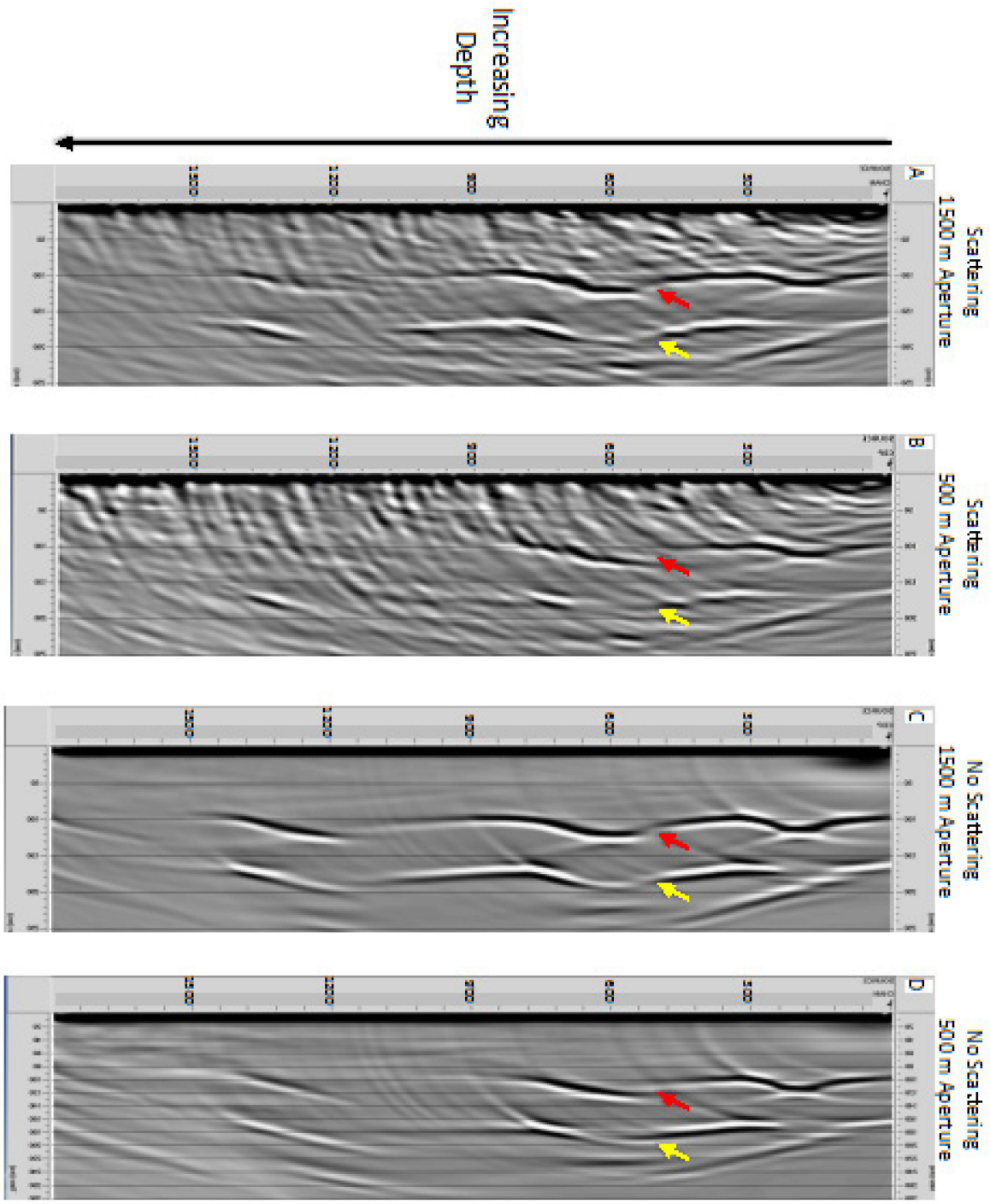

Figure 5.13 Decimated Corrugated Model
(A) The source aperture is 1500 m and the source spacing is 10 m in an isotropic heterogeneous model with a RC of 0.067. (B) The source aperture is 500 m and the source spacing is 20 m in an isotropic heterogeneous model with a RC of 0.067. (C) The source aperture is 1500 m and the source spacing is 10 m in a homogeneous medium. (D) The source aperture is 500 m and the source spacing is 20 m in a homogeneous medium.

reflections are aparent because everything involved is signal, but much of this signal is non-stationary phase causing the reflections to be kinematically incorrect. The outcome gives evidence that the amount of stationary phase produced has been significantly decreased, due to the decrease in source aperture and source density. Unfortunately, the beneifits that scattering provide are too limited to replace the significant benefits of increasing the surface source aperture.

5.5 Concluding Remarks

Chapter 5 studied a complex imaging target with varying dips, similar to a real world target. The corrugated model was designed to diagnostically test benefits of the scattering wavefield. To test this the model was processed in a number of ways, including; (i) cross-correlating with only the coda, (ii) reducing the source aperture and (iii) running a pre-stack migration on the cross-correlated data.

It was observed that the coda + direct case produces the highest quality migrated seismic image, although only marginally. The marginal improvements are most noticeable when the corrugated model is dipping away from the adjacent borehole. Since, the comparison between the direct case and the direct + coda case was not conclusive, another model that cross-correlated with only coda was completed. This model demonstrated that kinematically correct events are produced. Also, the results suggest that the introduction of the scattered wavefield disturbs the non-stationary phase contributions, allowing greater cancellation of these events. These outcomes indicate that

including the coda during cross-correlation with real world data would be beneficial to the overall image quality as more stationary phase and less non-physical events could be present.

Although the research was enlightening to the overall understanding of the effectiveness heterogeneity has on the seismic image quality, not all of the results were positive. Including the coda during cross-correlation does not have the same effectiveness as surface sources for producing constructive interference of kinematically correct events and cancellation of artifacts. Unfortunately, it is more beneficial to extend the surface source aperture than to cross-correlate using coda if possible during a real world VSP survey. Another processing technique that did not work out as planned was the pre-stack depth migration. Pre-stack migration is supposed to provide a solution when imaging with conflicting dips, however a lot of the noise from the heterogeneities was not cancelled out, causing the final migrated image to be overloaded with unwanted signal between the receivers and the target. When processing data with the virtual source technique stacking the data benefits the migrated image as many artifacts are summed out during this stage.

Chapter 6: Discussion

The research completed for this master's thesis was designed to investigate how seismic scattering from geological heterogeneity (example; sedimentary layering or gneissic foliations) may enhance imaging when using the virtual source technique. This topic of imaging complex, near vertical structures surrounded by a heterogeneous medium has limited research completed, which allowed me to extend the understanding from the current literature. Since, these geological scenarios are of high significance to the petroleum and mining exploration industry this study could aid in drilling programs, by more accurately locating and orientating targets of interest.

Chapter 3 demonstrated, through the analysis of ray tracing (Brand, and Hurich 2012; Hurich and Deemer, 2013) that even if a VSP walk away survey is unable to meet the requirements that receivers must be surrounded by sources the virtual source method is still valid. However, caution must still be taken with the geometric design of the experiment particularly with respect to source density, aperture and dip of the structure of interest. The source aperture must be wide enough to capture a sufficient number of stationary phase points, because the range of offsets contained within the CMP virtual gathers are related to the amount of kinematically correct virtual sources and thus the final image quality. Appropriate source spacing prevents spatial aliasing from occurring in the correlation gather so that summation is more effective. Further research in Chapter 3 used straight ray analysis to examine the impacts that reflector orientation, source aperture and the distance between the reflector and borehole can have on both the

depth at which stationary phase points can be created, and the fold of the virtual CMP-gathers. All of this work indicates that great care must be taken when designing a VSP walk away survey, to ensure sufficient stationary phase points are captured.

The next step in the research was to analyze how heterogeneous mediums influence the seismic wavefield. The beginning of Chapter 4 experimented with a variety of heterogeneous mediums, testing which geological conditions affect seismic scattering. This research was completed using zero and 1000 m offset 2-D synthetic VSP surveys. Analysis of these heterogeneous models identified two heterogeneous models, one in the strong scattering regime and another in the weak scattering regime that were carried forward for further experimentation. Running VSP walk away surveys in both geological scenarios determine which conditions will produce optimal seismic images with the virtual source technique.

Before introducing heterogeneities to the virtual source method a model with a homogeneous background and a vertical target was completed. The homogeneous model was designed to gain insight into imaging capabilities of the virtual source method before adding complexities into the interpretation. The interpretation of the virtual source and CMP gathers identified some key artifacts that are a result of the cross-correlation and summation of the VSP shots gathers. The most noticeable artifacts are the multiples from the front and back reflections, the non-hyperbolic moveout of far offset virtual source – receiver pairs and events with no apparent physical meaning. Further analysis was conducted on the final stacked image, which demonstrated that the vertically dipping

target is imaged kinematically correctly when sufficient stationary phase points are captured. Unfortunately, the limited source aperture results do not produce enough destructive interference of artifacts, and image the shallow and deeper portions of the borehole poorly due to insufficient stationary phase points.

Using the research completed with scattering fields and the reference model, the idea that wave field scattering may mitigate the effects of limited source apertures by providing a larger range of angles was evaluated. Once the virtual source technique was completed in a heterogeneous medium it was evident that when a mute that included the direct wave + coda was applied to the VSP shots gathers the highest quality seismic image was produced. There is evidence throughout the processing workflow suggesting that the scattered wavefield allowed for increased illumination angles without introducing excessive noise to the data. Analysis of the CMP gathers demonstrates that the increased angles gets you closer to simulating surrounding the receivers with sources, resulting in improved cancellation of non-stationary phase events. In an attempt to gain further insight into how the coda affects the virtual source methods results, the direct + coda case was subtracted from the direct only case. If differencing gives definitive results it indicates that, increasing the illumination angles creates more ray paths with the appropriate geometry to create stationary phase points, which would increase the signal to noise ratio.

However enlightening the vertically dipping model was, a model that is more sensitive to increased angle illumination was required for a diagnostic test of the effect of

heterogeneity and scattering on the virtual source method. The corrugated model allowed for further investigation into the benefits of using coda to increase the constructive interference of kinematically correct events, and decrease the summation of artifacts. After imaging the corrugated model in a heterogeneous medium a similar result to chapter 4 occurred, the coda + direct case was able to produce the highest quality image, which is most noticeable when the corrugated model is dipping away from the borehole. Since the results from the corrugated model continued to produce subtle imaging improvements, further research into the benefits of using coda was needed. A mute that removed the direct wave was created and applied to the VSP shot gathers. The coda only case produced a sufficient amount of stationary phase points as well as the destructive interference of non-physical events, allowing the complex model to be imaged. So, this proves that while conducting the virtual source method on real world data it would benefit from including coda. Although, this is a positive result the increased illumination angles do not replace the effectiveness of real surface sources in the ability to produce stationary phase rays as shown at the end of chapter 5.

The research during this master's thesis has been very enlightening into the capabilities of the virtual source method in a simulated real world environment. First, proving that the virtual source method is still a valid imaging technique even if the VSP walk away survey violates the requirement that receivers must be surrounded by sources. This statement holds up if there is sufficient constructive interference of stationary phase points and destructive interference of non-physical events. Throughout this thesis a number of experiments suggesting that heterogeneous mediums could increase stationary

phase rays and removal of non-physical events were conducted. The use of the ray tracing method helped to back up observations made when modeling and thus exposing potential benefits of implementing the coda during cross-correlation. Finally, heterogeneities are thought to cause noise and usually are removed during traditional seismic processing, however this thesis suggests that the virtual source method can benefit from the scattered media and should be included when processing a real world seismic survey.

Chapter 7 References

Bakulin. A., and Calvert. R., 2004. Virtual Source: New method imaging 4D below complex overburden: 74'" Annual International Meeting. SEG Extended Abstracts, 2477-2480.

Bakulin. A., and Calvert. R., 2006. The virtual source method: Theory and case study: Geophysics, 71, SI139-SI150.

Bal, G., Ryzhik, L., 2005, Wave field correlation in weakly mismatched random media: Stochastics and Dynamics, 6(3), pp. 301-328

Boreca, L., Papanicolaou, B., Tsogka, C., 2006, Coherent interferometric imaging in clutter: Geophysics, 71(4), SI165-SI175.

Brand, E., 2011, The virtual source method for imaging steeply dipping structures using a walk-away VSP acquisition geometry: M.S. thesis, Memorial University of Newfoundland.

Brand, E., Hurich, C., 2013, Geometrical considerations in the acquisition of borehole interferometric data for imaging near-vertical features: design of field experiments: Geophysics: 78, this issue, doi: 10.1190/geo2012-0171.1.

Curtis, A., Gerstoft, P., Sato, H., Snieder, R., Wapenaar, K., 2006, Seismic interferometry – turning noise into signal: The Leading Edge, 25(9), 1082-1092.

Duff, D., 2007, Physical Property Analysis, Numberical and Scale Modeling for Planning of Surface Seismic Surveys: Voisey's Bay, Labrador: M.S. thesis, memorial University of Newfoundland.

Frankel, A., and Clayton, R.W., 1986, Finite Difference Simulations of Seismic Scattering: Implications for the Propagation of Short-Period Waves in the Crust and Models of Crustal Heterogeneity: Journal of Geophysical Research, 91, no. B6, pp.6465-6489.

Holliger, K., Green, A.G, and Juhlin, C., 1996, Stochastic Analysis of sonic logs from the upper crystalline crust: Methodology: Tectnophysics, 264, 341-356.

Hornby, B.E., and Yu, J., 2006, Interferometric imaging of a salt flank using walkaway VSP data: The Leading Edge Jun 2007, Vol 26, No. 6, pp 760-763.

Hurich, C., and Deemer, S., 2013 Combined surface and borehole seismic imaging in a hard rock terrain: A field test of seismic interferometry: Geophysics, Vol. 78, No. 3, pp. B103-110.

L'Heureux, E., and Milkereit, 2005, Building 3-D Petrophysical models based on the stochastic analysis of borehole logs: 75th Annual International Meeting, SEG, Expanded Abstracts, 1779-1782.

L'Heureux, E., 2006, Scattering regimes and the influence of heterogeneity on the seismic detection of mineral exploration targets: SEG Technical Program Expanded Abstracts 206: pp. 1338-1342.

Mehta, K., Snieder, R., and Sheiman, J., 2008, Acquisition geometry requirements for generating virtual-source data: The Leading Edge, 27, 620-629.

Schuster, G.T., 2001, Theory of Daylight/Interferometric Imaging: Tutorial: 63rd Annual International Conference and Exhibition, EAGE Extended Abstracts, A-32.

Schuster, G.T., 2009, Seismic Interferometry: Cambridge Press.

Vanconcelos, I., Gaiser, J., Calvert, A., and Calderon-Macias, C., 2008, Retrieval and suppression of surface waves using interferometry and correlation and by deconvolution: 78th Annual International Meeting, SEG Extended Abstracts, 2566-2570.

Xue, Y., Dong, S., and Schuster, G.T., 2009, Interferometric prediction and subtraction of surface waves with a nonlinear local filter: Geophysics, 74, S11-S18.

Yilmaz, O., Tanir, I., Gregory, C,. 2001, A unified 3-D seismic workflow: Geophysics, 66(6), 1699-1713. doi:10.1190/1.1487112.